STRUCTURE AND PROPERTIES OF COPPER OXIDE THIN FILMS

by

Andrew J. Wnuk

Thesis submitted to the Graduate Faculty of the

Virginia Polytechnic Institute and State University

in partial fulfillment of the requirements for the degree of

MASTER OF SCIENCE

in

Materials Engineering

APPROVED:

L. H. Slack, Chairman

J. J. Brown, Jr.

W. R. Hibbard, Jr.

October, 1977

Blacksburg, Virginia

ACKNOWLEDGMENTS

The author is pleased to express his appreciation to Dr. Lyle H. Slack for providing him the opportunity to study ceramic engineering at VPI&SU. He is also grateful to Dr. Slack for reviewing and strengthening this thesis. Appreciation is also extended to Dr. Jesse J. Brown, Jr. and Dr. Walter R. Hibbard, Jr. for their willingness to serve on the graduate committee.

Dr. G. V. Gibbs and Dr. F. K. Ross are also acknowledged for their assistance with the crystallographic aspects of this thesis. The aid of , who helped gather the optical data, and , who typed the manuscript, is also appreciated.

Finally, the author wishes to thank his parents, for their encouragement and understanding.

TABLE OF CONTENTS

Page

ACKNOWLEDGMENTS ii

LIST OF TABLES. v

LIST OF FIGURES vi

I. INTRODUCTION. 1

II. LITERATURE REVIEW 4

A. Cupric Oxide. 4
1. Structure 4
2. Nonstoichiometry. 4
3. Electrical Properties 5
B. Cuprous Oxide 7
1. Structure 7
2. Nonstoichiometry. 8
3. Electrical Properties 8
C. Copper Oxide Thin Films 9
D. Radio Frequency Sputtering of Oxides. 13
1. Sputtering Principles 13
2. R. F. Sputtering Variables. 14

III. EXPERIMENTAL PROCEDURE. 18

A. Film Preparation. 18
1. R. F. Sputtering. 18
a. Apparatus 18
b. Sputtering Targets. 18
c. Substrates. 20
d. Thin Film Thermocouples 21
e. Sputtering Atmospheres. 23
f. Sputtering Procedure. 23
2. Annealing Experiments 24
a. Air 24
b. Reducing Atmospheres. 26
3. Electrode Fabrication 27
B. Film Characterization 29
1. X-Ray Diffraction 29
2. SEM-EDAX. 29
3. Film Thickness Determination. 30
4. Electrical Measurements 31
a. Resistivity 31
b. Activation Energy 32
c. Charge Carrier Type 33

TABLE OF CONTENTS (Continued)

Page

5. Optical Properties 34

IV. RESULTS 35

A. Effects of Deposition Variables 35
B. X-Ray Analysis 35
1. Sputtered Films 39
2. Annealed Films 43
3. Reduced Films 46
C. SEM-EDAX Results 46
D. Electrical Properties 52
1. Sputtered Films 52
2. Annealed Films 62
3. Cu_2O Films 62
E. Optical Properties 67
1. Sputtered Films 67
2. Annealed Films 71
3. Cu_2O Films 71

V. DISCUSSION 83

A. Radio Frequency Sputtering of CuO 83
B. Structure and Properties of Copper Oxide Films 84
1. CuO/Cu_2O Films 84
2. CuO Films 87
3. Cu_2O Films 93

VI. CONCLUSIONS 95

VII. FUTURE WORK 97

REFERENCES 99

APPENDIX 103

VITA 105

ABSTRACT

LIST OF TABLES

Table | Page

I. Film Composition as Function of the O_2 Partial Pressure in a Plasma 12

II. R. F. Sputtering Parameters for CuO Deposition 25

III. X-Ray Diffraction Data 37

IV. Electrical Properties of Sputtered Copper Oxide Films. . . 53

V. Electrical Properties of Films Annealed at 300°C for 100 Hours. 65

VI. Electrical Properties of Reduced Films 68

VII. Optical Transmittance Data of Copper Oxide Films 69

VIII. Conversion of Wavelength to Energy 70

LIST OF FIGURES

Figure | Page

1. Sputtering Phase Diagram for the Cu-O System 11

2. Effect of sputtering variables on deposition rate of SiO_2 15

3. Effect of substrate temperature on NiO film density and stoichiometry. 17

4. Schematic diagram of the radio frequency sputtering apparatus. 19

5. Calibration curve for nickel/iron thin film thermocouples. 22

6. Resistivity specimen 28

7. Dependence of the CuO deposition rate on the percent O_2 in the sputtering atmosphere 36

8. X-Ray diffraction pattern of Film 24 sputtered in 100% Ar 40

9. X-Ray diffraction pattern of Film 15 sputtered in 90% Ar - 10% O_2. 41

10. X-Ray diffraction pattern of Film 21 sputtered in 50% Ar - 50% O_2. 42

11. Change in the X-ray diffraction pattern of Film 26 during annealing at 300°C in air 44

12. Change in X-ray diffraction pattern of Film 9 during annealing at 300°C in air. 45

13. Change in X-ray diffraction pattern of Film 12 during annealing at 300°C in air. 47

14. X-Ray diffraction pattern of Film 31 before and after reduction to Cu metal. 48

15. X-Ray diffraction pattern of Film 33 before and after reduction to Cu_2O. 49

16 A. SEM micrograph of Film 15 sputtered in 90% Ar - 10% O_2 . . 50

LIST OF FIGURES (Continued)

Figure Page

16 B. SEM micrograph of Film 16 sputtered in 100% Ar 50

17 A. SEM micrograph of Film 15 after annealing in air 51

17 B. SEM micrograph of Film 16 after annealing in air 51

18. Dependence of copper oxide film resistivity on oxygen content of the sputtering atmosphere 54

19. Temperature dependence of resistivity for CuO/Cu_2O films sputtered 1 hour in 100% Ar. 56

20. Temperature dependence of resistivity for CuO/Cu_2O films sputtered 4 hours in 100% Ar 57

21. Temperature dependence of resistivity for CuO films sputtered for 1 and 2 hours in 90% Ar - 10% O_2 58

22. Temperature dependence of resistivity for CuO films sputtered for 4 hours in 90% Ar - 10% O_2 59

23. Temperature dependence of resistivity for CuO films sputtered for 2 hours in 50% Ar - 50% O_2 60

24. Temperature dependence of resistivity for CuO films sputtered for 4 hours in 50% Ar - 50% O_2 61

25. Change in room temperature resistivity after annealing in air at $300^{\circ}C$. 63

26. Temperature dependence of resistivity for CuO films after annealing at $300^{\circ}C$ 64

27. Temperature dependence of resistivity for Cu_2O films after annealing at $300^{\circ}C$ 66

28. Change in absorbance, reflectance, and transmittance (with wavelength) for CuO/Cu_2O Film 6 sputtered in 100% Ar. 72

29. Change in transmittance with wavelength for CuO/Cu_2O Film 24 sputtered in 100% Ar 73

30. Change in transmittance with wavelength for CuO Film 8 sputtered in 90% Ar - 10% O_2 74

LIST OF FIGURES (Continued)

Figure | Page

31. Change in transmittance with wavelength for CuO Film 15 sputtered in 90% Ar - 10% O_2 75

32. Change in transmittance with wavelength for CuO Film 13 sputtered in 50% Ar - 50% O_2 76

33. Change in transmittance with wavelength for CuO Film 22 sputtered in 50% Ar - 50% O_2 77

34. Change in transmittance with wavelength for CuO Film 26 after annealing. 78

35. Change in transmittance with wavelength for CuO Film 9 after annealing. 79

36. Change in transmittance with wavelength for CuO Film 12 after annealing. 80

37. Change in transmittance with wavelength for Cu_2O Film 27R. 81

38. Change in absorbance, reflectance and transmittance with wavelength for an uncoated Corning 7059 glass substrate. . 82

39. Resistivity dependence of CuO/Cu_2O films on Cu_2O content . 86

I. INTRODUCTION

Current interest concerning the utilization of transition metal oxide thin films on foreign substrates arises from the varied chemical, electrical, and optical properties associated with these materials. A wide range of possible applications have been proposed for oxide films but detailed characterization is necessary before their practical value can be assessed.

To date, the majority of oxide film studies have been directed towards the development of selective transparent coatings for architectural glass. Pure and mixed oxide films capable of reflecting long wavelength radiation have been investigated.[1,2]

Selectively absorbent layers are also of interest, especially in the design of flat plate solar collectors. Thin films of CuO and Co_3O_4 on polished metal sheets, for example, have been shown to absorb greater than 80% of the incident solar radiation while retaining a very low infrared emissivity.[3] These types of coatings are also capable of operating at temperatures as high as 500°C allowing them to be used under focused solar radiation.

Oxide films may someday take an active role in photovoltaic energy conversion. Thin films of cuprous oxide, Cu_2O, on copper sheets were known to be rectifying and photovoltaic as far back as 1920.[4] Recent calculations[5] have pointed out that the Cu_2O-Cu solar cell may be capable of up to 10% conversion efficiency compared to 14% achieved by the heavily researched silicon solar cell. Even higher efficiencies may be attained if another oxide film can be used

in place of the copper layer to form a rectifying p-n junction with Cu_2O. Such an application would require that the second film have a smaller band gap than Cu_2O so that a greater portion of the solar spectrum could be absorbed by the cell.

Although the electrical properties of some of the other stable transition metal oxides such as MnO, CoO and NiO are well known, those of CuO have not been clearly established. Since single crystals of CuO have apparently never been grown, previous studies of electronic conduction have been carried out on sintered pellets or compressed powders. The effects of grain boundaries and porosity have not been sufficiently correlated with electrical properties to warrant much faith in these measurements. Similarly, the effect of nonstoichiometry on the electrical and optical properties of CuO has not been ascertained. A study of CuO films could provide valuable insight into the semi-conducting nature of the same.

In contrast to CuO, cuprous oxide is probably the most investigated copper compound. Due to its unique photoconductive properties, many single crystals of Cu_2O have been grown and characterized.

However, the preparation of thick Cu_2O films, free of CuO, has been complicated by the tendency of Cu_2O to oxidize to CuO above $250^{\circ}C$. An improved technique for obtaining Cu_2O films is needed if thin film rectifiers and photocells composed of Cu_2O and another oxide are to be fabricated and tested.

In view of the potential offered by copper oxide films for solar energy control, this study was undertaken to provide an insight into

the preparation and properties of both CuO and Cu_2O films. This investigation entailed the preparation of CuO films by radio frequency sputtering of the oxide in various argon-oxygen atmospheres. It was believed that a study of the pure undoped oxide would lead to a better understanding of the electrical and optical properties of CuO. A less extensive study of Cu_2O films prepared by chemical reduction of the previously sputtered CuO films was also included.

The overall goal of preparing and characterizing thin films of CuO and Cu_2O was sought by fulfilling the following objectives:

1. To prepare thin films of CuO on glass substrates by radio frequency sputtering.
2. To examine the effects of the deposition variables on the resulting film properties.
3. To observe the effects of nonstoichiometry on the optical and electrical properties of CuO.
4. To evaluate the properties of Cu_2O thin films prepared by a new technique: the reduction of CuO films with carbon monoxide.

II. LITERATURE REVIEW

A. Cupric Oxide

1. Structure. Tunell[6] et al. assigned CuO to the monoclinic system in 1933, and the lattice parameters were later refined by Swanson and Tatge.[7] The coordination in CuO has been identified as fourfold. Each copper atom is surrounded by four oxygens in a square planar array and each oxygen atom is surrounded by four copper atoms at the corners of a nonequilateral tetrahedron.

The other monoxides of the series Mn, Fe, Co, and Ni all crystallize in the cubic NaCl structure where the coordination is octahedral. The ionic radius of Cu^{+2} (0.69Å) is slightly smaller than that of Ni^{+2} and Co^{+2}.[8] Radius ratio rules predict octahedral coordination. The difference in crystal structure may be attributed to a distortion of the octahedral symmetry in which a shortening of the four planar bonds is accompanied by an elongation of the opposite bonds.[9] This distortion may be explained on the basis of 3d orbital splittings[10] but a complete discussion is beyond the scope of this study.

2. Nonstoichiometry. Very little is known about the stoichiometry of CuO below 1000°C except that it is metal deficient. Tretyakov et al.[11] have investigated the degree of nonstoichiometry above 1000°C. Their results showed that the quantity x in CuO_{1+x} could be estimated by

$$x = -5.46 \times 10^{54} \exp\left(\frac{-365{,}000 \pm 20{,}000}{RT}\right) \cdot P_{O_2}^{-2}$$

They have further concluded that the dominant defects at high temperatures are interstitial copper atoms.

3. Electrical Properties. The tendency for CuO to be metal deficient at low temperatures and therefore a p-type semiconductor is somewhat unusual. Generally, if a metal forms several oxides, the oxide containing the lower valent metal ion will be a p-type semiconductor, whereas the oxide containing the higher valent ion will be n-type.[12]

The band gap of CuO has not been precisely determined. Stecker[13] found that the electrical conductivity in the range 700-900°C was independent of the partial pressure of oxygen, indicating intrinsic excitation. The activation energy in this range was estimated at about 2.2 eV. Shapiro[14] determined the band gap of CuO to be 1.44 eV from spectroscopic measurements on powdered specimens.

Models for the conduction mechanism in CuO have traditionally been assumed from data on other transition metal oxides. Verwey[15] first proposed that conduction in NiO or CuO occurred by hole transfer between Ni^{+2} and Ni^{+3} or Cu^{+1} and Cu^{+2} respectively. Later, in 1957, Heikes and Johnston[16] studied the effect of Li substitution on the electrical properties of MnO, CoO, NiO, and CuO using sintered pellets. Their results showed that the room temperature resistivity of CuO could be lowered from 10^8 Ω-cm to about 2 Ω-cm by addition of 2% Li. The activation energy and resistivity were found to increase sharply at the antiferromagnetic Curie point of CuO which occurred at 180°C. Heikes and Johnston[16] concluded that electrical conduction in CuO occurred by the diffusion of self trapped holes (positive holes trapped by lattice distortions induced by cation vacancies) and that

mobility was a thermally activated quantity. This mechanism, they reasoned, was responsible for the low hole mobility and negligible Hall effect in CuO. Young[17] et al. measured the effect of high pressure on the electrical properties of NiO, CoO, CuO, and Cu_2O. Values for mobility calculated from conductivity and Seebeck effect data indicated that hole mobility decreased with increasing pressure. The authors concluded that the hopping mechanism proposed by Heikes and Johnston[16] was correct.

The hopping model was accepted until 1963 when precise Hall measurements on lithium doped NiO single crystals indicated that carrier density increased exponentially with temperature and that mobility increased with increasing lithium content.[18] The hopping model incorrectly predicted that the carrier concentration remained essentially constant and that mobility increased with increasing temperature. Similar work on CuO has not been reported.

Conduction mechanisms such as the hopping model were proposed because simple band theory predicted that materials with unfilled energy levels would show metallic conductivity. Such behavior was not observed in CuO and other related oxides with unfilled 3d orbitals. More recent work concerning the electronic nature of these compounds has been aimed at establishing the position of the 3d energy levels relative to those of the oxygen derived bands. Theories describing both localized and collective behavior of the 3d electrons have been proposed.

Quantum mechanical calculations have predicted the presence of non-overlapping, localized 3d energy levels within the band gap of MnO, CoO, NiO, and CuO.[19] The 3d orbital splittings described by crystal field theory provided a basis for the calculations.

A different picture of the valence band structure of transition metal compounds has resulted from the application of X-ray photoemission spectroscopy (XPS) to the problem. After completing a systematic study of the 3d transition metal oxides, Huffman and Wertheim[20] have concluded that a narrow 3d band lies just above the oxygen 2p band. The low hole mobility in CuO and other oxides could be explained on the basis of a narrow band model which predicts that the effective mass of the carriers is large. However, the XPS studies could not account for the location of the unfilled 3d energy levels since the technique depends upon ejection of excited electrons from occupied levels.

Bhattacharyya and Mukherjee[21] have studied the effects of doping CuO with Li^{+} and Ga^{+3}. Addition of Li^{+} increased the number of holes and therefore increased conductivity. The decrease in conductivity with addition of Ga^{+3} was explained as a decrease in the number of holes.

B. Cuprous Oxide

1. <u>Structure</u>. Cuprous oxide possesses a peculiar crystalline form in which the oxygen atoms form a body centered cubic lattice. Four copper atoms are tetrahedrally coordinated to each oxygen atom. This

structure is also observed in Ag_2O, the only other transition metal oxide containing a stable monovalent cation.[22]

2. Nonstoichiometry. Like CuO, cuprous oxide is metal deficient. The primary defects have been identified as either singly ionized vacancies and holes or neutral copper vacancies.[23]

Above 950°C the quantity x in Cu_2O_{1+x} varies with the oxygen partial pressure raised to the ¼ power.[11] Simple mass action formalism predicts that the concentration of vacancies will be proportional to $P_{O_2}^{1/8}$.[24]

3. Electrical Properties. Cuprous oxide is a p-type semiconductor. Reported values of the band gap range from 1.69[14] to 2.67 eV.[25].

Brattain[26] reviewed the work on electrical properties of Cu_2O published before 1951. The reported room temperature hole concentrations and mobilities ranged from 10^{12} - $10^{14}/cm^3$ and 20 to 100 cm^2/volt·sec, respectively. In the same publication a band scheme for the Cu-Cu_2O rectifier was developed.

The high hole mobility in Cu_2O could not be explained by earlier workers through observation of electrical properties alone. Since high electron mobilities, observed in both ZnO[27] and CdO[28], had been explained on the basis of a "wide band" semiconductor model, the same term was used to describe Cu_2O. However, both ZnO and CdO were n-type semiconductors and the high carrier mobility was easily explained as the motion of weakly bound electrons in a wide conduction band. A simple model for hole transport in a wide valence band was not

proposed. Huffner and Wertheim[29] concluded from XPS investigations that the full Cu 3d and O 2p bands overlapped, thus forming a wide valence band. Holes, created in the valence band, would possess a low effective mass and therefore a high mobility.

Toth et al.[30] observed that the conductivity of Cu_2O above 750°C was proportional to $P_{O_2}^{1/n}$ where n ranged from 7 to 8. This result agreed with that predicted from the dependence of hole concentration on oxygen partial pressure.

The conduction mechanism in Cu_2O crystals has been investigated by Kuzel and Weichman.[31] Differences in activation energy for conduction were observed for bulk (0.3 eV) and surface (0.1 eV < E_a < 0.3 eV) conductivity. Changes in the activation energy between 100 and 200°C were attributed to ionization of copper vacancies. Derry et al.[32] have measured the conductivity of Cu_2O films between 20° and 200°C. Values for the activation energy in oxygen and in a vacuum were reported as 0.29 and 0.33 eV respectively. Smith and Wieder[33] investigated the relation between oxygen uptake and conductance of oxidized and reduced Cu_2O films.

C. Copper Oxide Thin Films

The preparation of copper oxide thin films on glass by oxidation of evaporated copper films has been studied by Wieder and Czanderna.[34,35] Using a vacuum microbalance technique they were able to isolate CuO and Cu_2O films. A metastable oxide phase of composition $CuO_{0.67}$ was identified and postulated to be a "gross defect form" of

Cu_2O.[35] The authors indicated that the above composition corresponded to Cu_2O with one copper ion vacancy per unit cell, on the average. Although the optical properties of these films were investigated, no electrical measurements were reported.

Cupric oxide films have been obtained by the pyrolytic decomposition of cupric nitrate[3] and cupric acetate[36] solutions. The latter method required high decomposition temperatures due to the formation of stable intermediates.

Reactive d.c. sputtering has been employed by Perny[37] to prepare films of CuO and Cu_2O. Generally, films consisting of mixtures of CuO as the minor phase and Cu_2O as the major phase were obtained. A refinement of this technique[38] led to the development of a sputtering "phase diagram" based on the oxygen content of the sputtering atmosphere and a quantity termed the reduced field given by

$$E^* = \frac{\text{Cathode Voltage}}{\text{Cathode Anode Spacing x Pressure}}$$

The relationship between the reduced field, oxygen content of the sputtering atmosphere, and the resulting film composition is illustrated in Figure 1. It is interesting to note that all three phases of the Cu-O system may be obtained regardless of the oxygen content of the gas by selecting the proper reduced field. Perny did not characterize the films as to their electrical and optical properties.

Sachse and Nichols[39] utilized triode sputtering to directly sputter CuO in atmospheres of varying oxygen content. Table I lists the compositions of the films they obtained. The oxygen partial

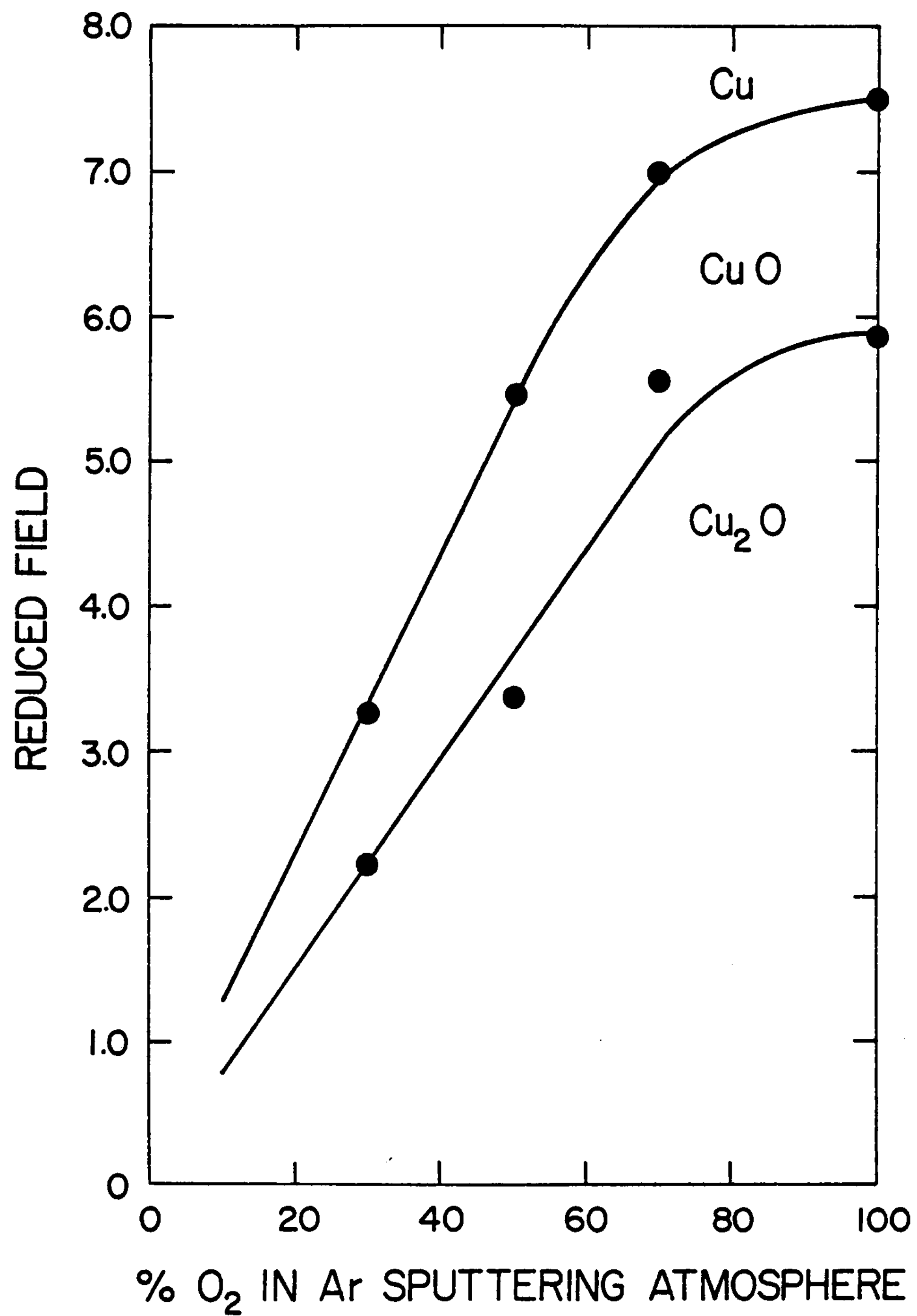

Figure 1. Sputtering "Phase Diagram" for Cu-O System (after Perny[38]).

TABLE I

Film Composition as Function of the O_2 Partial Pressure in a Plasma

Oxygen Metal Ratio in Target	O_2 Partial Pressure in Plasma μ Torr	Film Composition	Film Thickness (Å)	Deposition Rate Å/h
O/Cu		O/Cu ratio		
1.00	<< 1	0.125	1820	225
	3	0.98	3660	407
	8	0.98	4300	268
	23	0.99	2280	143
	23	1.00	2950	185
	160	1.00	1030	147

(After Sachse and Nichols[39])

pressure for the sputterings in pure argon was assumed to be less than 1μ torr. The data indicated that CuO undergoes severe dissociation when sputtered in pure argon.

D. Radio Frequency Sputtering of Oxides

Although CuO films may be obtained by various methods, radio frequency sputtering was chosen as the mode of preparation for this study. Radio frequency sputtering has proven to be a valuable deposition technique in that both conducting and insulating materials may be deposited. Precise control over film thickness, uniformity, stoichiometry, and crystallinity is possible through careful maintainence of the deposition parameters.

1. Sputtering Principles. The sputtering process depends upon the bombardment of a target material by positive ions, usually Ar^{+}. The ions are obtained by the application of a high potential between two parallel plates separated by a small distance. As long as the applied potential exceeds the ionization energy of the gas, a self contained glow discharge, or plasma, will form.[40]

In conventional d.c. sputtering systems, the target acts as the cathode and consequently must be a good electrical conductor. High energy positive ions are continuously accelerated towards the target where a negative charge is maintained. Ions with enough kinetic energy to exceed the binding energy of the target atoms eject material from the target. The nature of the sputtered material is complex. Neutral atoms, ions, or polyatomic species may be ejected.

An insulator, if placed in such a system, would allow a sheath of positive ions to form at its surface, thus preventing further bombardment. This difficulty is overcome by the application of a time varying potential to a metal plate behind the target such that another time varying potential develops at the target face. During the positive half cycle, the electrons, by virtue of their small mass, flow rapidly from the plasma to the target surface. A net negative charge results and is responsible for attracting the heavier positive ions. The intensity of the ion bonbardment increases during the negative half cycle due to the increased negative charge at the target. This "self biasing" action was first explained by Wehner in 1955.[42]

2. R. F. Sputtering Variables. Control of the deposition rate is perhaps the most important aspect of the sputtering process. It effects such properties as crystallinity, uniformity, and adhesion. The rate of film growth is heavily influenced by the following factors:

a. nature of the gas
b. gas pressure
c. r.f. power
d. target to substrate distance.

Figure 2 illustrates the dependence of the deposition rate of SiO_2, as presented by Vossen and O'Neill,[41] upon the above parameters. No data of this type is available for CuO. The area of the target is important in determining the uniformity of the film. Vossen and O'Neill[41] report that the radius of uniformity of the film is approximately 0.5 inch less than the radius of the target.

Using a liquid nitrogen cooled substrate holder, Frey[43] studied the effect of substrate temperature on structure, density, and

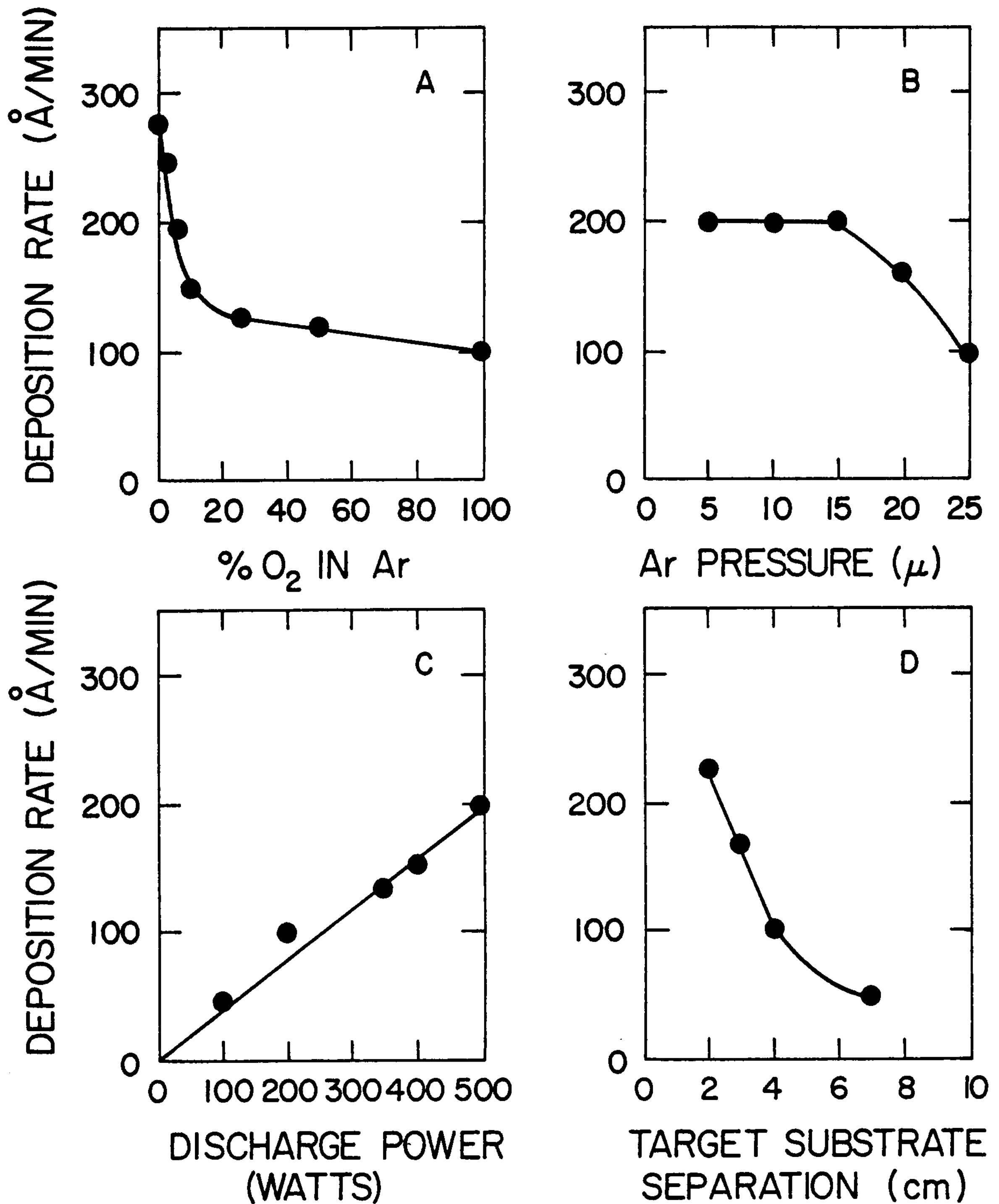

Figure 2. Effect of sputtering variables on deposition rate of SiO_2 (after Vossen and O'Neill[41]).

stoichiometry of r.f. sputtered NiO films. Decreasing crystallinity was observed for decreasing substrate temperature and completely amorphous films resulted below -100°C. The effect of substrate temperature on NiO film density and stoichiometry are shown in Figure 3.

The high energy required for r.f. sputtering makes dissociation of some materials inevitable. Frey[43] observed that NiO dissociated into nickel metal when sputtered in pure Ar. Films sputtered from pure Co_3O_4 targets have exhibited CoO diffraction peaks indicating partial dissociation.[44]

Vossen and O'Neill[41] have compiled a table of oxide materials based upon their heats of dissociation. Since the dissociation energy of NiO (58.4 kcal/mole) is greater than that of CuO (37.6 kcal/mole), some dissociation of CuO is also expected.

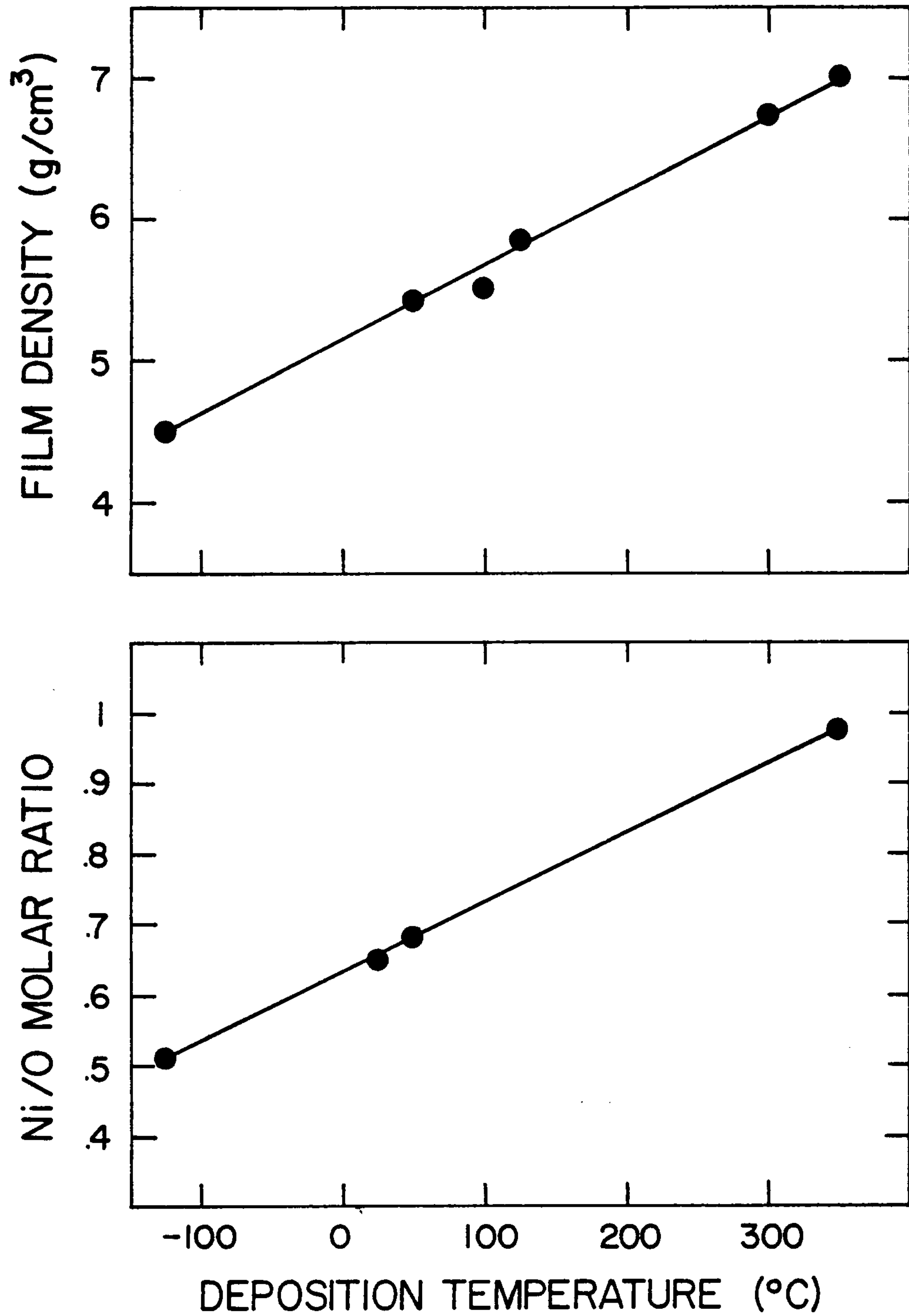

Figure 3. Effect of substrate temperature on NiO film density and stoichiometry (after Frey[43]).

III. EXPERIMENTAL PROCEDURE

A. Film Preparation

1. R. F. Sputtering.

a. Apparatus. An R. D. Mathis* Mk III r.f. generator and sputtering module was used to prepare the CuO films. Deposition was carried out inside a 9 inch by 9 inch Pyrex pipe which contained a 3.375 inch water cooled cathode and an 8 inch diameter water cooled substrate pedestal which also served as the anode. The target assembly was attached to the cathode by means of three small screws. The cathode shield, which prevented sputtering of the backing plate, exposed only the target face.

Evacuation of the deposition chamber was carried out by an oil sealed roughing pump,** for achieving the forevacuum, and a 4 inch diameter oil diffusion pump.*** Pressure was monitored by means of Pirani+ and discharge type++ vacuum gauges. Figure 4 schematically represents the sputtering apparatus.

b. Sputtering Targets. Since the CuO films used in this study were obtained by r.f. sputtering the oxide itself, a reasonably

---

*R. D. Mathis Corp., Long Beach, California.

**Model 1397, Welch Scientific Co., Skokie, Ill.

***Type BLN-60, Consolidated Electrodynamics Corp., Rochester, N.Y.

+Type GP 140, Consolidated Electrodynamics Corp., Rochester, N.Y.

++Type GPH-100A, Consolidated Electrodynamics Corp., Rochester, N.Y.

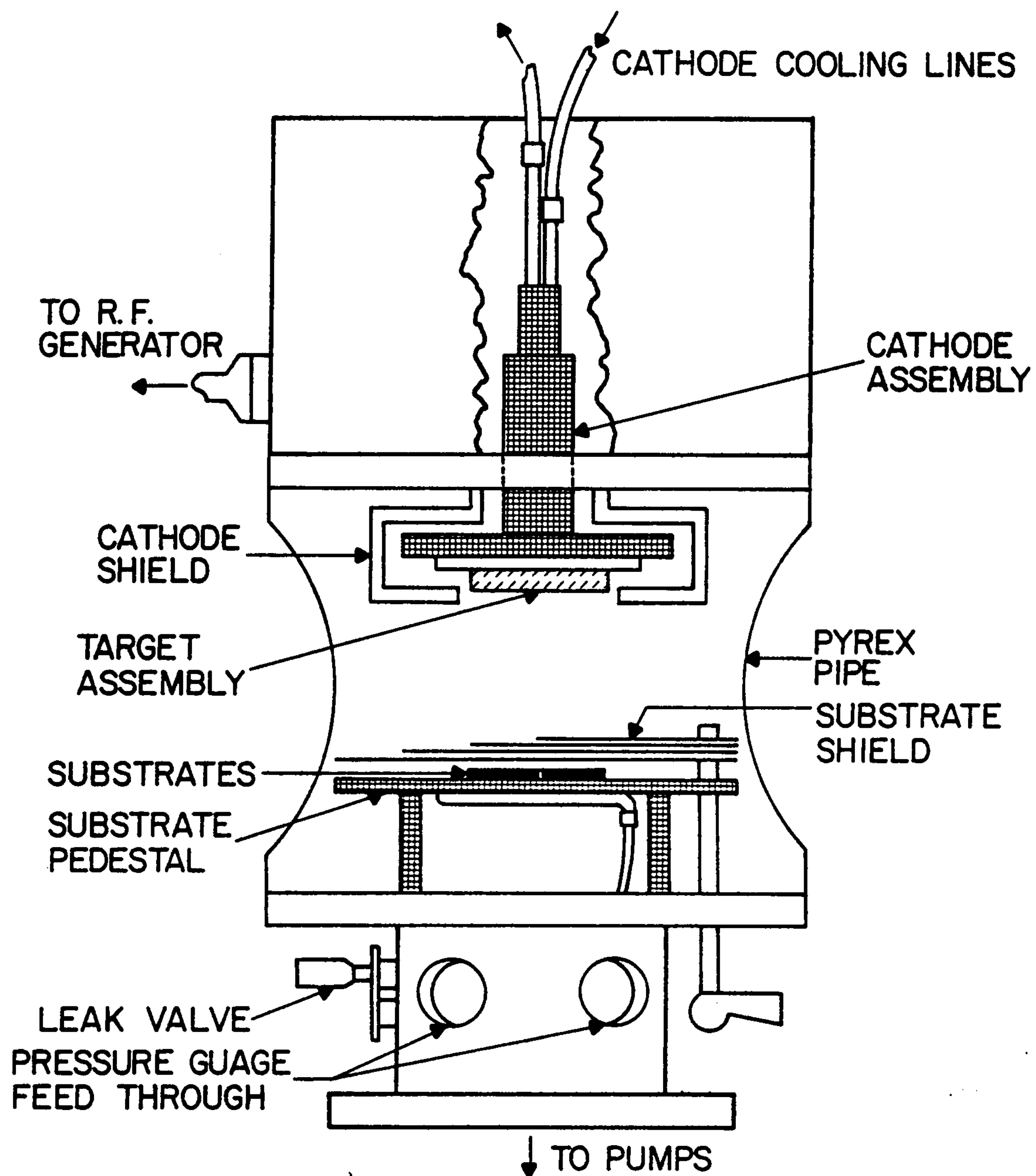

Figure 4. Schematic diagram of the radio frequency sputtering apparatus.

dense sintered target was necessary. Cupric oxide powder* was hot pressed** in a two inch diameter graphite die for three hours at 500°C and 3000 psi. After removal from the die, the target was sintered for 12 hours at 900°C. The resulting disk was approximately 1.75 inches in diameter by 0.25 inch thick and roughly 70% of its theoretical density. The compact was then cemented to a 3.375 inch diameter by 0.25 inch thick aluminum backing plate with a conducting silver filled epoxy.***

Iron, nickel, and molybdenum targets were fabricated from high purity sheets,+, 3.375 inches in diameter by 0.005 inch thick, and fastened to aluminum backing plates with small screws. Small tabs of metal were folded over the screws to prevent sputtering of the screw heads.

c. Substrates. Corning #7059++ glass slides were used exclusively as substrates for this study. This glass contained no alkali or iron which could affect electrical and optical measurements. The standard substrate for electrical and optical experiments was 1.0 inch by 1.5 inches by 0.05 inches. Additional substrates for Ni/Fe thin film thermocouples and SEM specimens were obtained by cutting

---

*Fisher Certified Reagent, Fisher Scientific Company, Pittsburgh, PA.

**Model RH 1512, Alfred Ceramic Enterprises, Inc., Alfred, N.Y.

***Transene Company, Inc., Rowley, Mass.

+Alfa Products, Beverly, Mass.

++Corning Glass Works, Danville, VA.

the larger slides into 1.0 inch by 0.25 inch and 0.25 inch square pieces on a diamond saw.

d. Thin Film Thermocouples. As mentioned earlier, deposition temperature plays an important role in determining film density and structure. Although the substrate temperature was not varied in this research, a knowledge of this quantity might prove useful in explaining film behavior. The preparation and use of Ni/Fe thin film thermocouples for substrate temperature determination has been previously described by Morrison and Lachenmayer,[45] Marshall et al.,[46] and Frey.[43]

Alternate layers of iron and nickel, each roughly 3000Å thick, were sputtered on to the substrates cut for this purpose. Opposite ends of the substrate were masked during deposition to provide contact areas of pure Ni and Fe. One batch of 20 thermocouples was prepared in this manner and a representative sample calibrated to 300°C in air inside a tube furnace. The calibration curve, which agrees well with literature data, is shown in Figure 5.

Contact was made to the thermocouples inside the deposition chamber with small Ni and Fe plates welded to the respective wires. The wires and contact plates were protected from the discharge by mullite thermocouple tubing. The wires were run through a compressed rubber stopper situated in one of the feedthrough ports at the base of the sputtering module. Thermal emf measurements were made with a millivolt potentiometer equipped with an internal temperature compensator.*

---

*Model 8690, Leeds and Northrup Co., Philadelphia, PA.

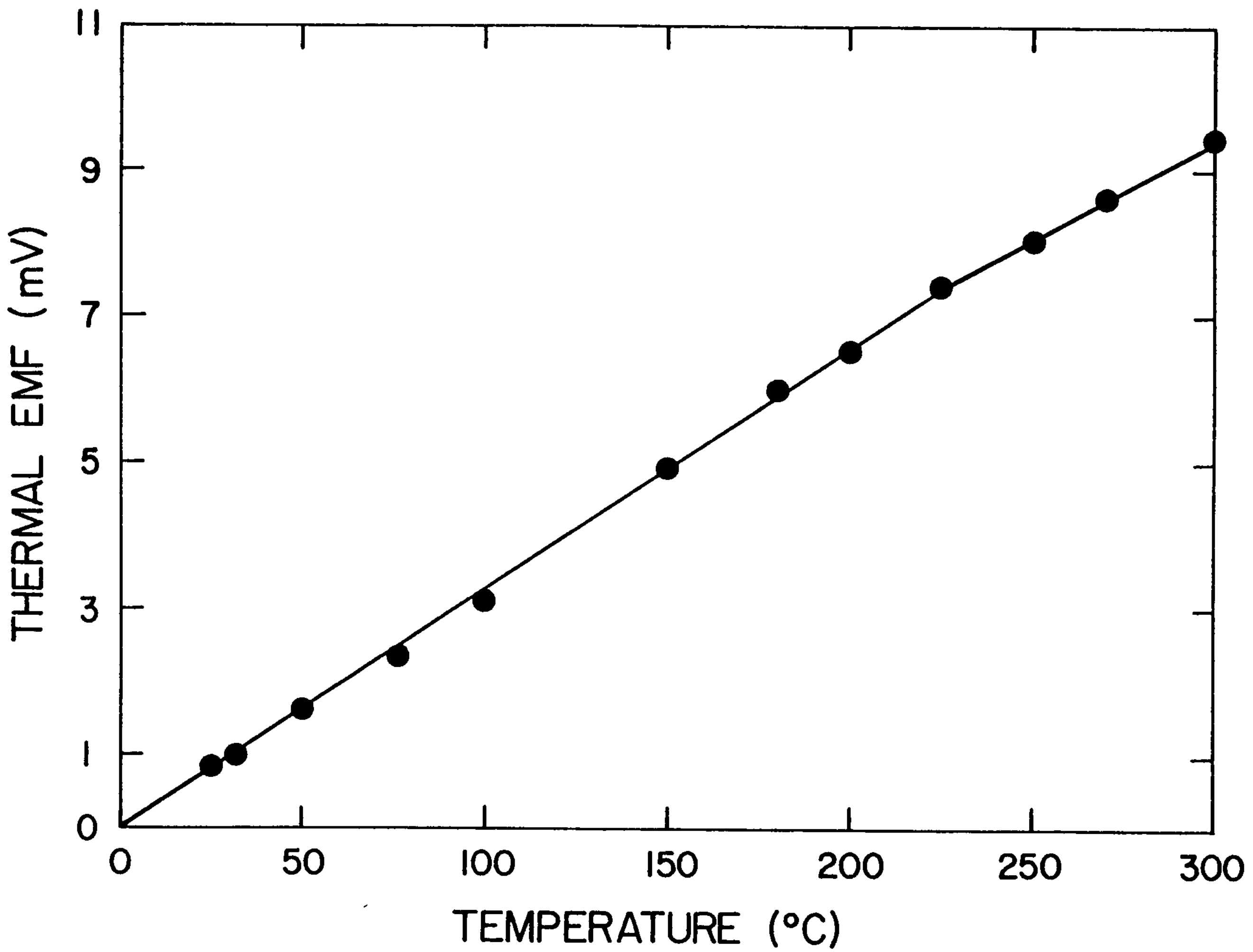

Figure 5. Calibration Curve for the nickel/iron thin film thermocouples.

e. <u>Sputtering Atmospheres</u>. Pure Ar, 90% Ar-10% O_2, and 50% Ar-50% O_2 atmospheres were employed to provide CuO films of varying oxygen content. The 90% Ar-10% O_2 gas was a commercially* prepared mixture. The 50% Ar-50% O_2 atmosphere was obtained by carefully mixing pure Ar and O_2 with the aid of flowmeters prior to admittance to the sputtering chamber. The possibility of ruining the pump oils prevented the use of higher oxygen containing atmospheres.

f. <u>Sputtering Procedure</u>. Prior to sputtering, the substrates were cleaned of dirt and grease by simply wiping with acetone or, in more severe cases, an ultrasonic treatment. A stream of dry nitrogen was used to blow the substrates free of dust immediately before they were placed in the deposition chamber. The large slides were partially masked at one end by a 22 mm square by 0.12 mm thick glass coverslip which provided a step for subsequent film thickness measurements. The small SEM substrate was placed on top of the coverslip where it also prevented the mask from moving during deposition. Once the substrates were in place, the substrate shield was drawn across them and the deposition chamber sealed. At this point, the system was evacuated until a pressure less than 10^{-5} torr was achieved.

After the desired vacuum had been obtained, the sputtering gas was admitted through the leak valve in the base of the module. After the pressure had stabilized, a discharge was started by slowly

---

*Airco Company, Inc., Riverton, N.J.

increasing the current to the cathode. Sputtering was allowed to continue on the substrate shield for 15 minutes. During this time the pressure and plasma stabilized and "matching" or minimization of reflected power was carried out by carefully adjusting the controls on the module.

As soon as the system had stabilized, the shield was drawn back and a timer was started. During the deposition process, pressure was closely monitored to prevent unwanted pressure surges and drops. At the end of a run the shield was pulled back across the substrates and the discharge terminated. The substrates were allowed to cool inside the chamber for at least 30 minutes before removal.

To simplify the sputtering experiments, the gas pressure, sputtering power, and substrate-target separation were kept constant throughout this study. Film thickness was varied solely through the use of different sputtering times. Table II lists the sputtering parameters used in obtaining the CuO films. Slight changes in the settings resulted from the use of different atmospheres.

2. Annealing Experiments

a. Air. The effect of annealing in air on film resistivity and structure was studied. The films were treated in a small muffle furnace* at a constant temperature of 300°C. Room temperature resistivity measurements of each specimen were recorded at intervals

---

*Model M10A-1A, Blue M Electric Co., Blue Island, Ill.

TABLE II

R. F. Sputtering Parameters for CuO Deposition

Atmosphere	Pressure (μ)	Target Substrate Separation (cm)	Plate Current (Amps)	D.C. Voltage (Volts)	R.F. Power (Watts)	Sputtering Time (min)
100% Ar	10	10	0.170	3000	200	60,240
90% Ar-10% O_2	10	10	0.170	3000	200	60,120,240
50% Ar-50% O_2	10	10	0.170	280	200	60,240

of 0, 1, 2, 5, 10, 50, and 100 hours. X-ray diffraction patterns were recorded at intervals of 0, 1, 10, and 100 hours.

b. Reducing Atmospheres. Syphon grade CO_2 and pure CO were used to reduce the CuO films to Cu_2O. The desired reducing atmosphere was obtained by metering CO_2 and CO flow similar to the procedure described earlier for mixing the sputtering atmospheres.

A tube furnace* equipped with a 4 foot length of 1.5 inch diameter Pyrex tubing was used to prepare the Cu_2O films. A 6.0 inch length of 1.0 inch diameter mullite tubing made a convenient "boat" in which to mount the CuO films.

The boat, loaded with 1 to 3 films, was pushed into the center of the tube with a metal rod. The furnace was immediately sealed and the contents allowed to heat up under a flow of CO_2 at 250 ml/min. After 15 minutes the CO_2 flow rate was lowered to 95 ml/min and the CO flow set at 5 ml/min. After 30 minutes the CO flow was discontinued and the boat was drawn to the cool end of the furnace with a Ta wire which passed through the wall of the tygon tubing supplying the gas flow. The specimens were allowed to cool under a CO_2 flow of 25 ml/min. for 45 minutes before they were removed from the furnace.

The optimum combination of gas composition, flow rate, reducing time, and temperature were determined by a trial and error process. A review of the thermodynamics of the reduction pointed out that control of the CO_2/CO ratio to prevent the formation of Cu metal was

---

*Type G-02720-T, Hevi Duty Electric Co., Milwaukee, WI.

impractical. The analysis is presented in the appendix. Since the reduction of CuO to Cu is a stepwise process, involving the formation of Cu_2O as an intermediate, the desired oxide was obtained by controlling the reaction time.

3. Electrode Fabrication. During the course of this research difficulties in selecting metal electrode materials became evident. Problems with adhesion, chemical stability, and mechanical strength were encountered.

Figure 6 illustrates the type of sample used for resistivity measurements. Four strips or "islands" were deposited on top of a previously prepared copper oxide film through a special mask. Initially, evaporated* aluminum was used because of its ease of deposition and low cost. However, aluminum tended to diffuse into the film at temperatures as low as 200°C. Despite its excellent adherence, the aluminum was very easily scratched.

Sputtered molybdenum was examined and showed great promise due to its adherence and durability. Unfortunately, Mo oxidized rapidly at temperatures as low as 300°C.

Evaporated gold films were highly stable above 300°C and did not react with film components or oxidize. The chief disadvantages of gold were its high cost and very poor adhesion to the film surface.

The bulk of the electronic measurements in this study were made using Mo electrodes. Specimens used in the annealing experiments

---

*Type CVE-20, Consolidated Vacuum Corp., Rochester, N.Y.

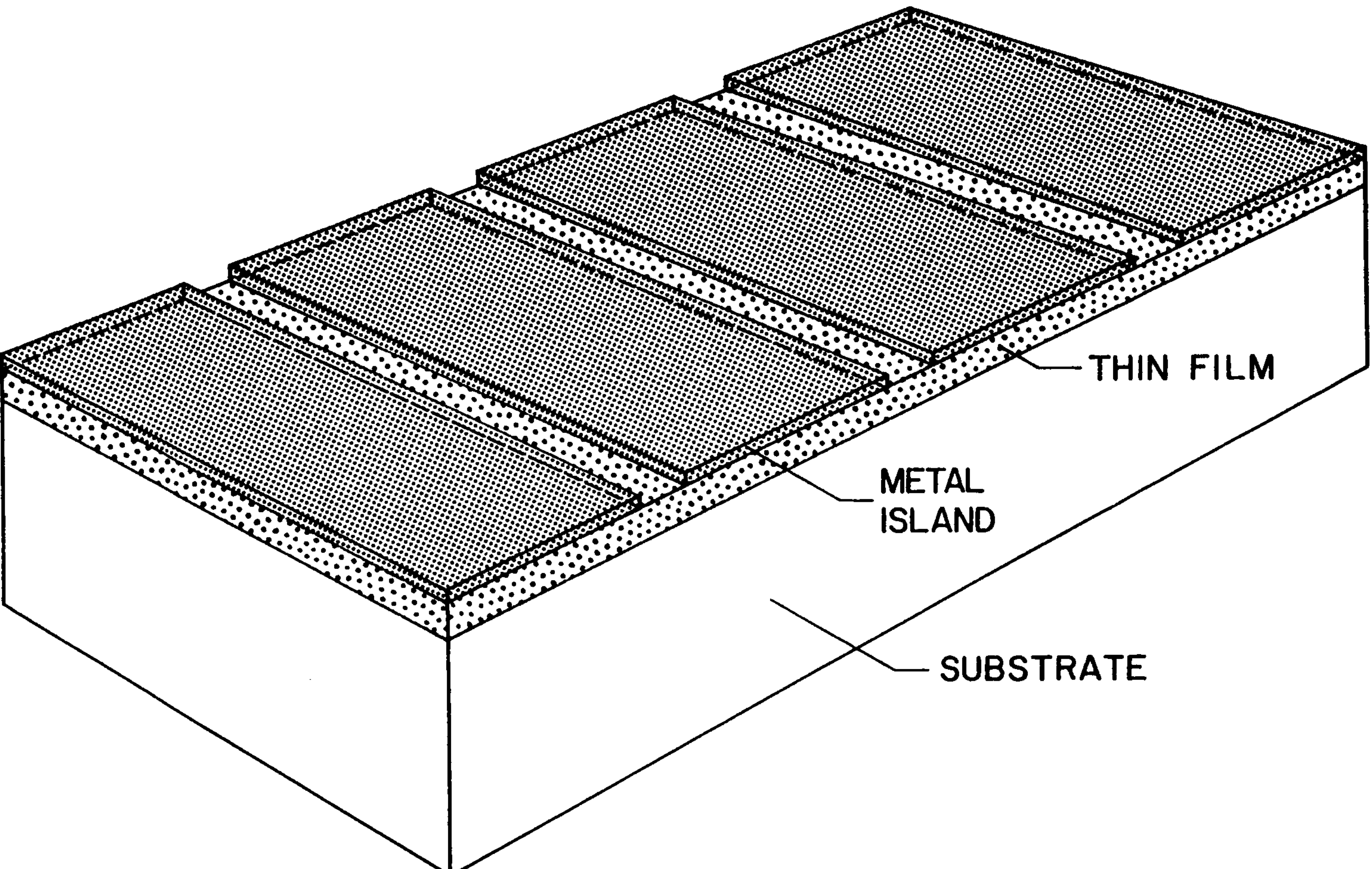

Figure 6. Resistivity specimen.

were coated with gold. In each case the electrode thickness was calculated to be 1000 Å.

B. Film Characterization

1. X-Ray Diffraction. The effects of sputtering, annealing, and reducing on film structure and chemistry were investigated by X-ray diffraction. Peak widths were examined for evidence of grain growth during annealing. Films consisting of very fine grains generally show broad diffraction peaks which become narrower as the grains increase in size.

A Norelco diffractometer operating at 40 kV and 15 ma was used to scan each specimen over a constant 2θ range of 20° to 60°. The range, time constant, and scan speed were kept constant at 100 cps, 2, and 1° 2θ per minute respectively.

2. SEM-EDAX. The surface morphology of the sputtered films was observed with the aid of a scanning electron microscope.* The specimen was irradiated with a focused electron beam which released secondary electrons, backscattered electrons, and characteristic X-rays. Photographs of the film surfaces were obtained from secondary electron images.

Possible chemical contamination of the films was investigated with an Energy Dispersive Analysis of X-Rays (EDAX) attachment. Characteristic X-ray emission spectra, generated by the ejection of core electrons from their parent atoms, were recorded and photographed

---

*AR 900, Burlington, Mass.

on a cathode ray display tube. The chemical composition of the glass substrates was also studied in this manner.

3. Film Thickness Determination. As previously described, a small area at the end of each substrate used for electrical measurements was masked during CuO deposition. The size of the masked area was approximately 22 mm long and 3 mm wide. Subsequent electrode deposition created a reflective step which permitted the determination of film thickness by interferometry.

Thickness measurements were carried out on a Varian Å-Scope multiple beam interferometer.* The instrument employed a sodium vapor lamp with a wavelength of 5892 Å. The monochromatic radiation, after reflecting off the film surface, passed through a small air wedge and was transmitted to a special eyepiece. The spacing of the interference fringes, produced in the air wedge, was measured in arbitrary units with the aid of a movable hairline controlled by a graduated knob. Light reflected from the area of the step formed interference fringes that were offset an amount proportional to the height of the surface variation. The fringe offset was also measured with the hairline. Film thickness (t) was calculated from the following relation.

$$t = \frac{\text{fringe offset}}{\text{fringe spacing}} \times 2946 \text{ Å}$$

Since the fringe spacing is always equal to $\lambda/2$ [47], the quantity

---

*Varian Associates, Palo Alto, California.

(2946 Å/fringe spacing) is actually a proportionality constant relating the observed offset to the actual film thickness.

Three thickness measurements were made at different points along the step. These values were averaged and rounded to the nearest 100 Å. The accuracy of the instrument, as reported by the manufacturer, is $\pm$ 30Å.

4. Electrical Measurements.

a. Resistivity. Measurement of semiconductor resistivity is generally performed by a four point probe technique.[48] In this study, a modification[44] of the four point probe method was used to determine film resistivity.

Electrical leads were attached, by means of small alligator clips, to the four metal islands on the resistivity specimen shown in Figure 6. A constant current (I), obtained from a power supply,* was passed through the outer contacts on the specimen. A sensitive multimeter**, with a range of 10^{-9} to 10^{-1} amps, was employed to measure the current. The high resistance of the films limited the maximum current to about 10^{-4} amps. The voltage drop (ΔV) across the gap between the two inner electrodes was measured with a digital voltmeter*** sensitive to 10^{-3} volts.

---

*Model 865C, Harrison Laboratories.

**Model 153, Keithley Instruments, Inc., Cleveland, Ohio.

***Model 160B, Keithley Instruments, Inc., Cleveland, Ohio.

The resistance (R) of the film was calculated from Ohm's Law:

$$R(\Omega) = \Delta V/I$$

Sheet resistance ($R_{\square}$), the resistance of any size square of material, was determined by multiplying R by the film width (2.54 cm) and dividing by the gap width (0.15 cm), such that

$$R_{\square} = \frac{\Delta V}{I}\,\frac{(2.54\ \text{cm})}{(0.15\ \text{cm})}$$

Sheet resistance is commonly expressed as Ω/square. The product of sheet resistance and film thickness (t) yielded the resistivity (ρ) of the specimen in Ω-cm as shown below.

$$\rho(\Omega\text{-cm}) = \frac{\Delta V}{I}\left(\frac{2.54}{0.15}\right) t$$

b. Activation Energy. The dependence of film resistivity on temperature was determined using the same technique described in the preceeding section. The specimen was enclosed in a controlled temperature chamber* in which temperature gradients were limited to $\pm$ 1°C. Film temperature was measured by means of a chromel alumel thermocouple in contact with the bottom surface of the specimen.

Resistivity is related to the absolute temperature by an Arrhenius relation,

where $\rho = C \exp(Ea/kT)$

E_a = activation energy in eV

k = Boltzmann constant = 8.6×10^{-5} eV/°K

(Model MK 2300, Delta Design, Inc., La Mesa, California.

T = temperature (^oK)

C = a constant.

By taking logarithms of the above relation and differentiating with respect to 1/T, the following expression is obtained.

$$\frac{d \log_e \rho}{d\ 1/T} = \frac{E_a}{k}$$

Thus, the slope of the $\log_e \rho$ vs. 1/T relationship yields the activation energy.

The similarity in activation energy for a group of specimens prepared under the same conditions was taken as a measure of reproducibility. Activation energies for the sputtered and reduced films were determined in air between 25° and 200°C.

c. Charge Carrier Type. The sign of the charge carriers in the CuO and Cu_2O films was determined by taking advantage of their thermoelectric properties. Two probes connected to a sensitive voltmeter were placed on the film surface. The positive probe was heated with a soldering iron.

Charge carriers move away from the hot probe in an attempt to conduct heat. If the sample is n-type, the observed voltage is positive since the negative carriers will migrate to the negative probe. If the sample is p-type, positive carriers migrate to the negative probe and the observed voltage is negative.[50].

d. <u>Optical Properties</u>. The dependence of film absorbance on wavelength was observed on a Cary 14* recording spectrophotometer. Since the bulk of the sun's energy reaching the earth is concentrated between 0.3μ and 2.5μ, this wavelength region was examined. The optical data was calculated and plotted using a computer program developed by Viverito.[(1)]

---

*Cary 14, Varian, Inc., New York, N.Y.

IV. RESULTS

A. Effects of Deposition Variables

Increasing the oxygen content of the sputtering atmosphere decreased the deposition rate in a linear fashion as shown in Figure 7. The scatter in the data can be attributed to both gas pressure and discharge power fluctuations which occurred during some of the depositions, as well as errors in film thickness measurement. In spite of the latter possibility, film uniformity appeared to be excellent. The three film thickness measurements performed on each specimen rarely deviated more than $\pm$ 5% from their average value.

Through utilization of the Ni/Fe thin film thermocouples, substrate temperature was found to range between 110 and 130°C regardless of the sputtering atmosphere employed. No correlation with either deposition rate or oxygen content could be found. The effects of substrate temperature on CuO film properties will be reviewed in the Discussion section.

Adhesion of the sputtered films to the glass substrates was excellent. No problems with peeling or cracking were encountered.

B. X-Ray Analysis

The diffraction data, between 20° and 60° 2θ, for some of the films prepared during this study are listed in Table III. Films are listed according to their method of preparation. Data for the CuO target material as well as that listed for Cu, Cu_2O, and CuO in the Powder Diffraction File[50] is also included for comparison.

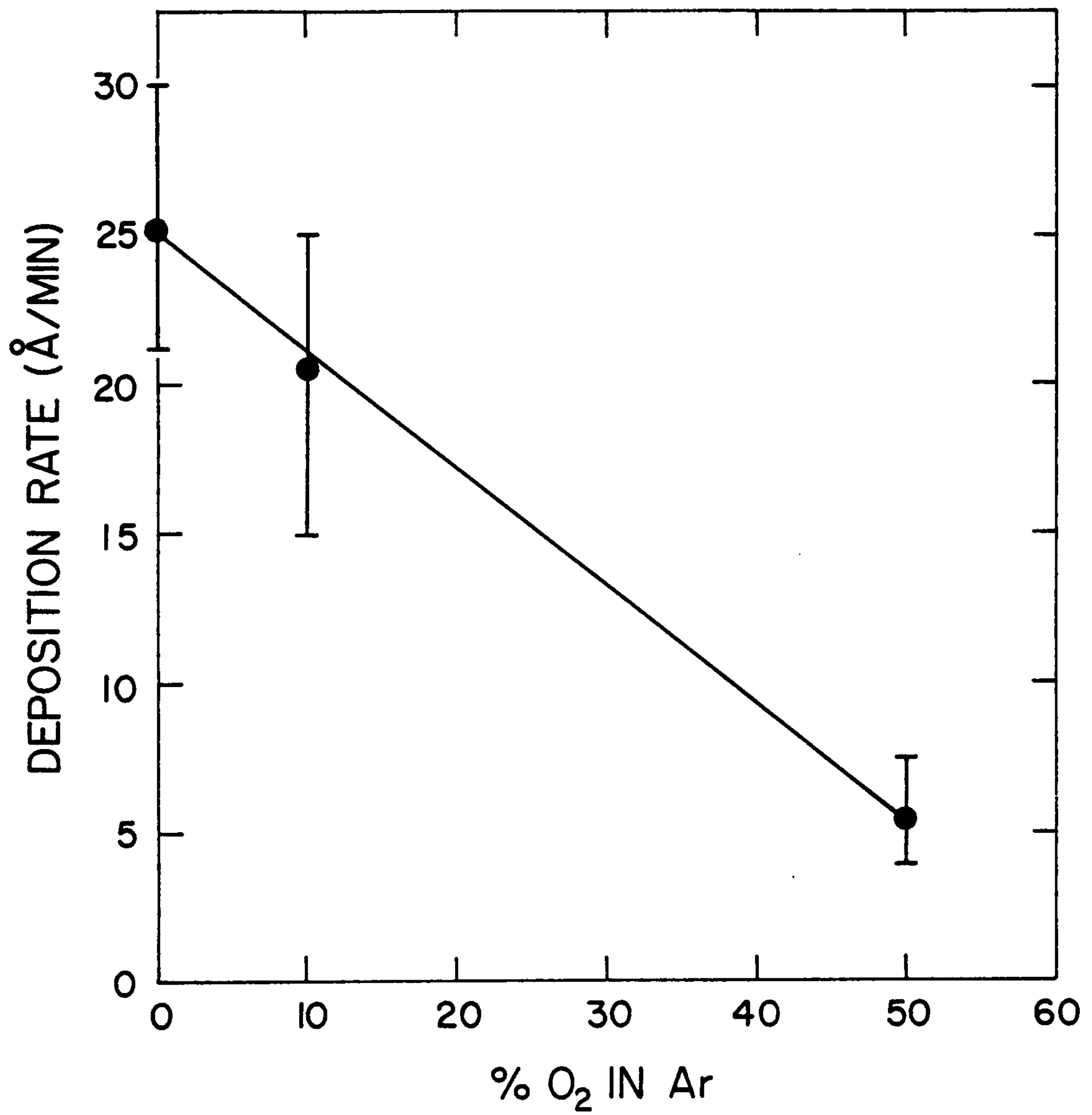

Figure 7. Dependence of the CuO deposition rate on the percent O_2 in the sputtering atmosphere.

Table III

X-Ray Diffraction Data

	Film No.	$2\theta^{o}$(Obs)	d(Å)	I/I_o	hkl
	Target Material CuO Powder	32.50	2.755	20	110
		35.50	2.529	100	002,$\bar{1}11$
		38.70	2.327	92	111,200
		46.20	1.965	6	$\bar{1}12$
		48.50	1.877	54	$\bar{2}02$
		53.30	1.719	15	020
		58.10	1.588	23	202
Films Sputtered in 100% Ar	24	35.50	2.529	10	002,$\bar{1}11$
		36.50	2.462	45	111(Cu_2O)
		38.30	2.350	100	111,200
		42.80		5	200(Cu_2O)
	26 Before Annealing	35.40	2.535	20	002,$\bar{1}11$
		36.10	2.488	100	111(Cu_2O)
		38.40	2.344	50	111,200
	After Annealing	35.40	2.535	40	002,$\bar{1}11$
		38.50	2.338	100	111,200
Films Sputtered in 90% Ar - 10% O_2	15 & 29	38.25	2.353	100	111,200
	9 Before Annealing	37.70	2.386	100	111,200
	After Annealing	38.50	2.338	100	111,200
		53.50	1.713	5	020
Films Sputtered in 50% Ar - 50% O_2	21	35.25	2.546	10	$\bar{1}11$,002
		38.40	2.535	100	111,200
	12 Before Annealing	38.25	2.353	100	111,200
	After Annealing	38.50	2.338	100	111,200
Reduced Films	33R	36.20	2.481	100	111(Cu_2O)
		42.00	2.151	40	200(Cu_2O)
	31R	43.0	2.103	100	111(Cu)
		50.25	1.816	30	200(Cu)

Table III(continued)

	Card No.	2θ°(Obs)	d(Å)	I/I_o	hkl
Powder Diffraction File	CuO 5-0661	32.52	2.751	12	110
		35.48	2.530	49	002
		35.58	2.523	100	$\bar{1}11$
		38.76	2.323	96	111
		38.95	2.312	30	200
		46.35	1.959	3	$\bar{1}12$
		48.80	1.866	25	$\bar{2}02$
		51.39	1.778	2	112
		53.46	1.714	8	020
		58.36	1.581	14	202
	Cu_2O 5-0667	29.58	3.020	9	110
		36.45	2.465	100	111
		42.33	2.135	37	200
		52.50	1.743	1	211
	Cu 4-0836	43.33	2.088	100	111
		50.48	1.808	46	200

1. <u>Sputtered Films</u>. X-ray diffraction data revealed that the oxygen content of the sputtering atmosphere had an important effect on film composition and structure. Partial dissociation of CuO to a mixture of CuO and Cu_2O was observed in all films sputtered in pure argon. No evidence of elemental copper was observed. The diffraction pattern of such a film is shown in Figure 8. Thinner films displayed similar peaks but of much lower intensity. The (200) peak of Cu_2O was not present in all these films, however, and the relative intensities of the CuO (111) and Cu_2O (111) peaks varied considerably.

The diffraction patterns of films deposited by sputtering CuO in 10% and 50% O_2 are shown in Figures 9 and 10 respectively. No peaks corresponding to Cu_2O or Cu were found in any of these specimens. Only one major peak, attributable to the overlap of the (111) and (200) reflections, appeared in these diffraction patterns at approximately 38.3^{o} 2θ. An additional peak of very low intensity, corresponding to the $(\bar{1}11)$-(002) overlap, appeared in the patterns of a few films sputtered in 50% O_2.

The presence of only one peak in the diffraction patterns of films sputtered in 10% O_2 suggested that preferred orientation might exist in these films. Since the (111) and (200) planes in CuO possess very similar d-spacings, the resulting peak is actually an overlap of two reflections. Slow scan diffraction patterns ($\frac{1}{4}^{o}$ 2θ/min) were recorded between 36° and 40° 2θ and the broad peak examined for the presence of a doublet or shoulder. No evidence for two peaks was found in this manner. Diffraction angles between 60° and 90° were

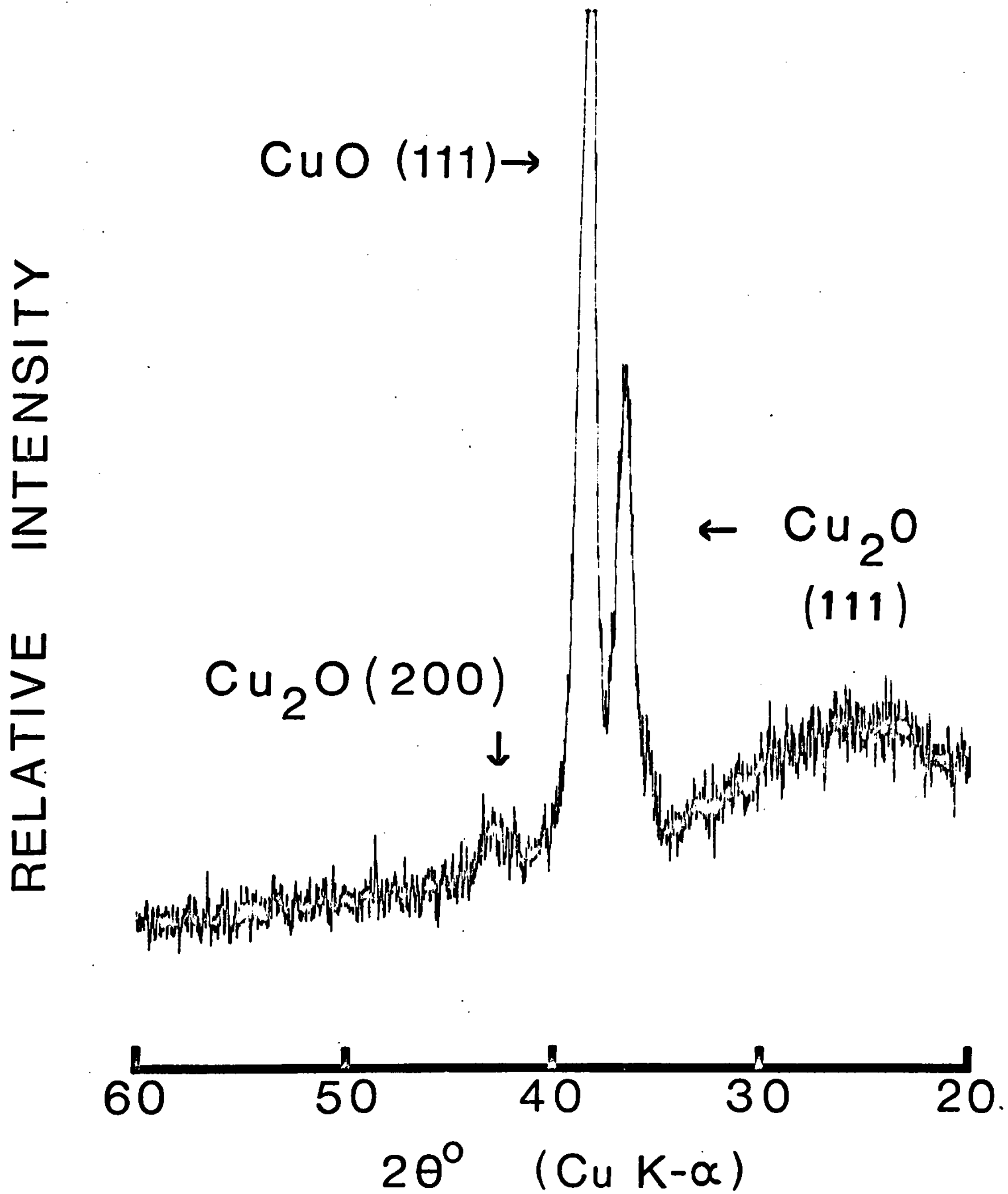

Figure 8. X-Ray diffraction pattern of Film 24 (5100Å thick) sputtered in 100% Ar.

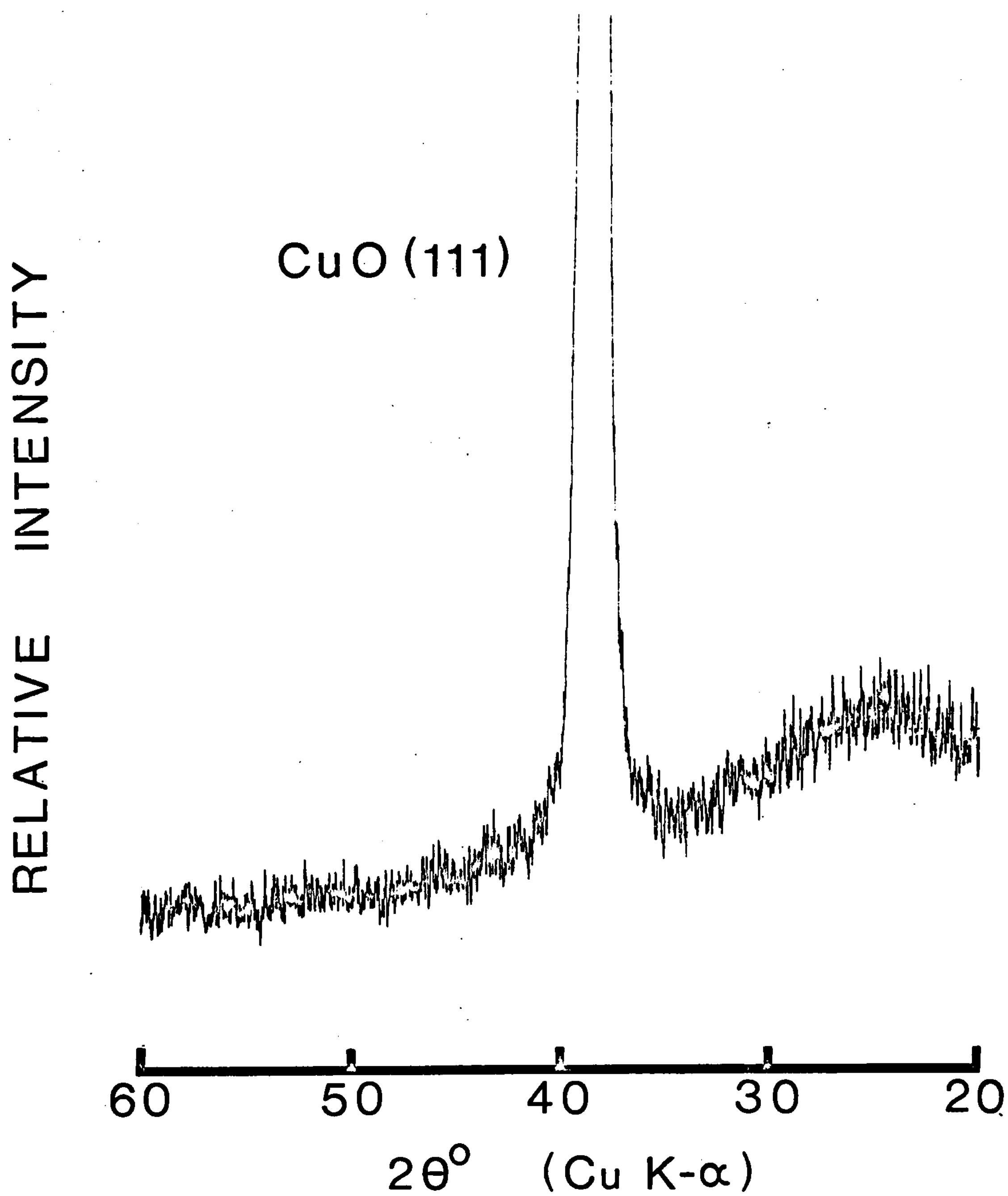

Figure 9. X-Ray diffraction pattern of Film 15 (5500Å thick) sputtered in 90% Ar - 10% O_2.

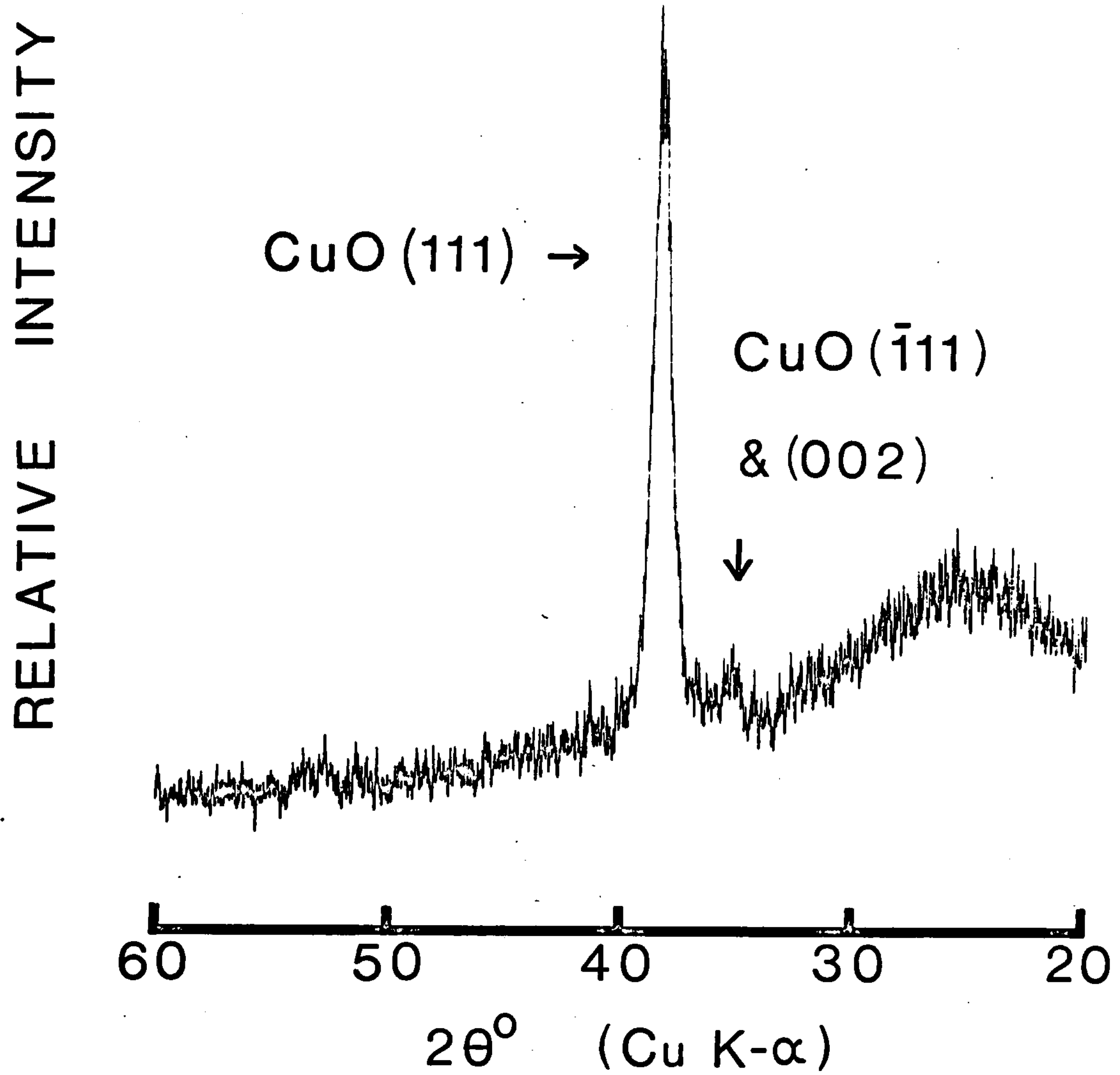

Figure 10. X-Ray diffraction pattern of Film 21 (1400Å thick) sputtered in 50% Ar - 50% O_2.

investigated for the presence of a (222) reflection as well as others. Within this range, only one peak of very low intensity was found at 83.10° corresponding to the (222) reflection of CuO. Observation of only the (111) and (222) reflections in several specimens confirmed the existence of preferred orientation because the (111) and (222) planes are parallel to one another.

The d-spacings of the planes represented in the diffraction patterns of the sputtered films varied from film to film. They were generally larger than those determined for the CuO target material and those listed in the powder diffraction file.

2. Annealed Films. Annealing in air at 300°C produced significant changes in a specimen initially sputtered in pure argon. As shown in Figure 11, the Cu_2O peak was virtually eliminated after one hour leaving a small broad peak at approximately 35.50°. The intensity of the new peak, which corresponded to the $(\bar{1}11)$-(002) overlap of CuO, increased with annealing time as did that of the CuO (111) peak. The position of the CuO (111) peak changed from 38.25 to 38.50° during the annealing process.

The effect of annealing a film sputtered in 10% O_2 is shown in Figure 12. After one hour, a small peak appeared at 53.5° which corresponded to the (020) reflection of CuO. The position of the (111) peak changed markedly, from 37.70° to 38.50°, during annealing. The intensity of the (111) peak also increased while that of the (020) decreased after 100 hours.

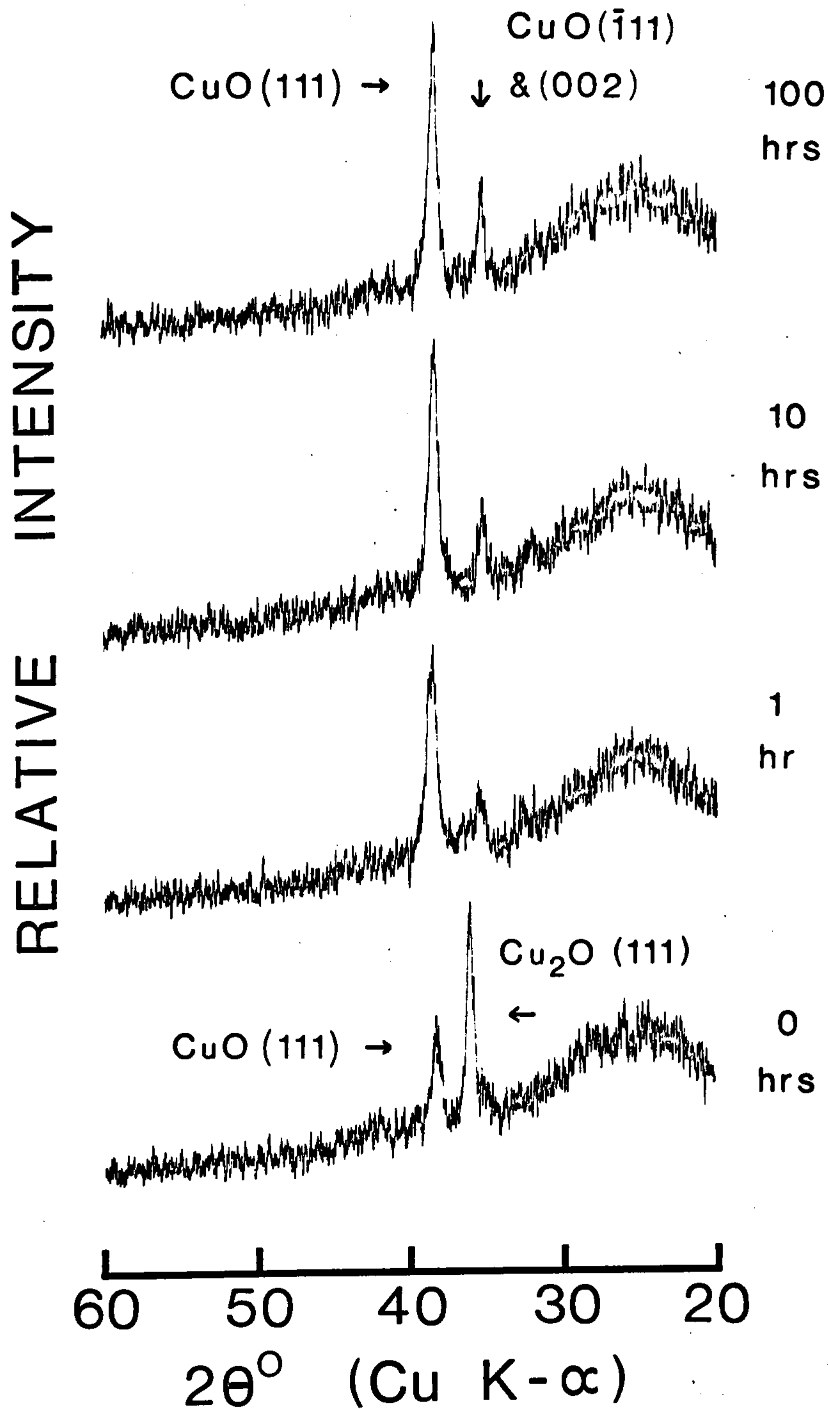

Figure 11. Change in the X-ray diffraction pattern of Film 26 (1500Å) during annealing at 300°C in air.

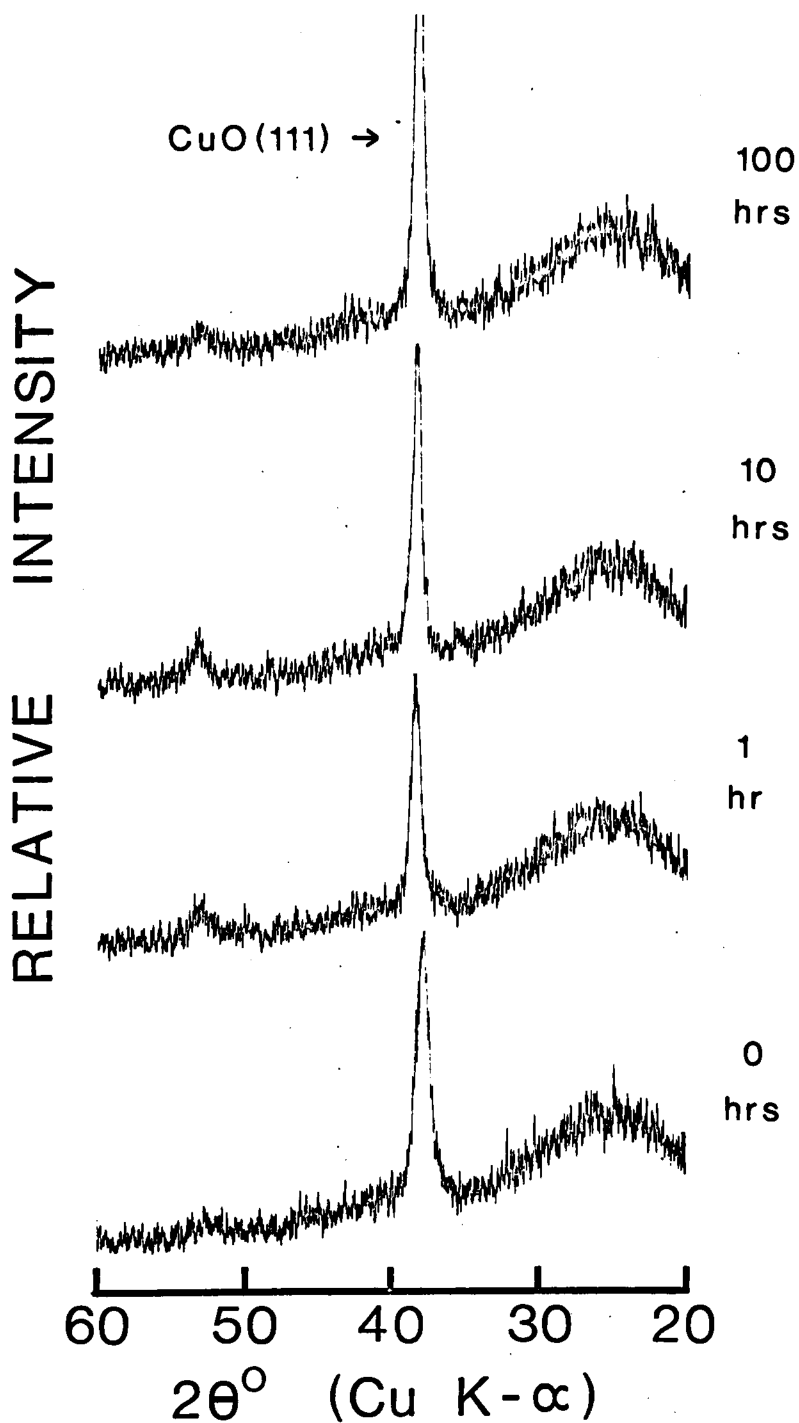

Figure 12. Change in the X-ray diffraction pattern of Film 9 (1200Å) during annealing at 300°C in air.

Annealing of a CuO film sputtered in 50% O_2 is represented in Figure 13. Again, the position of the (111) peak shifted from 38.25 to 38.50°.

3. <u>Reduced Films</u>. During the earlier stages of the reduction experiments several CuO/Cu_2O films were completely reduced to copper metal. Diffraction patterns, such as that in Figure 14B, possessed no peaks belonging to either CuO or Cu_2O.

Successful reduction of CuO to Cu_2O was carried out in an atmosphere containing 5% CO and 95% CO_2. No Cu or CuO peaks were present in any of the diffraction patterns of the Cu_2O films utilized in subsequent electrical and optical experiments. A typical result is shown in Figure 15.

C. SEM-EDAX Results

Radio frequency sputtering of CuO resulted in highly uniform film surfaces composed of submicron sized crystallites. Scanning electron micrographs of unannealed specimens sputtered in 10% O_2 and pure argon are shown in Figures 16A and B respectively. The film thicknesses were similar as indicated in the captions. It was apparent that the film sputtered in the presence of oxygen possessed a finer microstructure than that sputtered in pure argon. Sputtering in 50% O_2 resulted in surface morphologies similar to that depicted in Figure 16.

The scanning electron micrographs shown in Figures 17A and B represent the same specimens after annealing at 300°C in air for

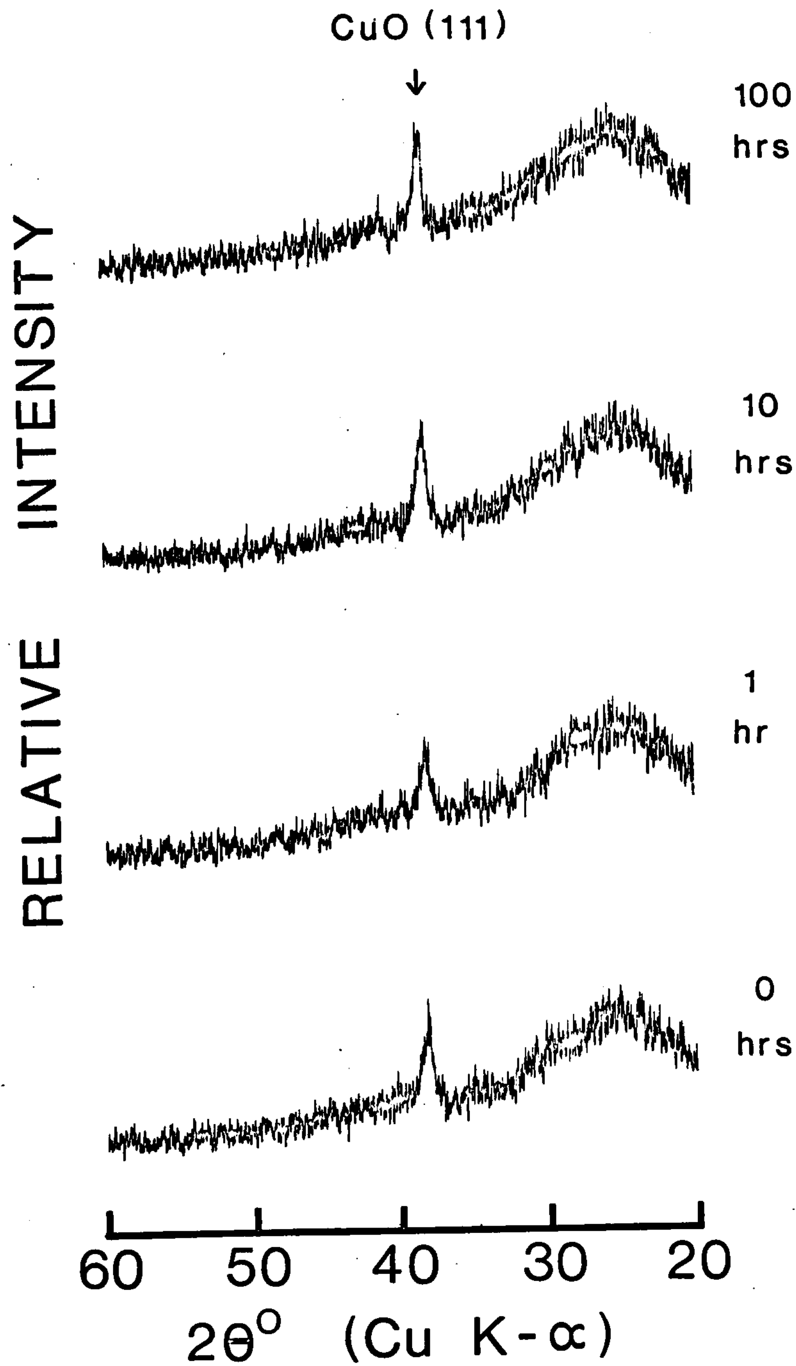

Figure 13. Change in the X-ray diffraction pattern of Film 12 (800Å) during annealing at 300°C in air.

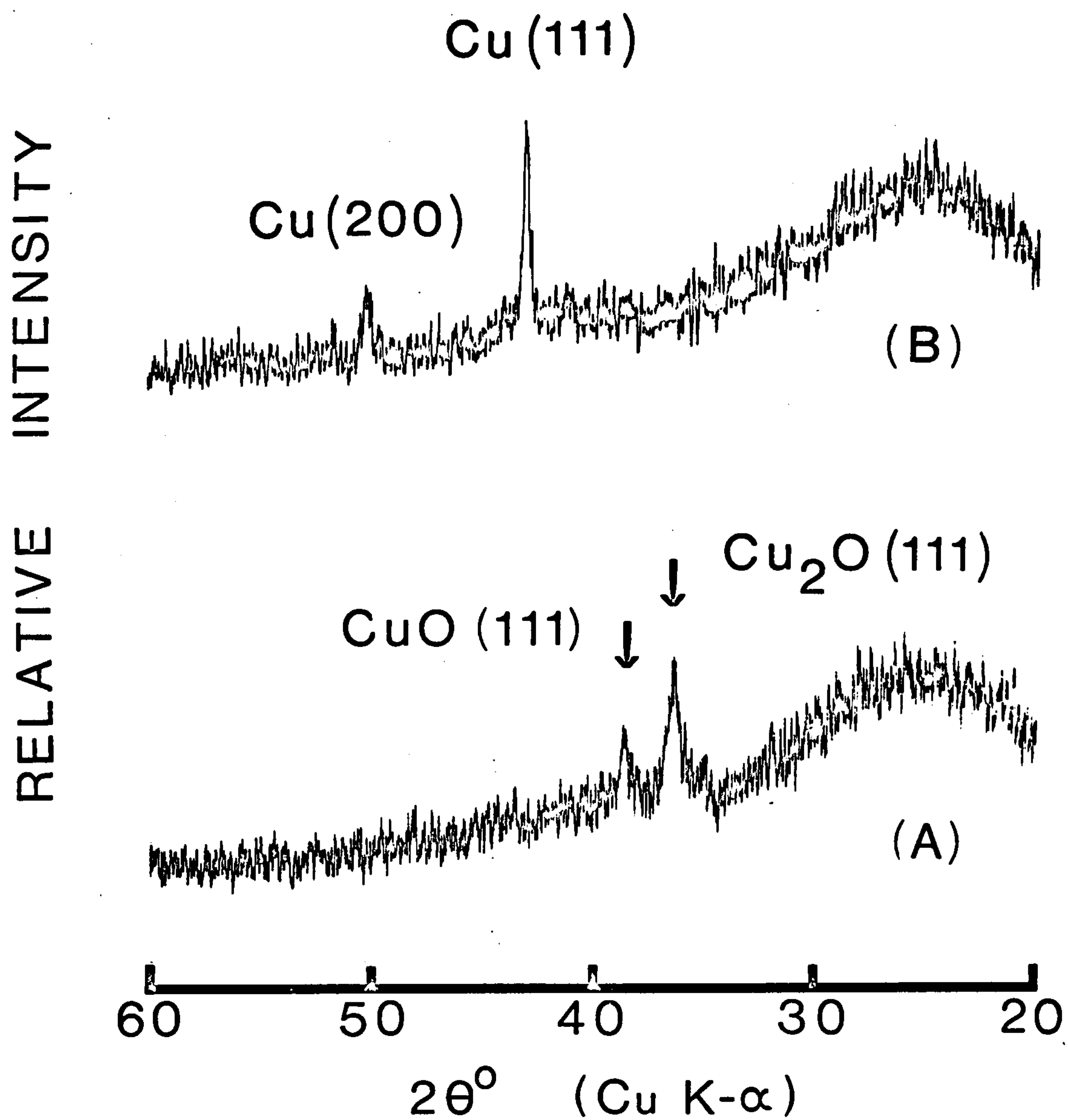

Figure 14. X-Ray diffraction pattern of Film 31 (1500Å) (A) as sputtered, and (B) after reduction to Cu.

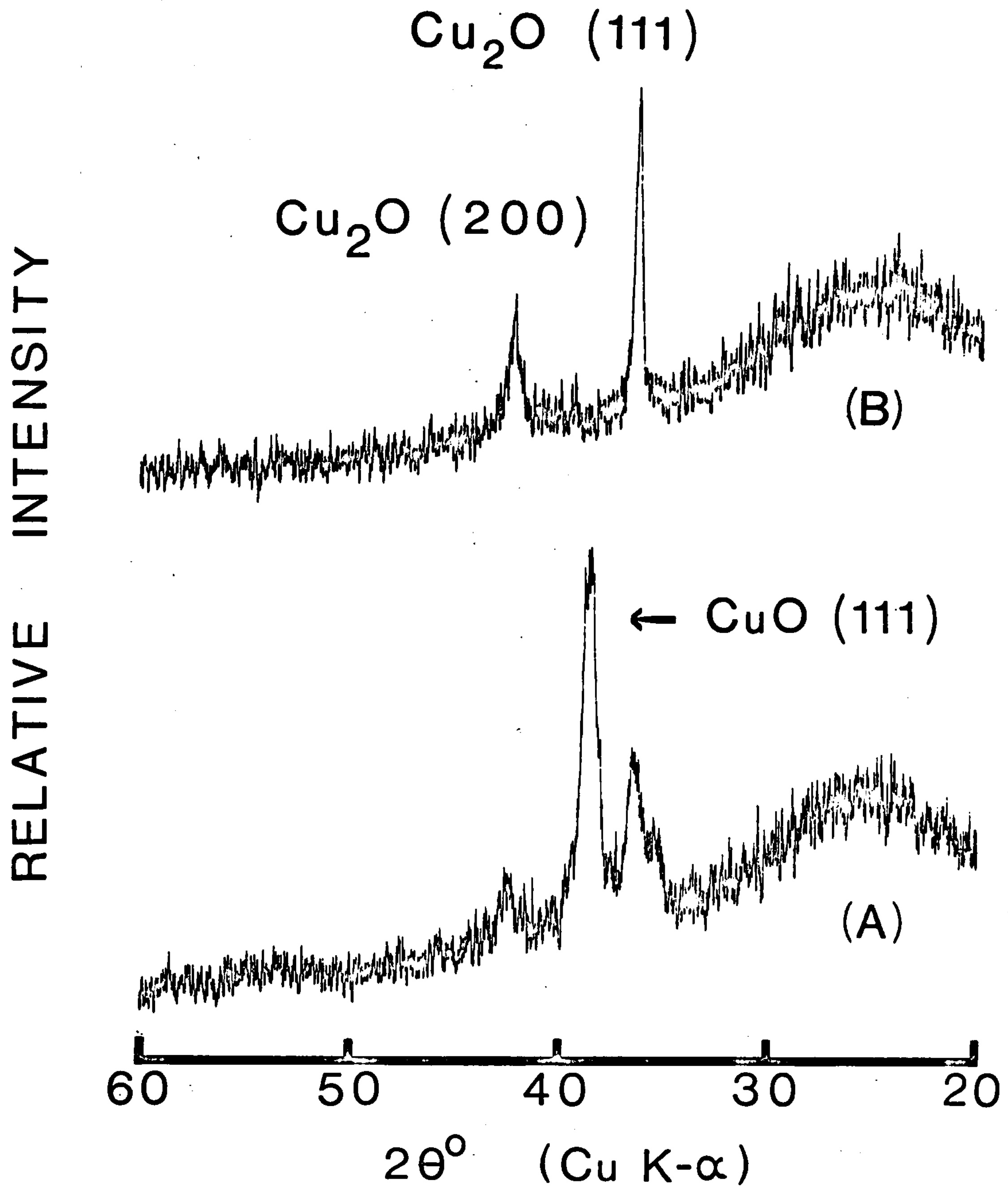

Figure 15. X-Ray diffraction pattern of Film 33 (1800Å) (A) as sputtered, and (B) after reduction to Cu_2O.

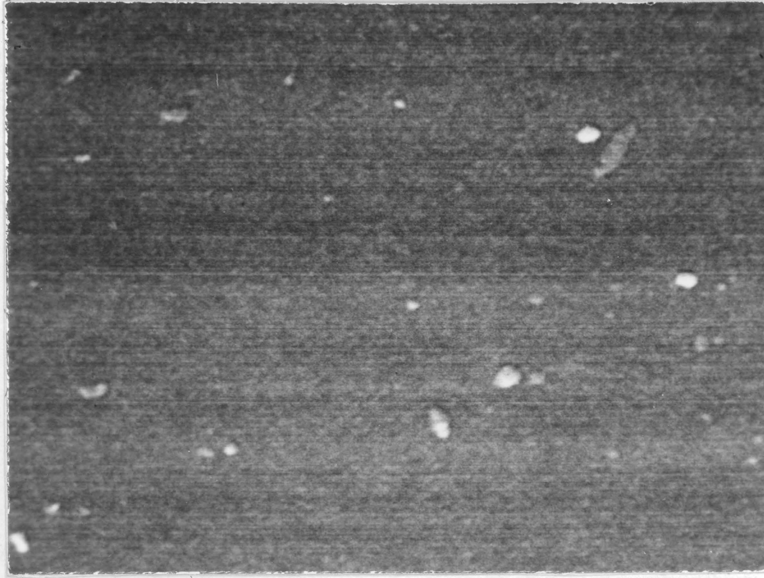

Figure 16A. SEM micrograph of Film 15 (5500Å) sputtered in 90% Ar -10% O_2.

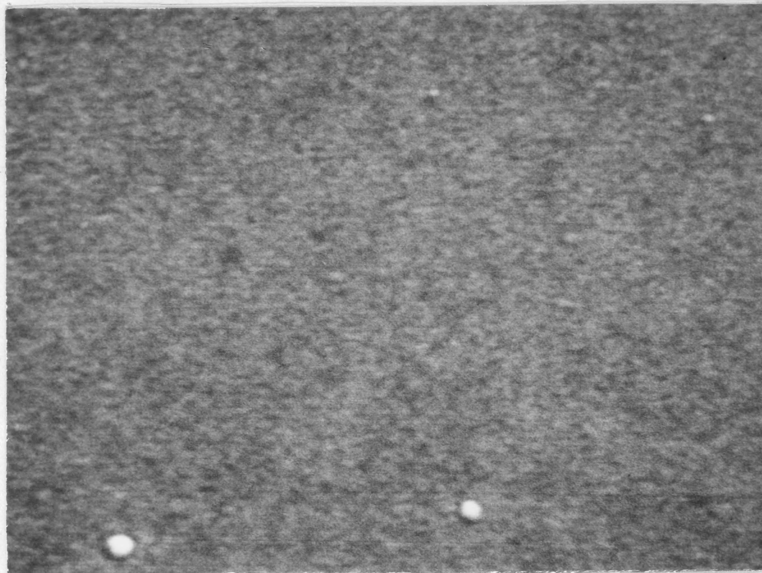

Figure 16B. SEM micrograph of Film 16 (6000Å) displaying increased grain size due to sputtering in 100% Ar.

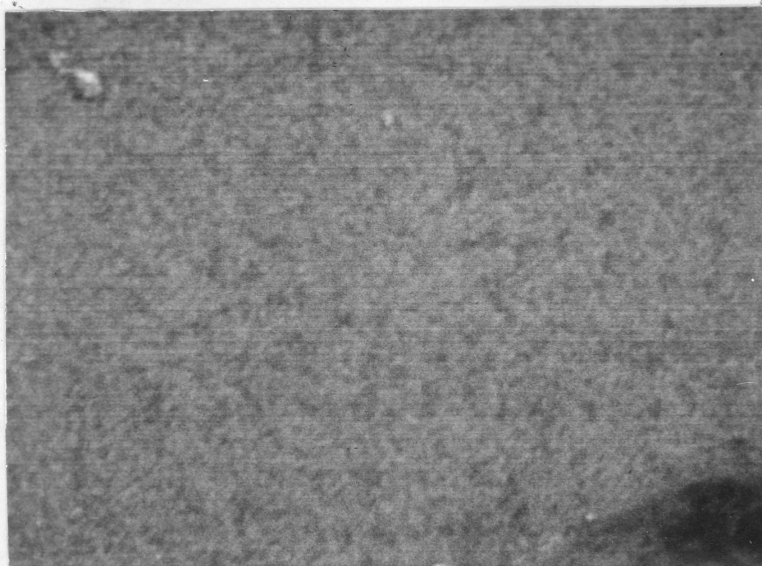

Figure 17A. SEM micrograph of Film 15 exhibiting grain growth after annealing in air at 300°C for 100 hours.

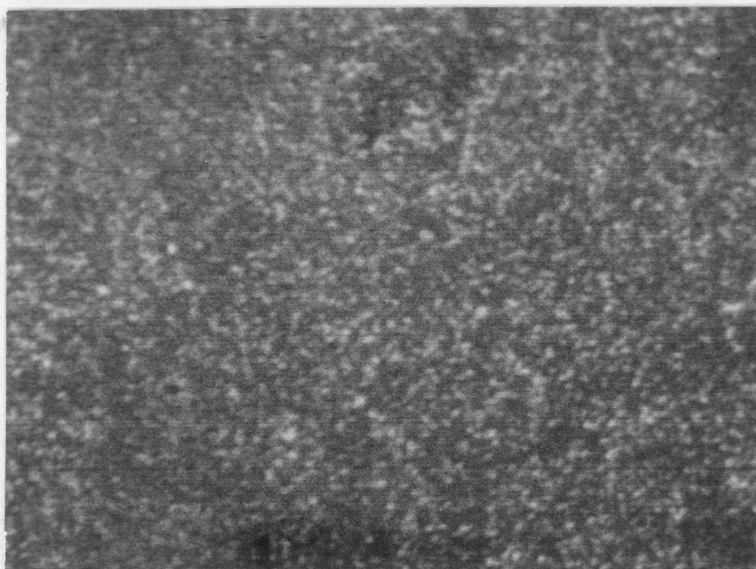

Figure 17B. SEM micrograph of Film 16 exhibiting grain growth after annealing in air at 300°C for 100 hours.

100 hours. The micrographs reveal that crystal growth has occurred during annealing.

The SEM micrographs also gave evidence of surface contamination. The large white masses on the film surfaces were probably organic dust since EDAX did not reveal any foreign impurities in the films.

D. Electrical Properties

The observed values of film thickness, resistivity, and activation energy (E_a) for the sputtered copper oxide films prepared in this study are listed in Table IV. The films are arranged according to the composition of the sputtering gas employed during their preparation.

1. Sputtered Films. All copper oxide films formed via r.f. sputtering of CuO were p-type conductors as determined by the hot probe experiments. Decreasing film resistivity and activation energy were observed with increasing oxygen content of the sputtering atmosphere. The resistivity of the films approached a lower limit as the oxygen content increased as can be seen in Figure 20. Further increases in the oxygen content would not be expected to cause further significant decreases in film resistivity.

The dependence of film resistivity on temperature between room temperature and 200°C is illustrated in Figures 21 through 26. In each figure, three curves, corresponding to three films, prepared under identical conditions, are shown. The slope or thermal activation energy is also indicated.

Table IV

Electrical Properties of Sputtered Copper Oxide Films

	Film No.	Sputtering Time (min)	Film Thickness (Å)	Room Temp. ρ (Ω-cm)	E_a (eV)	Room Temp. ρ after Heating to 200°C (Ω-cm)
Films Sputtered in 100% Ar	4	60	1500	318	0.26	405
	5	60	1800	653	0.25	698
	6	60	1600	255	0.25	339
	16	240	6000	515	0.27	658
	24	240	5100	790	0.27	860
	25	240	5800	700	0.28	746
	26	60	1500	359		
	27	60	1500	850		
	28	60	1500	450		
	30	60	1600	417		
	31	60	1500	270		
	33	60	1500	604		
	34	60	1600	833		
Films Sputtered in 90% Ar - 10% O_2	7	60	1500	13.6		
	8	60	1500	31.0	0.18	70.9
	9	60	1200	36.4		
	14	240	4000	42.8	0.19	55.5
	15	240	5500	130	0.26	145
	17	60	1200	43.1	0.18	52.0
	18	120	2400	116		
	19	120	1800	19.3	0.18	30.4
	29	240	5400	73.6	0.23	90.4
	39	60	1500	36.8	0.18	
Films Sputtered in 50% Ar - 50% O_2	11	120	800	4.50	0.16	8.60
	12	120	800	4.50		
	13	120	800	6.4	0.13	16.0
	20	240	1400	13.8	0.15	35.3
	21	240	1400	3.25	0.13	4.80
	22	240	1100	20.4	0.12	26.2
	23	120	800	20.4	0.14	30.6
	40	120	700	4.40		

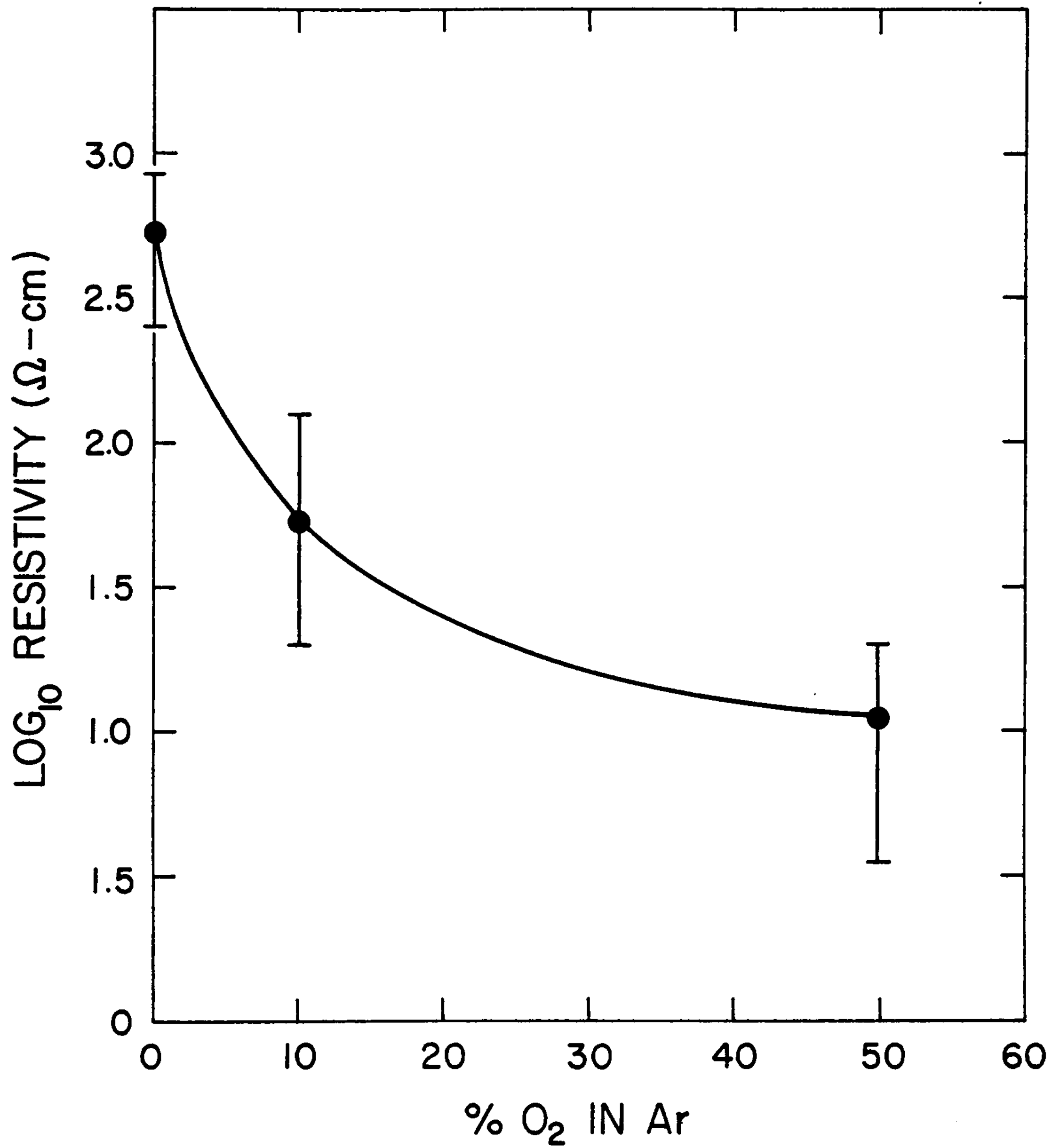

Figure 18. Dependence of copper oxide film resistivity on oxygen content of the sputtering atmosphere.

The resistivity data for three films, sputtered for one hour in pure argon, are illustrated in Figure 21. The calculated activation energies were very reproducible. Similar data for films sputtered for four hours, to achieve greater thickness, are shown in Figure 22. Again, the activation energies displayed very good agreement but were slightly larger than those of the thinner films.

Pure CuO films sputtered in 10% oxygen for one and two hours exhibited excellent agreement in activation energy at low temperatures as shown in Figure 23. However, on approaching 200°C, each curve was characterized by an upward curvature. Similar films sputtered for four hours showed considerable variation in their activation energies which were greater than those of the thinner films. As can be seen in Figure 24, breaks in two of the curves occurred at low temperatures. In view of the fact that such breaks occurred in only four of the eighteen specimens examined, they were assumed to be insignificant.

The temperature dependence of resistivity for the CuO films sputtered in 50% oxygen are illustrated in Figures 25 and 26. A similar range of activation energies existed in both sets of curves. These values were less than those of the films sputtered in pure argon or 10% oxygen. Each of the curves in Figures 25 and 26 deviated from linearity above 100°C.

The resistivity of the sputtered films increased after heating to 200°C. No changes in resistivity were observed after several weeks exposure to the atmosphere at room temperature either before or after heating.

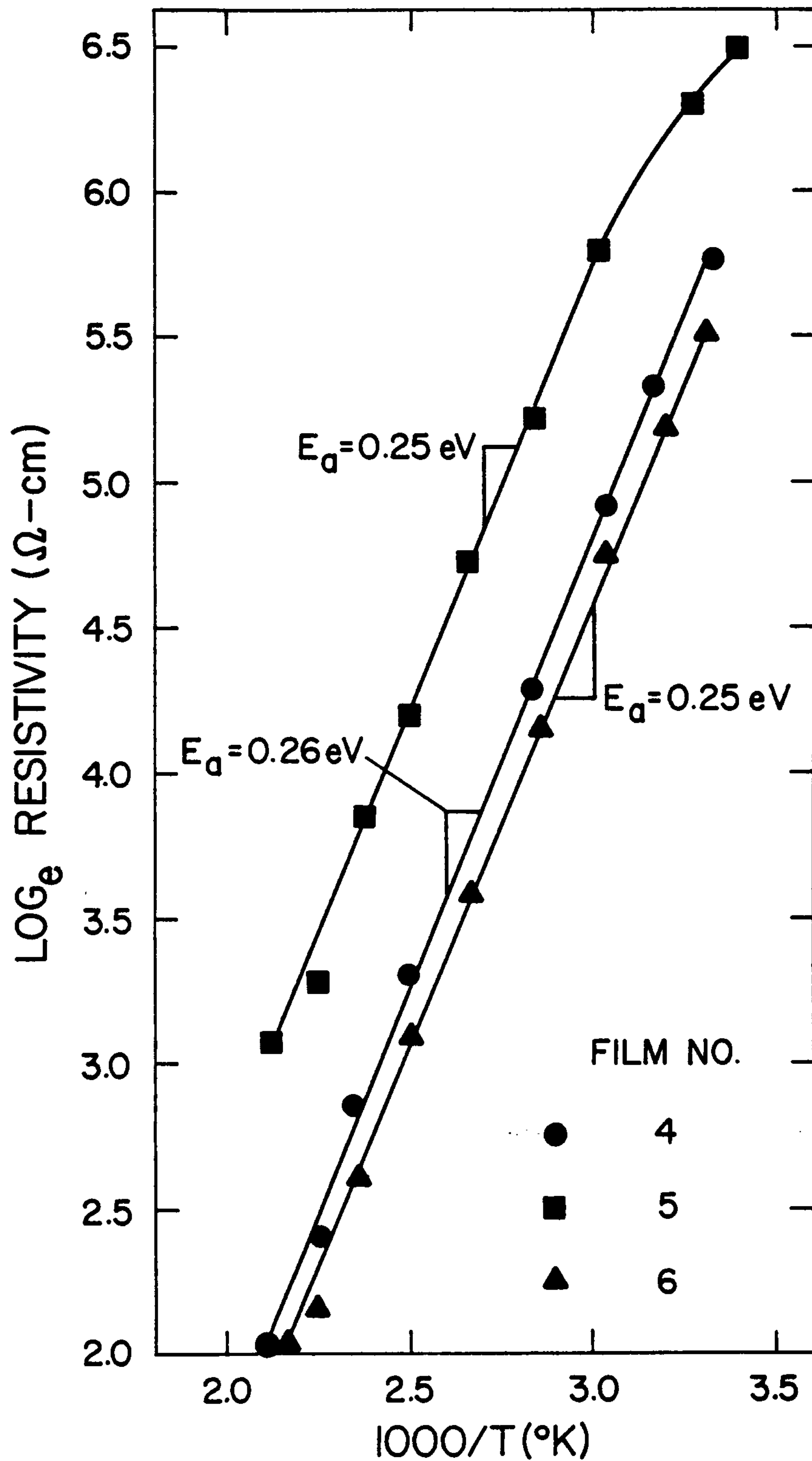

Figure 19. Temperature dependence of resistivity for CuO/Cu_2O films sputtered for 1 hour in 100% Ar.

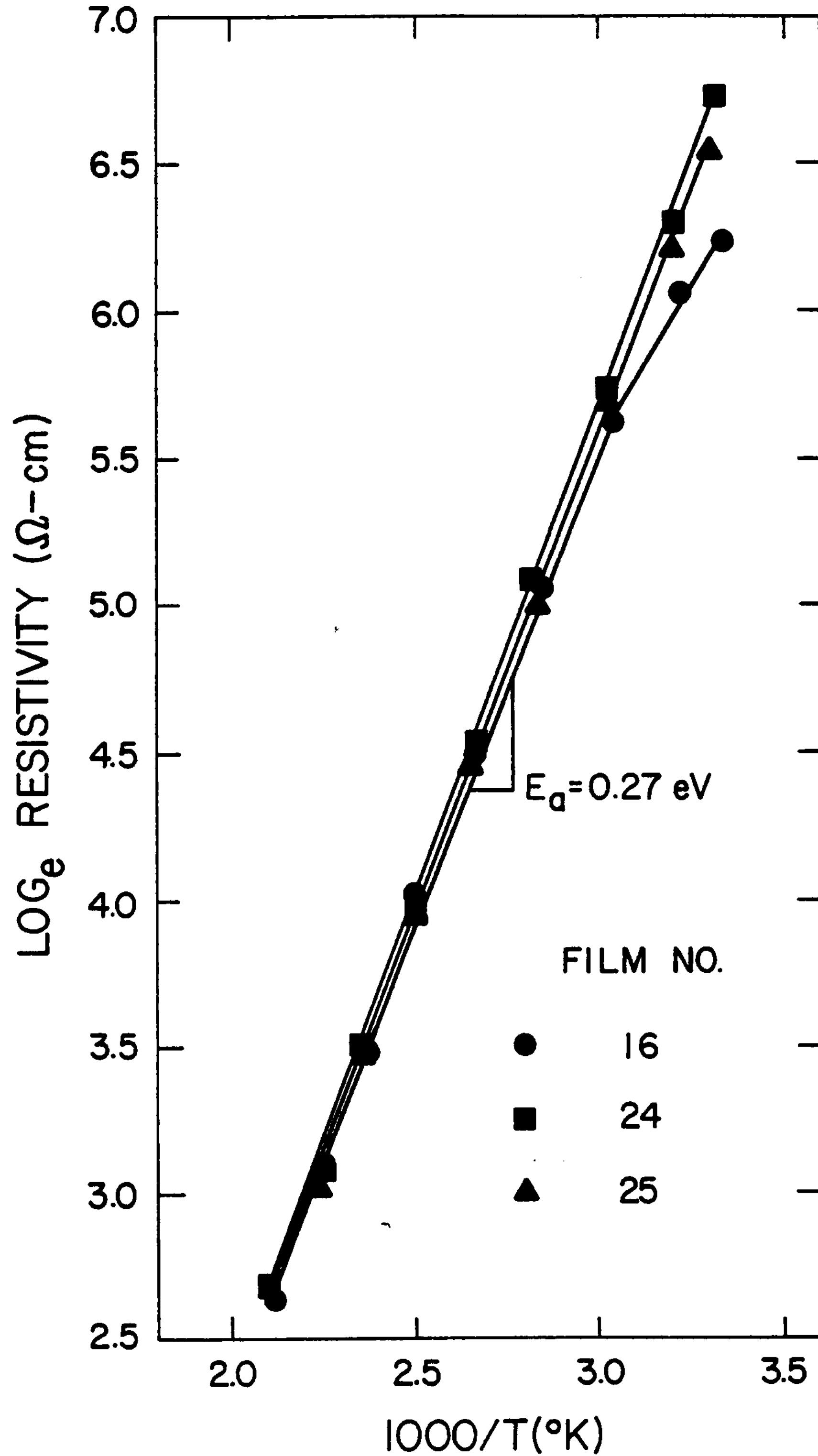

Figure 20. Temperature dependence of resistivity for CuO/Cu_2O films sputtered for 4 hours in 100% Ar.

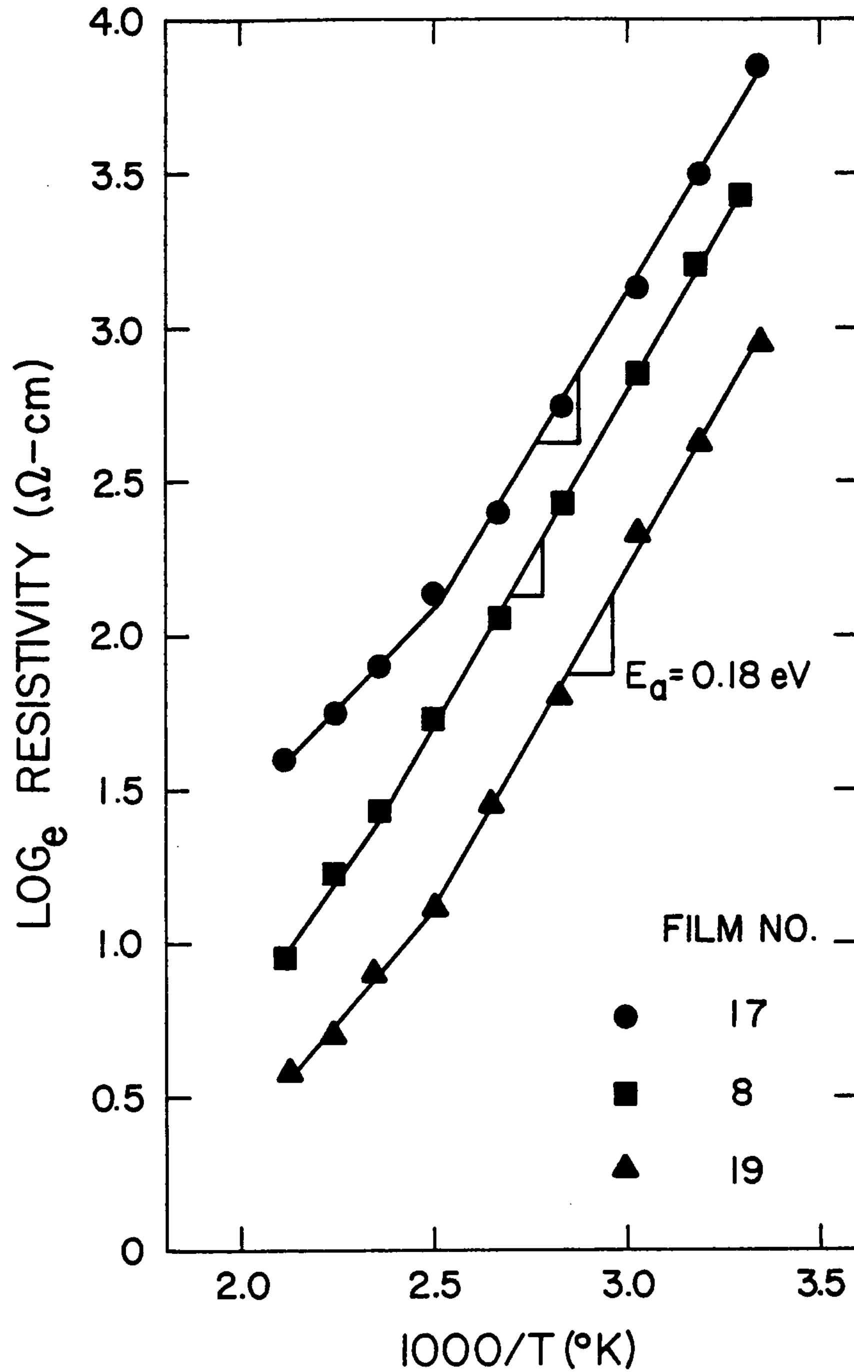

Figure 21. Temperature dependence of resistivity for CuO films sputtered for 1 hour (8 and 17) and 2 hours (19) in 90% Ar - 10% O_2.

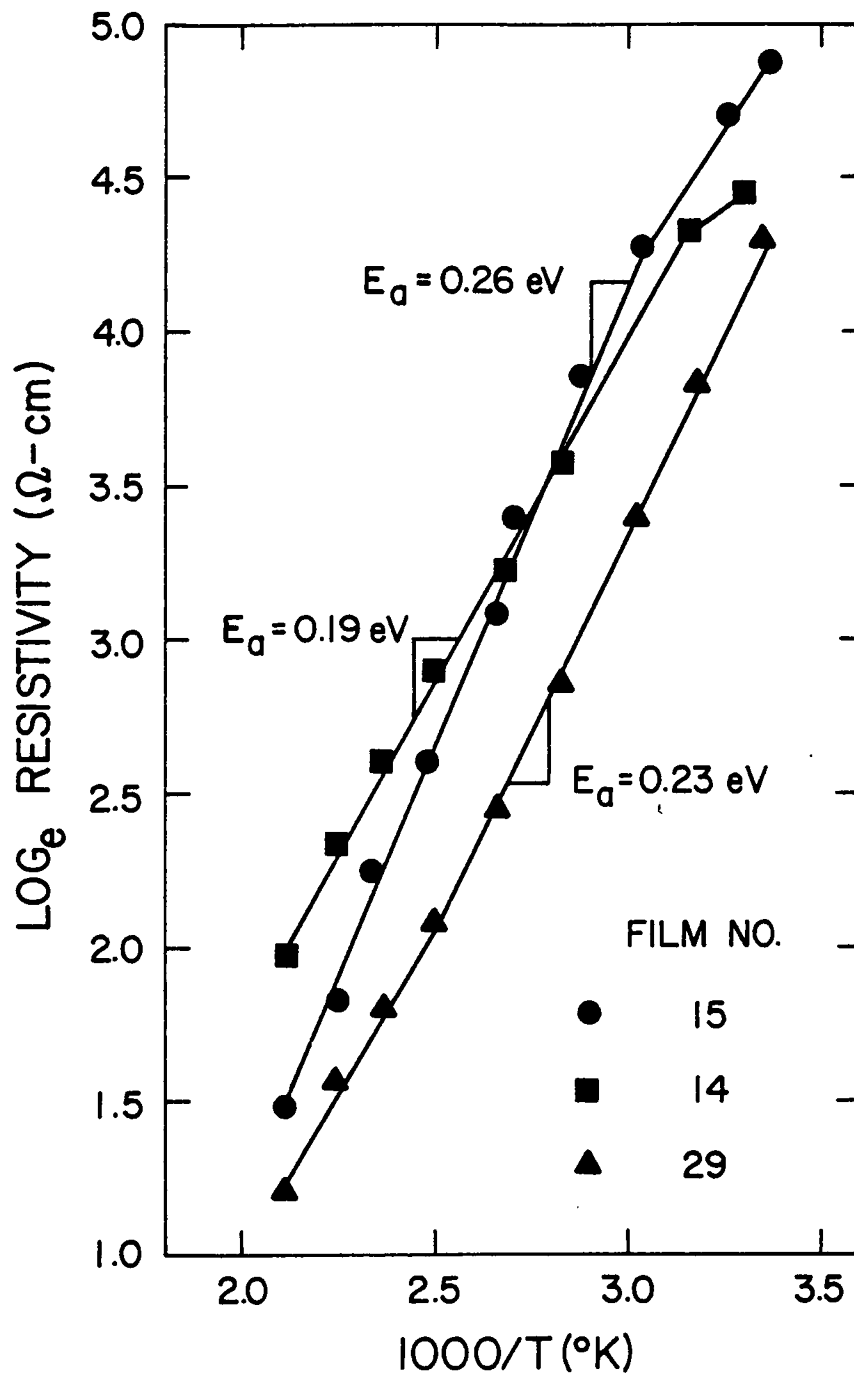

Figure 22. Temperature dependence of resistivity for CuO films sputtered for 4 hours in 90% Ar - 10% O_2.

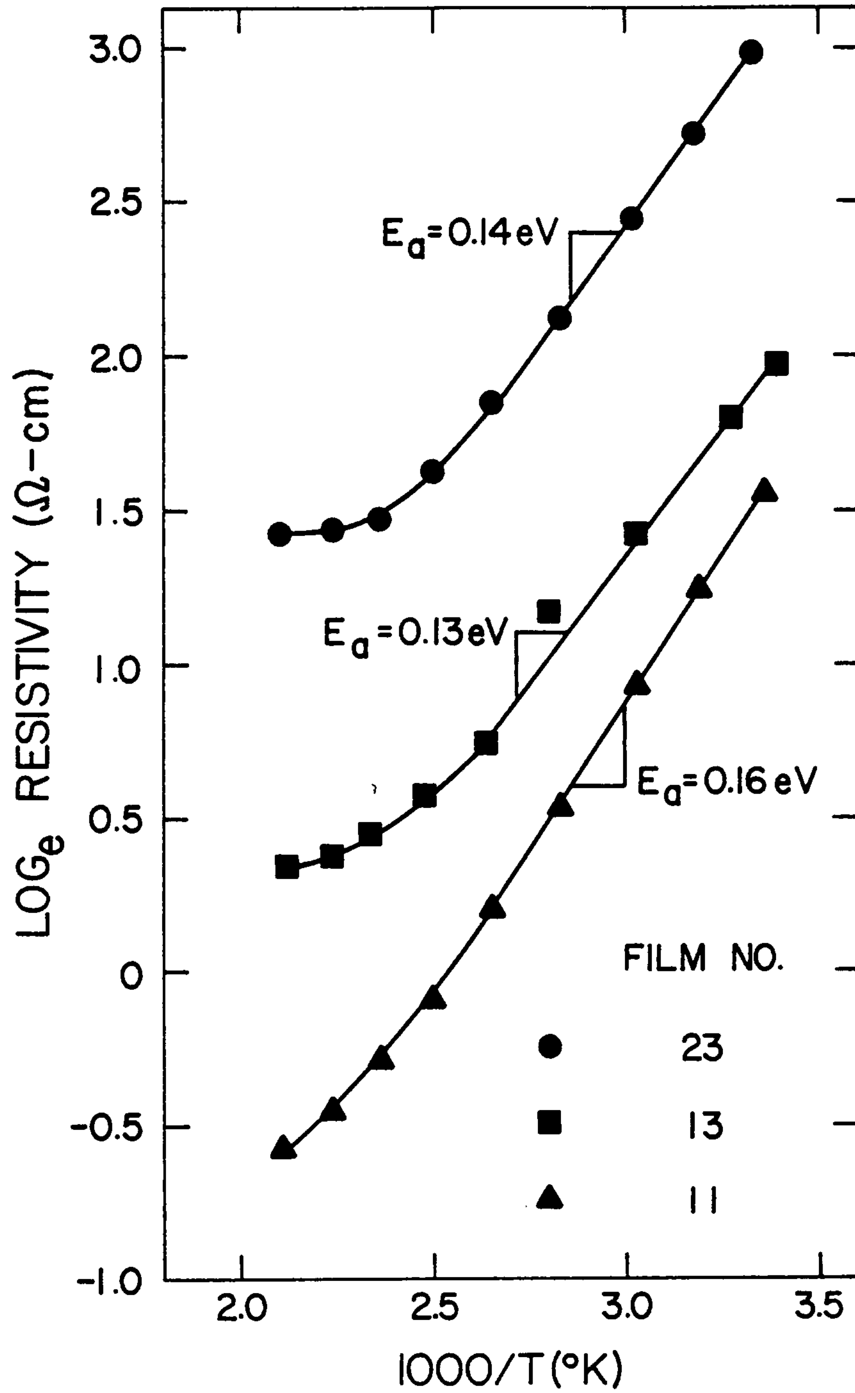

Figure 23. Temperature dependence of resistivity for CuO films sputtered for 2 hours in 50% Ar - 50% O_2.

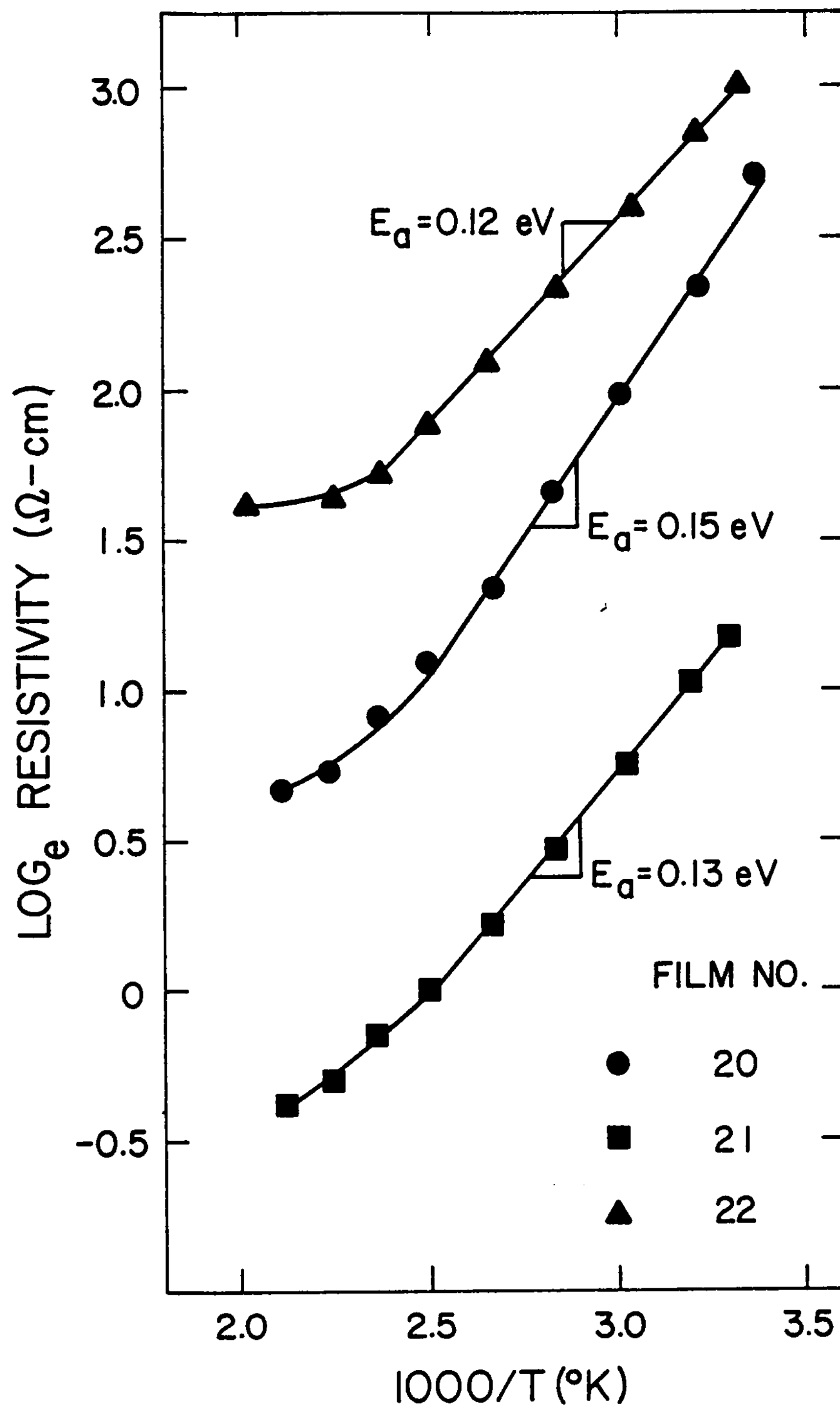

Figure 24. Temperature dependence of resistivity for CuO films sputtered for 4 hours in 50% Ar - 50% O_2.

2. Annealed Films. Changes in room temperature resistivity with time for three specimens, sputtered in different atmospheres and then annealed, are depicted in Figure 27. The three films were simultaneously annealed in air at 300°C. The resistivity of each film increased rapidly within the first several hours before approaching a constant value.

After the annealing experiments were completed, the temperature dependence of resistivity between room temperature and 200°C was determined for each specimen. The film sputtered in pure argon (Film 26) was highly resistive and only 10^{-7} ampere could be passed through the specimen. Outside interference, caused by the temperature controller on the test chamber, rendered accurate determination of this film's resistivity impossible at elevated temperatures. However, the films sputtered in 10% and 50% oxygen were conductive enough to permit the measurements to be made. The results are shown in Figure 28.

The activation energies of these specimens were slightly larger than those of similar unannealed specimens. The breaks in the curves, which occurred between 50 and 75°C, appeared in all other specimens heated to 300°C, and also occurred during cooling to room temperature. The results of annealing the sputtered films in air are summarized in Table V.

3. Cu_2O Films. The change in resistivity with temperature of three Cu_2O films prepared from sputtered CuO/Cu_2O films is shown in Figure 29. Breaks in the curves occurred consistently at 125°C. The

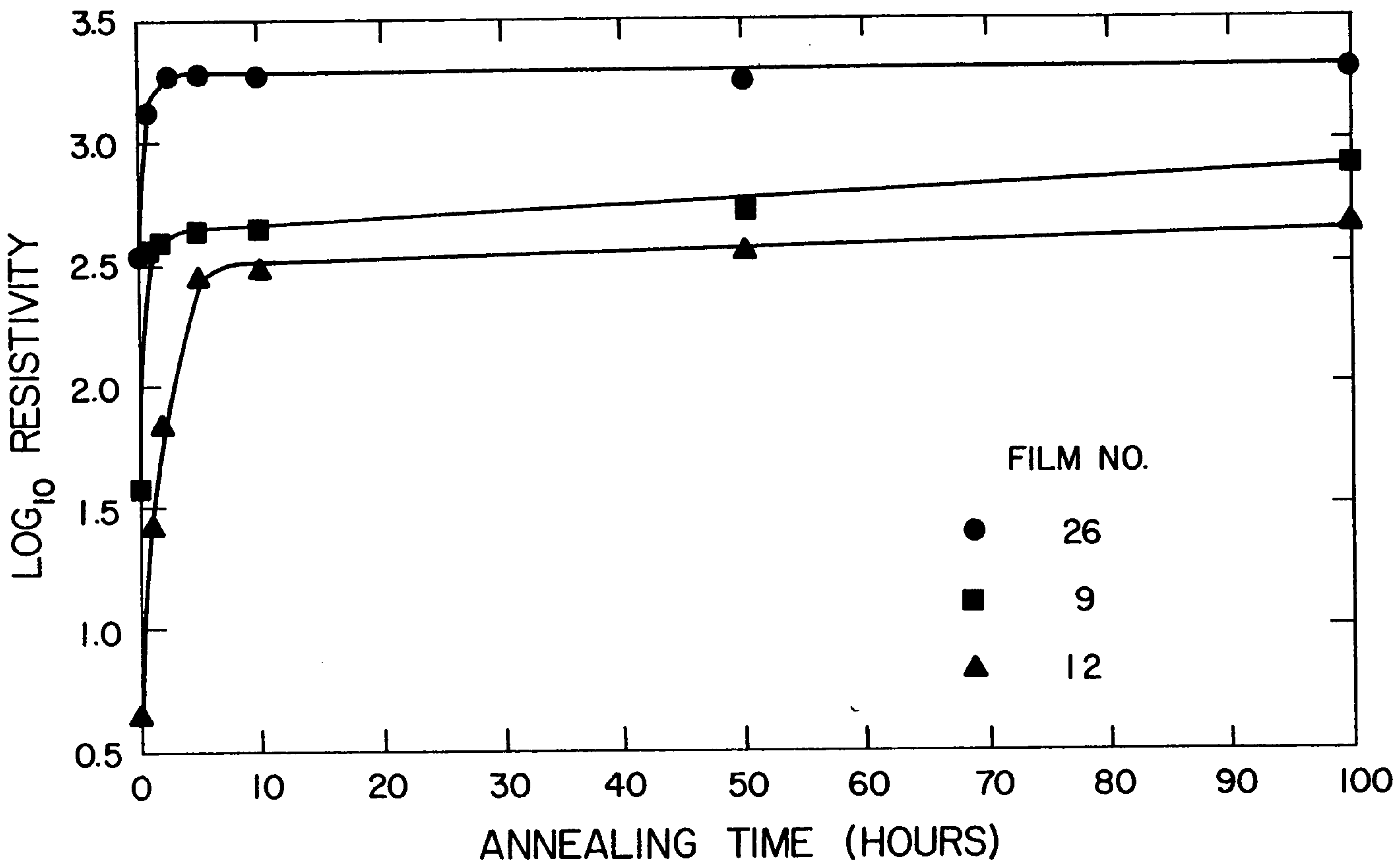

Figure 25. Change in room temperature resistivity after annealing in air at 300°C.

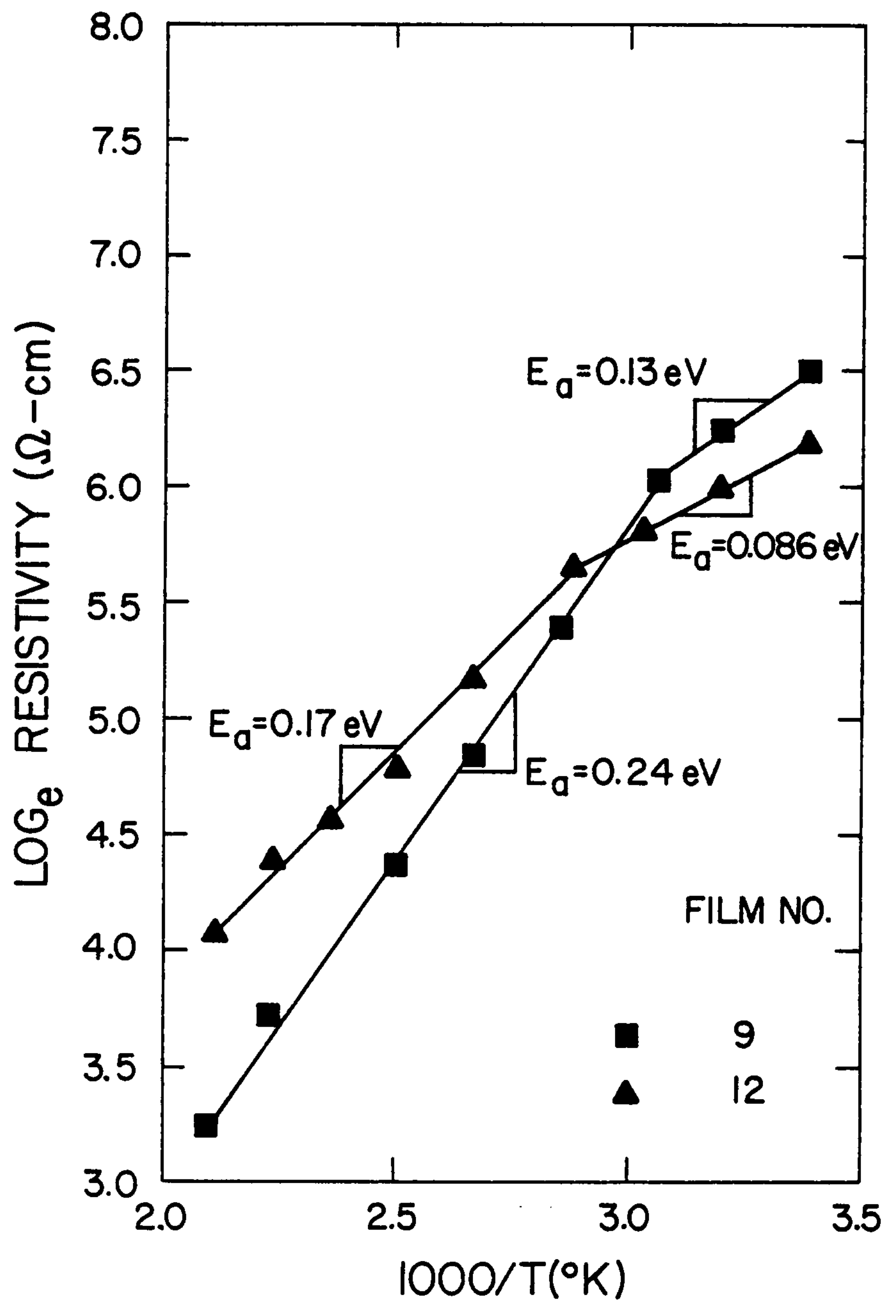

Figure 26. Temperature dependence of resistivity for CuO films after annealing at 300°C.

Table V

Electrical Properties of Films Annealed at 300°C for 100 Hours

Film No.	Thickness	Room Temp. Resistivity (Ω-cm) Before Annealing	After Annealing	Activation Energy (eV) Low Temp.	High Temp.
26	1500	359	2030	-	
9	1200	36.4	611	0.13	0.24
12	800	4.50	447	0.086	0.17

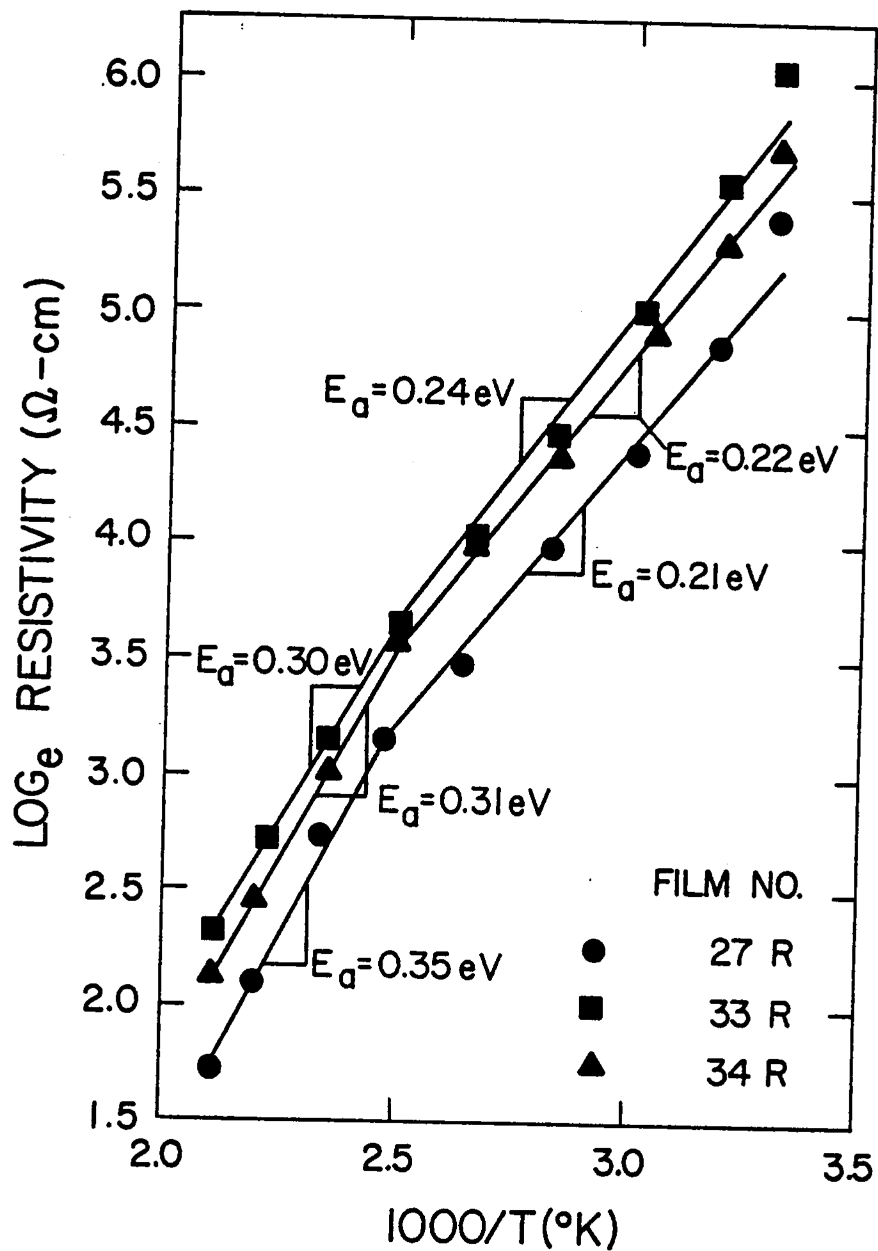

Figure 29. Temperature dependence of resistivity for Cu_2O films.

room-temperature resistivities of the Cu_2O films decreased slightly after heating to 200^oC as indicated in Table VI. All of the Cu_2O films were p-type conductors.

E. Optical Properties

Originally, measurement of absorbance, transmittance, and reflectance was to be carried out on the copper oxide films. Instrumental difficulties prevented reflectance data from being obtained for all but one copper oxide film and an uncoated substrate. Since the fraction of radiation not transmitted was both absorbed and reflected, discussion of film optical properties will be limited to transmittance data alone. For convenience, the optical data presented in Figures 30 through 40 are summarized in Table VII according to film preparation technique. The approximate thickness and room temperature resistivity of each film is listed along with transmittance data at 0.5, 1.0, and 2.0 μ. Conversion of wavelength to photon energy in electron volts is accomplished in Table VIII.

1. Sputtered Films. All as-sputtered copper oxide films were brown in color, the transparency of which depended on film thickness and composition. Films greater than 5000Å thick appeared black or very dark brown whereas those less than 1400Å thick were highly transparent.

Transmittance at 0.5 μ varied from 0% for the thickest films to 30% in the case of the very thin films sputtered in 50% O_2. Beyond 1.0 μ the films transmitted greater than 50% of the incident radiation.

Table VI

Electrical Properties of Reduced Films

	Film No.	Film Thickness (Å)	Room Temp. Resistivity (Ω-cm) Before Reducing	After Reducing	E_a (eV) Low Temp.	High Temp	Room Temp. ρ after Heating to 200°C (Ω-cm)
Cu_2O Films	27R	1500	850	264	0.35	0.21	182
	33R	1500	604	422	0.30	0.24	399
	34R	1600	833	281	0.31	0.22	241
Cu Metal Films	30R	1600	417	7.25×10^{-7}			
	31R	1500	270	1.73×10^{-6}			

Table VII

Optical Transmittance Data of Copper Oxide Films

Film Type	Film No.	Thickness (Å)	Room Temp. ρ (Ω-cm)	Fraction of Radiant Energy Transmitted Wave Length 0.5μ	1.0μ	2.0μ	Figure No.
Sputtered in 100% Ar	6	1600	255	0.20	0.50	0.65	30
	24	5100	790	0.00	0.42	0.80	31
Sputtered in 90% Ar 10% O_2	8	1500	31.0	0.02	0.90	0.70	32
	15	5500	130	0.00	0.65	0.57	33
Sputtered in 50% Ar 50% O_2	13	800	6.4	0.30	0.74	0.82	34
	22	1100	20.4	0.28	0.68	0.90	35
Annealed Films	26	1500	2031	0.07	0.75	0.60	36
	9	1200	611	0.24	0.72	0.90	37
	12	800	447	0.45	0.82	0.86	38
Reduced Films	27R	1500	264	0.34	0.72	0.70	39
Uncoated Corning #7059 Substrate		0.02"	-	0.90	0.92	0.90	40

Table VIII

Conversion of Wavelength to Energy

λ (μ)	Radiant Energy (eV)
0.30	4.13
0.35	3.54
0.40	3.10
0.45	2.75
0.50	2.48
0.55	2.26
0.60	2.07
0.65	1.91
0.70	1.77
0.75	1.65
0.80	1.55
0.85	1.46
0.90	1.38
0.95	1.31
1.00	1.24
1.50	0.83
2.00	0.62
2.50	0.50

Very sharp drops in transmittance were observed in films greater than 5000Å thick. The drops occurred at approximately 0.7 μ (1.77 eV). Such films also displayed transmittance cut offs between 0.62 μ (2.00 eV) and 0.5 μ (2.48 eV).

2. Annealed Films. Annealing in air at 300°C induced changes in the optical properties of the sputtered copper oxide films. Although differences in visible transmittance were observed, infrared transmittance remained very high such that no direct correlations could be made in this range.

Annealing resulted in decreased transmittance at 0.5 μ in the case of films sputtered in pure argon. Films sputtered in 10% and 50% O_2, and then annealed, exhibited greater visible transmittance than similar unannealed specimens.

3. Cu_2O Films. Cuprous oxide films displayed greater than 70% transmittance beyond 1.0 μ as shown in Figure 39. A sharp drop in transmittance occurred at 0.5 μ (2.48 eV). All the Cu_2O films were bright yellow in color.

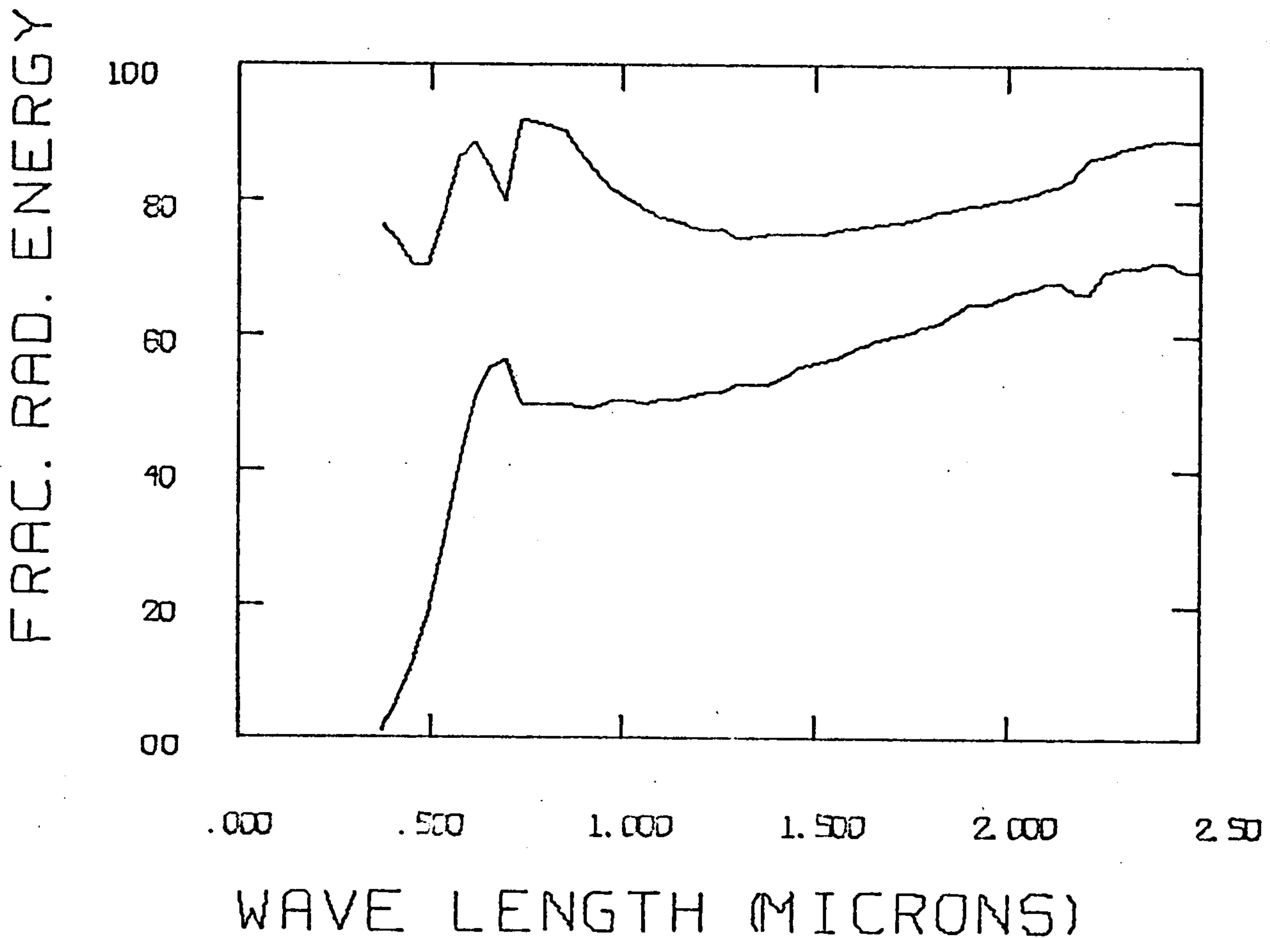

Figure 28. Change in absorbance (A), reflectance (R), and transmittance (T) with wavelength for CuO/Cu_2O Film 6 (1500Å sputtered in 100% argon.

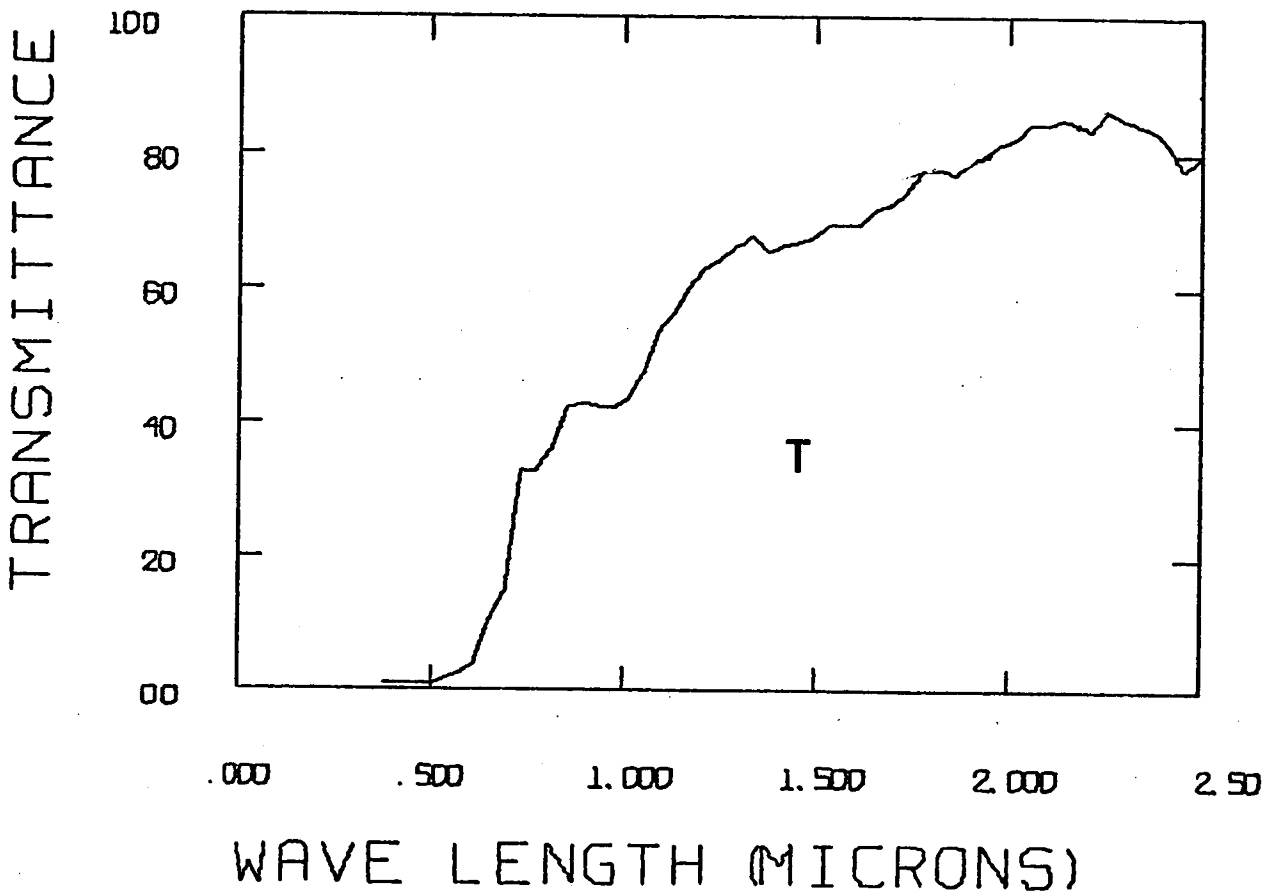

Figure 29. Change in transmittance (T) with wavelength for CuO/Cu_2O Film 24 (5100Å) sputtered in 100% argon.

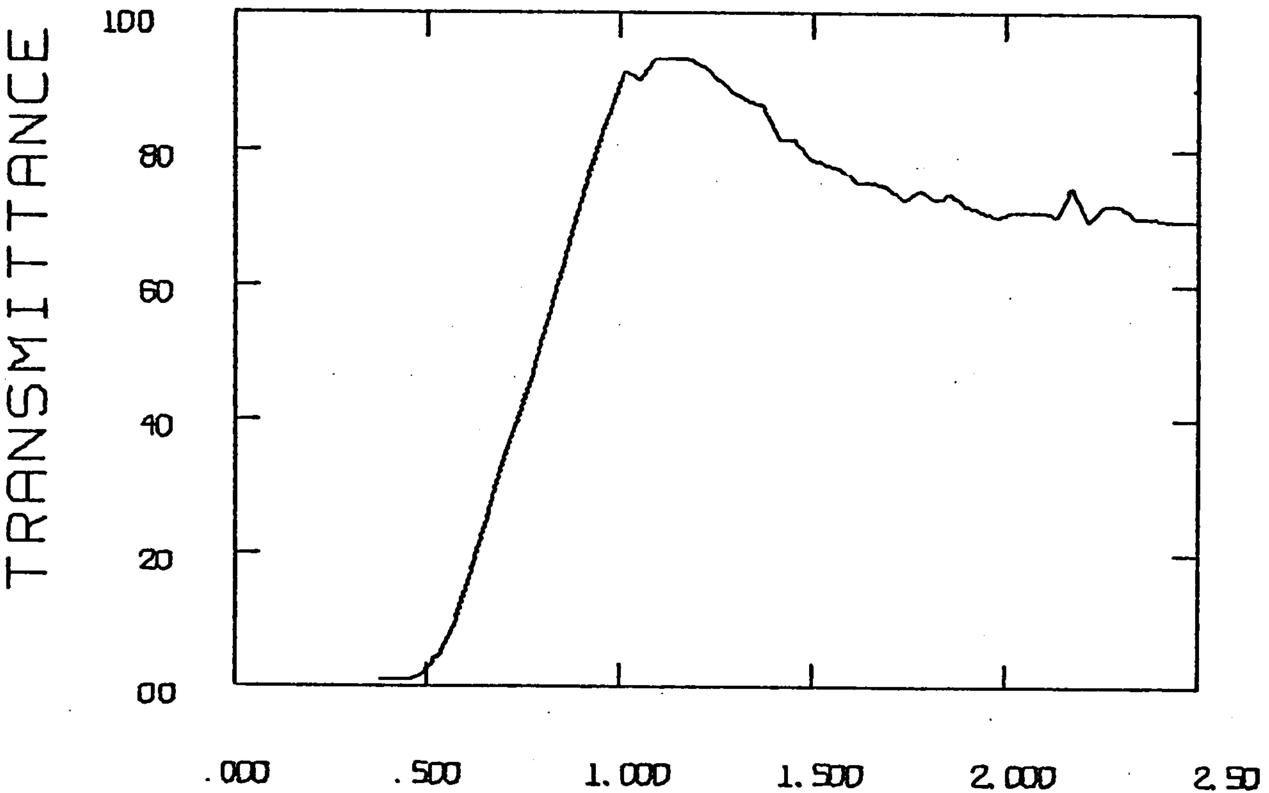

Figure 30. Change in transmittance (T) with wavelength for CuO Film 8 (1500Å) sputtered in 90% Ar - 10% O_2.

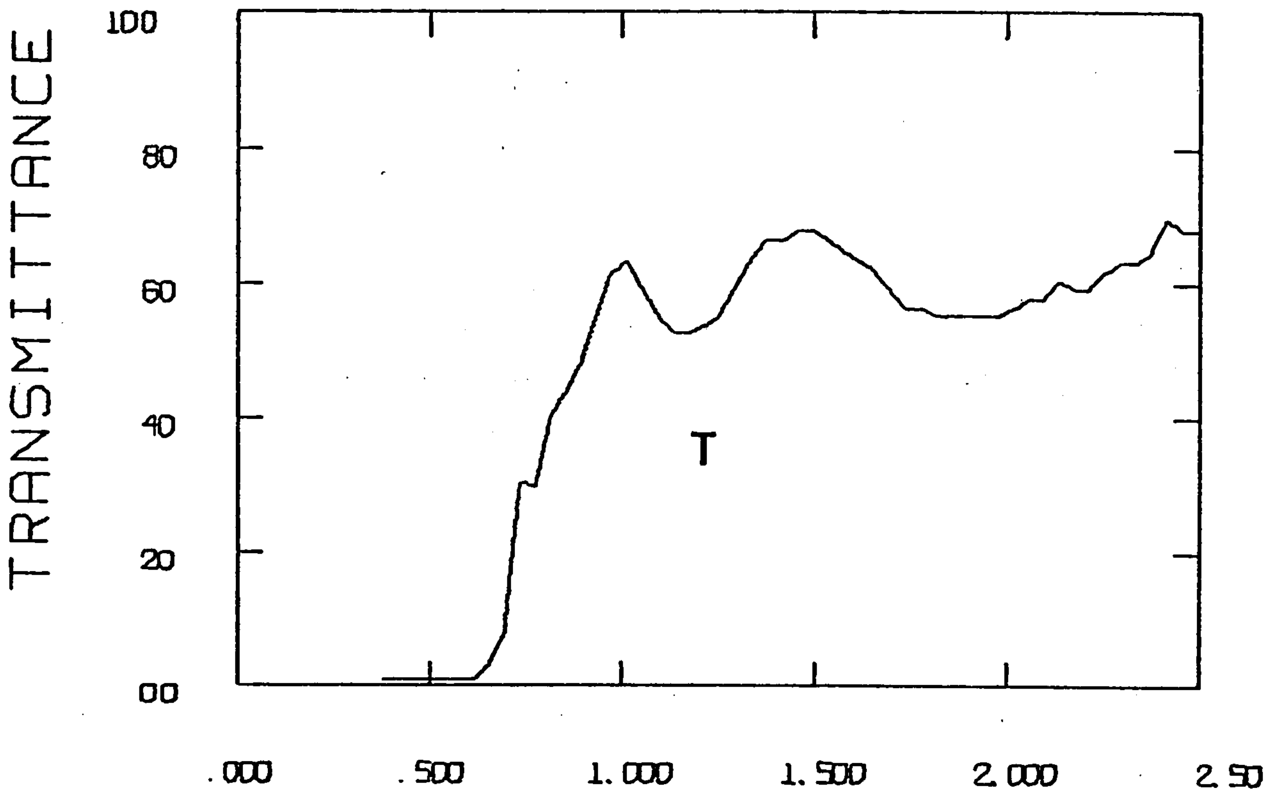

Figure 31. Change in transmittance (T) with wavelength for CuO Film 15 (5500Å) sputtered in 90% Ar - 10% O_2.

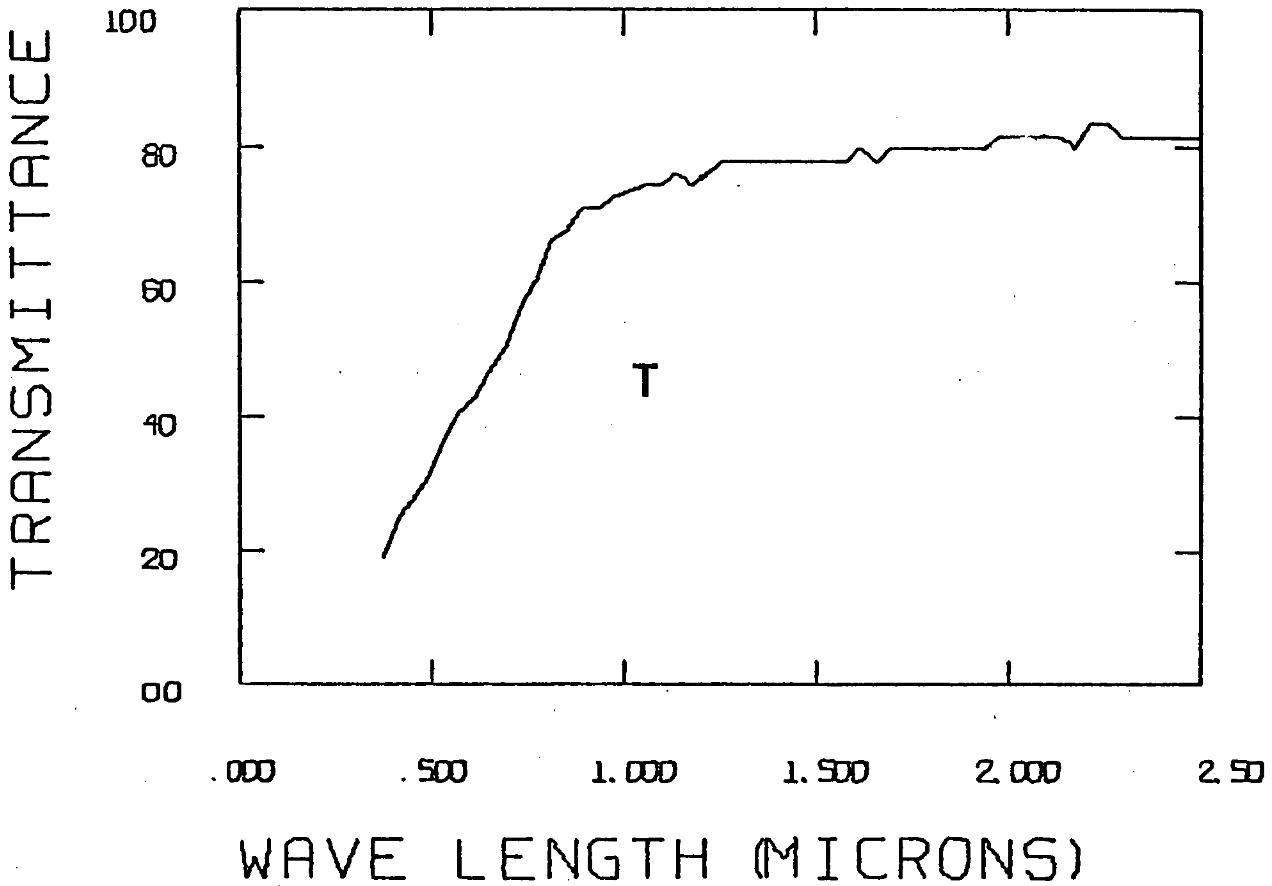

Figure 32. Change in transmittance (T) with wavelength for CuO Film 13 (800Å) sputtered in 50% Ar - 50% O_2.

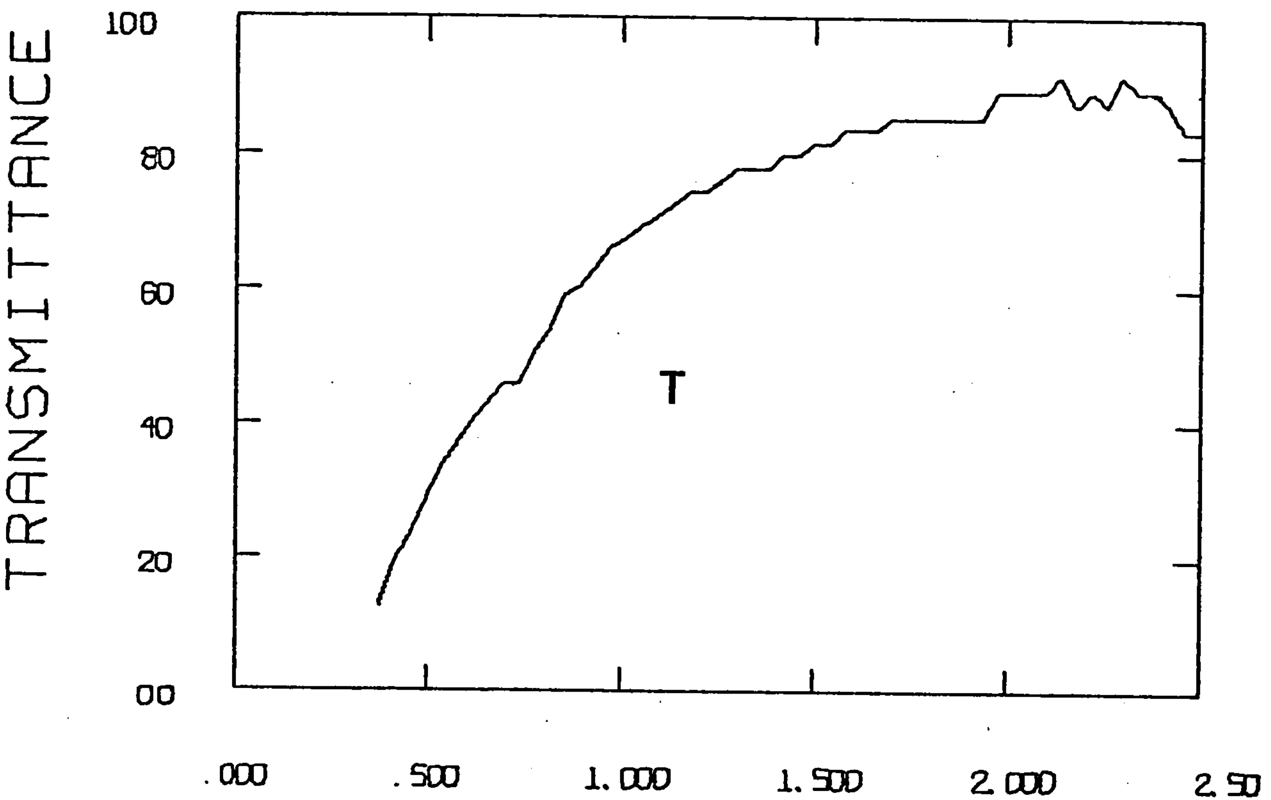

Figure 33. Change in transmittance (T) with wavelength for CuO Film 22 (1100Å) sputtered in 50% Ar - 50% O_2.

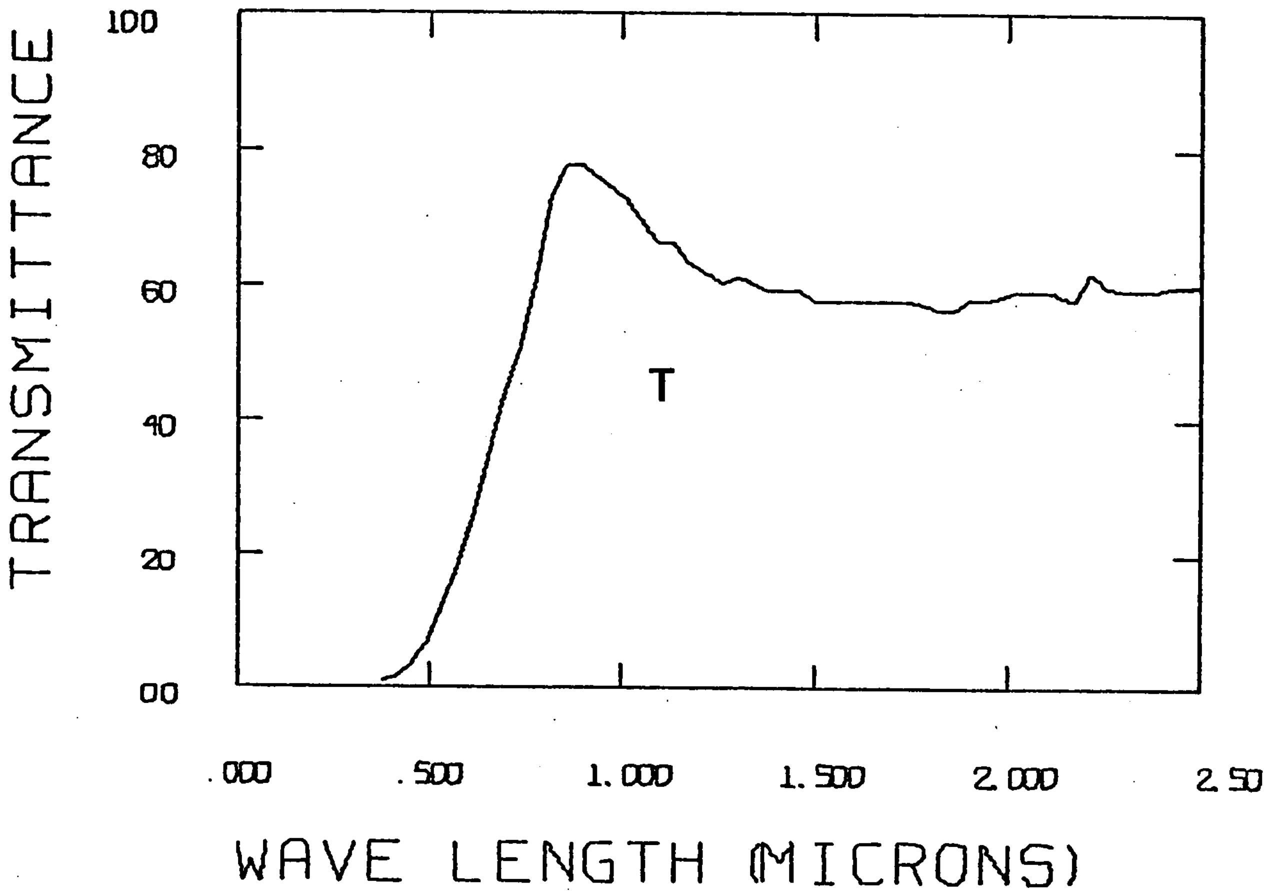

Figure 34. Change in transmittance (T) with wavelength for CuO Film 26 (1500Å) after annealing.

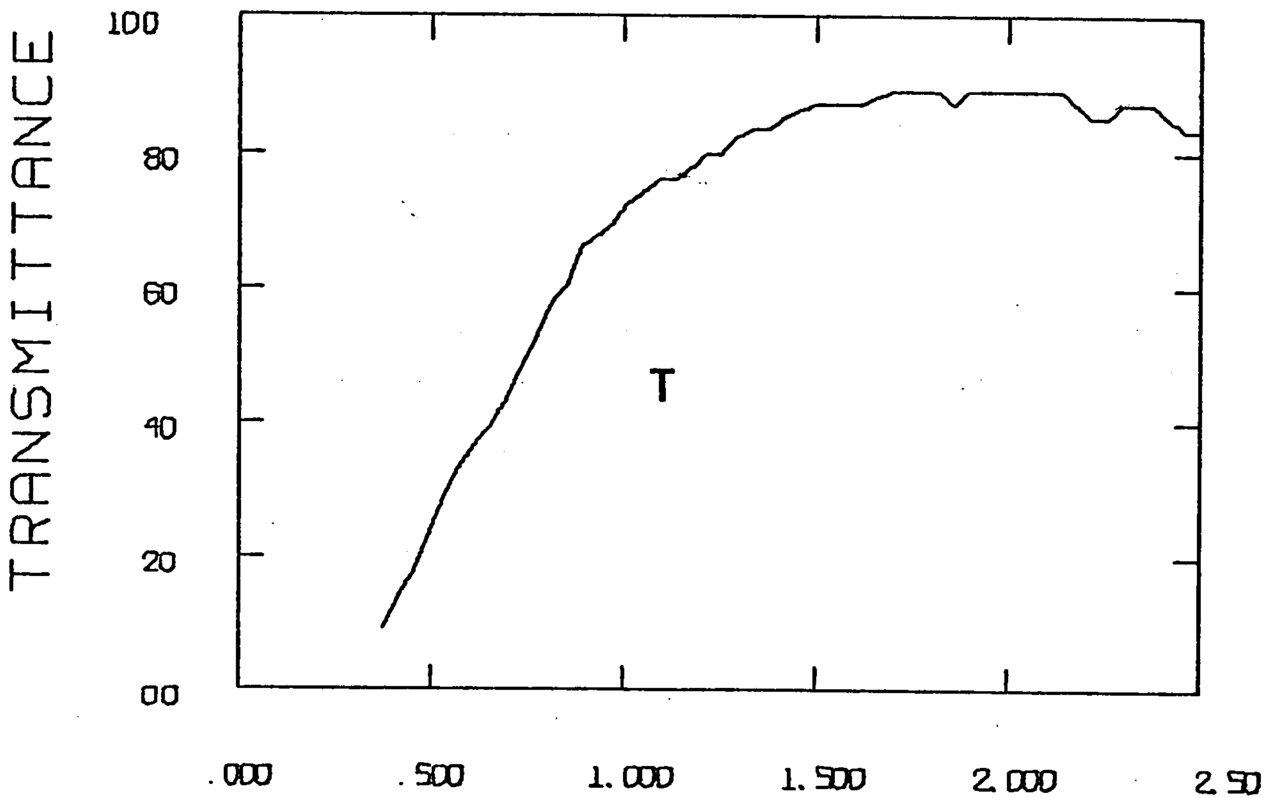

Figure 35. Change in transmittance (T) with wavelength for CuO Film 9 (1200Å) after annealing.

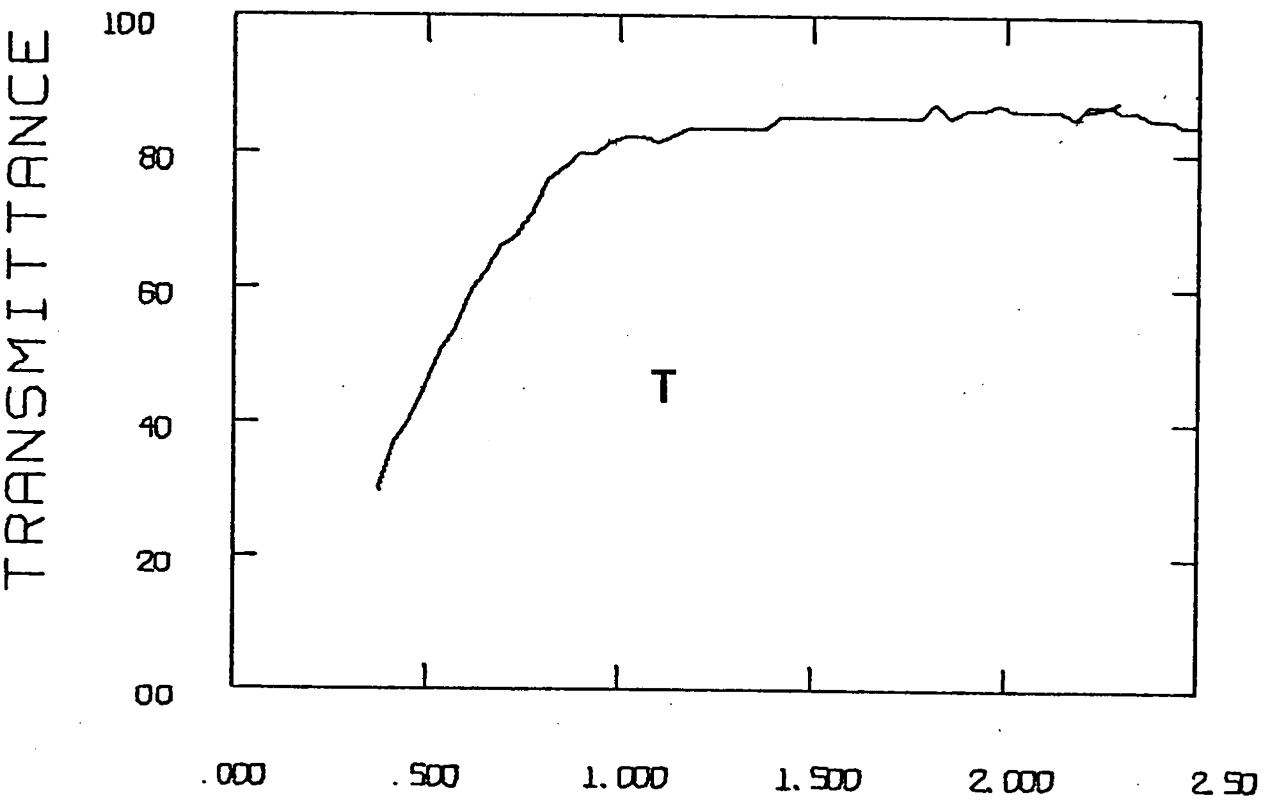

Figure 36. Change in transmittance (T) with wavelength for CuO Film 12 (800Å) after annealing.

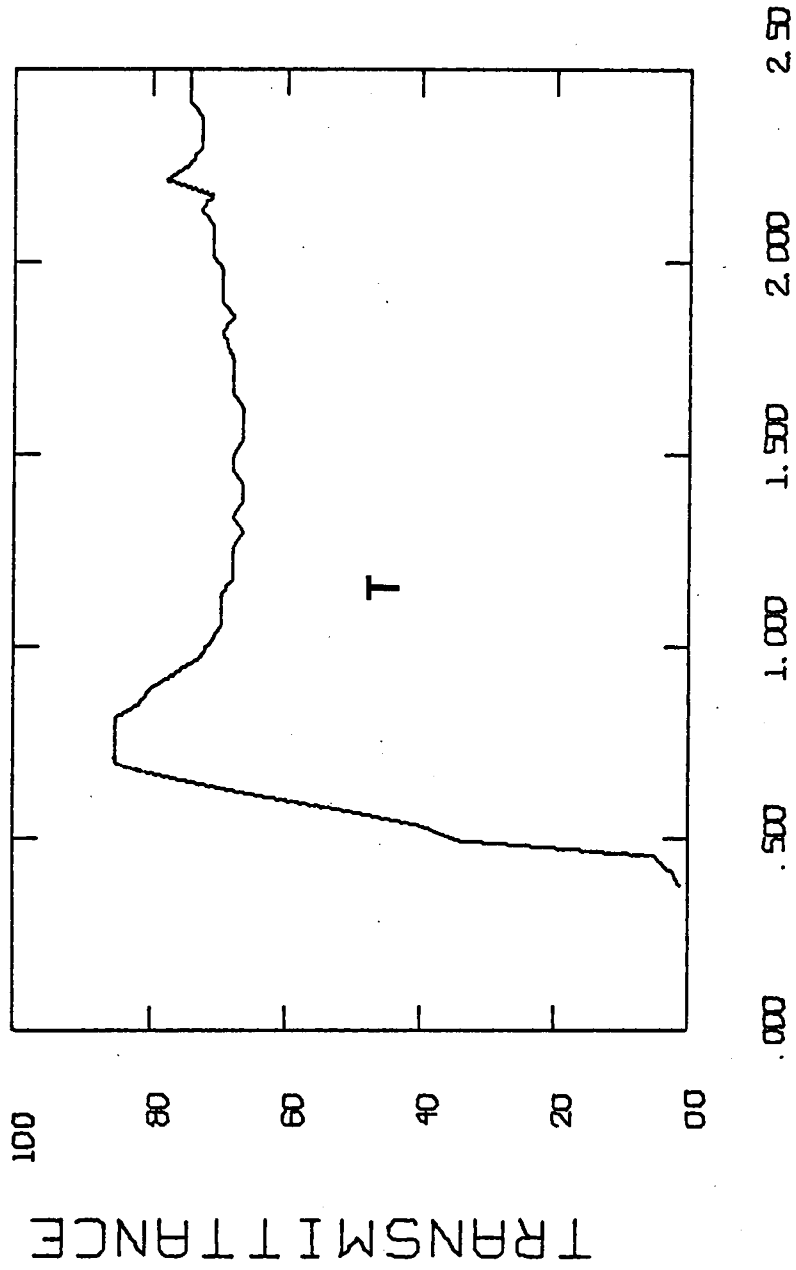

Figure 37. Change in transmittance (T) with wavelength for Cu_2O Film 27R (1500Å).

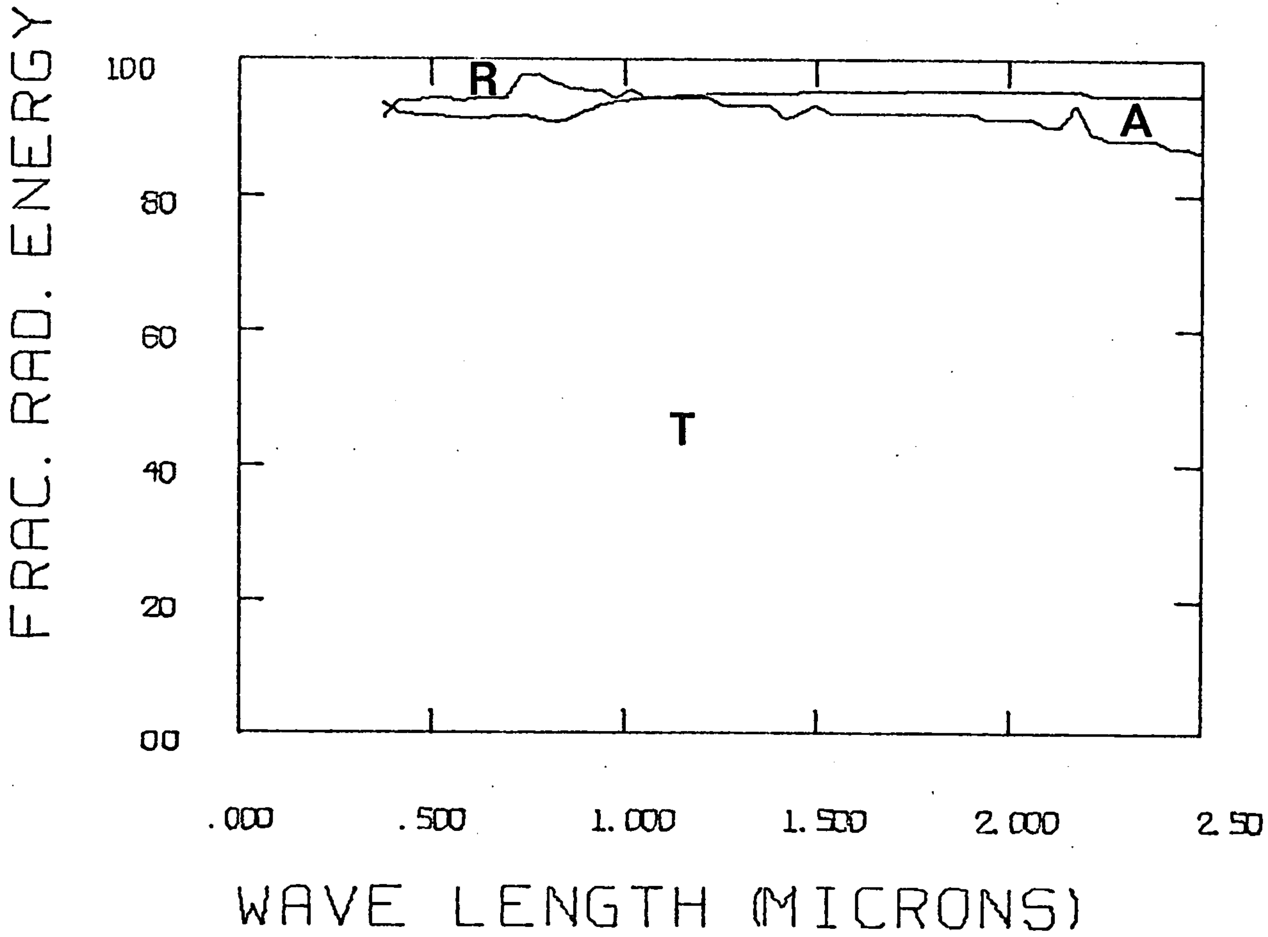

Figure 38. Change in absorbance (A), reflectance (R), and transmittance (T) with wavelength for an uncoated Corning 7059 glass substrate.

V. DISCUSSION

A. Radio Frequency Sputtering of CuO

Radio frequency sputtering from a CuO target in pure argon results in films composed of both CuO and Cu_2O. Vossen and O'Neill[41] have found that oxides with dissociation energies less than 70 kcal/mole are reduced when sputtered in pure argon. The reduction of CuO, observed by Sachse and Nichols[39] and this author, is due to the low dissociation energy (37.1 kcal/mole)[51] of the compound.

A mechanism explaining why only partial reduction of CuO occurs is not readily apparent. Little or no thermodynamic data exists for such partially reduced forms because the sputtered material may be in the gas, liquid, or solid state.[41] One or all of these states may be present in the sputtering environment, thereby complicating attempts at estimating the changes in stoichiometry which may occur.

Film stoichiometry is also affected by changes in the target surface. Heat generated in the target by ion bombardment and dissipation of r.f. energy may alter the surface composition of the target[52]. CuO is reduced to Cu_2O at 700°C under nitrogen at normal pressures[53], so it is conceivable that a Cu_2O layer may be present on the target surface during sputtering in pure argon. Differences in target stoichiometry from run to run may be responsible for the varying amounts of Cu_2O in the mixed films.

The utilization of a small sintered CuO target requires that a large target-to-substrate separation be employed to ensure uniform

film deposition. As shown by Vossen[41] (Figure 2D), a large separation also results in a significant decrease in deposition rate. The CuO deposition rates, obtained with a 10 cm separation, are less than 30 Å/minute which is in good agreement with Vossen's findings.

The addition of oxygen to the sputtering gas further decreases the deposition rate because a large portion of the sputtering power is used to form O^+ ions[41]. The ionization energy of Ar is 364 Kcal/mole whereas the dissocation and ionization energies of O_2 are 120 and 627 Kcal/mole respectively yielding a total energy of 747 Kcal/mole[54]. The decrease in the CuO deposition rate with increasing oxygen content is linear between 0 and 50% O_2.

Sputtering from larger targets would permit a much smaller target-to-substrate distance to be employed. Increasing the area to thickness ratio of the target would also allow higher sputtering powers to be utilized since target impedence would be decreased. Such changes would also increase the substrate temperature above the 120°C observed during this investigation.

B. Structure and Properties of Copper Oxide Films

1. <u>CuO/Cu_2O Films</u>. The diffraction peaks exhibited by the films sputtered in pure Ar correspond only to CuO or Cu_2O. The lack of any extraneous peaks or unusually large shifts in peak position indicates that two separate oxide phases are present in the mixed films. Integration of the diffraction peaks with a polar planimeter allows a rough approximation of the film composition to be made. Such analysis

indicates that the Cu_2O content of these films varies between 10 and 85 percent.

The dependence of resistivity on the Cu_2O content of the mixed films is illustrated in Figure 41. In spite of the scatter in the data, a linear or nearly linear decrease in resistivity with increasing Cu_2O fraction is suggested. The phases present in the mixed films must be nearly stoichiometric because the films have high resistivities and thermal activation energies. However, the phase controlling conduction must contain either interstitial oxygen atoms or cation vacancies because the films are p-type conductors.

The presence of two oxides in the films causes the fundamental absorption edge to be broadened over a range encompassing the band gaps of both Cu_2O and CuO. As shown in Figures 32 and 39, optical excitation in CuO begins at 1.0μ (1.24 eV) and that of Cu_2O begins at 0.7μ (2.07 eV). Films consisting of both oxides show a gradual decrease in transmittance with decreasing wavelength as shown in Figures 30 and 31.

Annealing the mixed films in air at $300^{\circ}C$ oxidizes the Cu_2O to CuO. The structure of the resulting CuO films appears to be less oriented than the films sputtered in the presence of oxygen, due to the appearance of two large peaks in the diffraction patterns (Figure 11). Although some randomness in the crystallite orientation must be present, these CuO films are still strongly oriented with the (111) planes parallel to the substrate. The (111) reflection possesses a much higher intensity relative to that of the overlapping (002)-($\bar{1}11$)

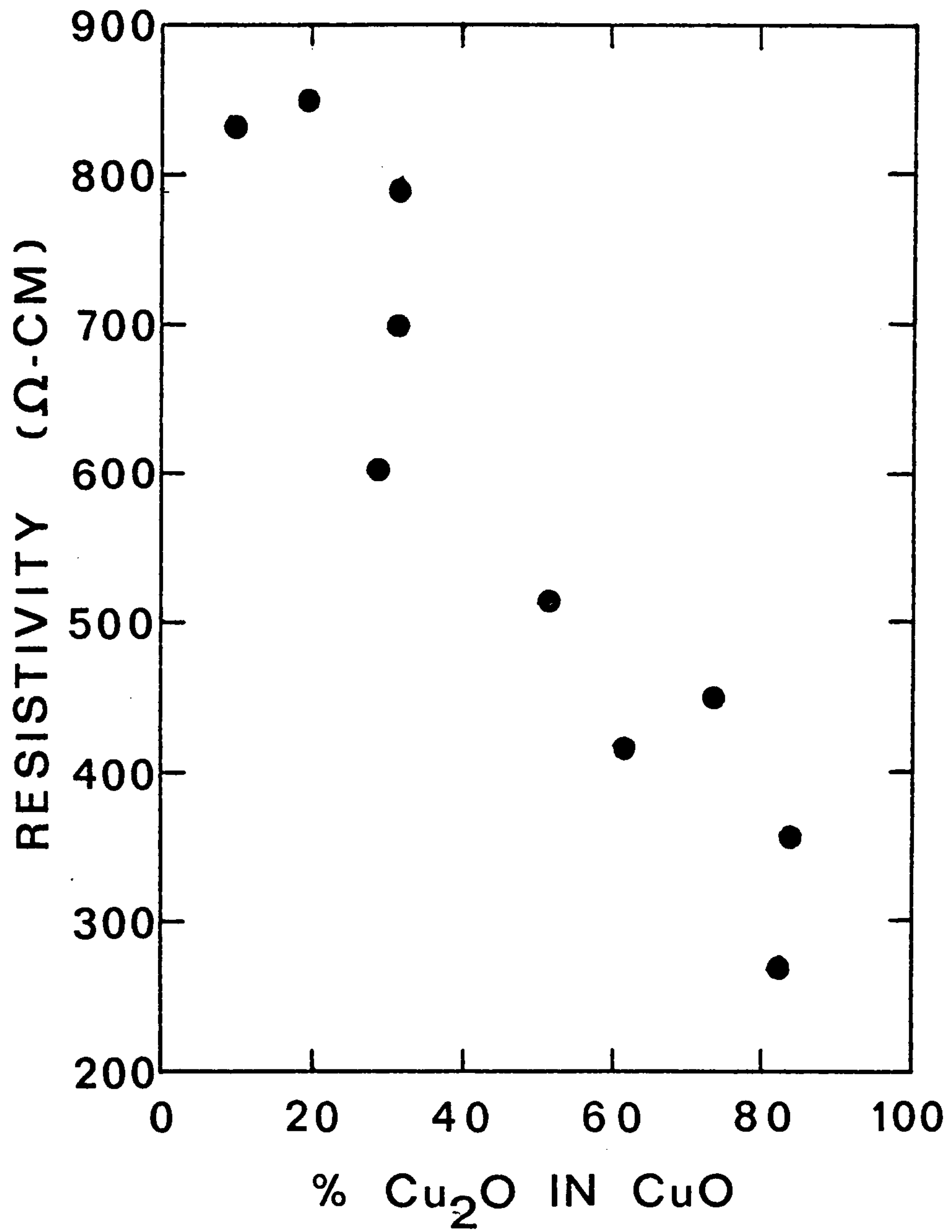

Figure 39. Resistivity dependence of CuO/Cu_2O films on Cu_2O content.

reflections. In the powder diffraction pattern of CuO, these reflections are of nearly equal intensity.

The resistivities of the CuO films, formed from the mixed films, are greater than those of the annealed CuO films which were initially sputtered in 10% and 50% oxygen. It is possible that small differences in orientation partially account for the difference in the resistivities of the annealed films. Lattice defects, as such, contribute to the scattering of charge carriers and therefore interfere with the conduction process.

Oxidation of the Cu_2O in the mixed films, to CuO also decreases their transmittance in the visible region. Thin films of CuO exhibit a dark brown color and are nearly opaque in layers as thin as 1800Å. On the other hand, Cu_2O films of similar thickness are bright yellow and transparent. The smaller band gap of CuO (~ 2.0 eV) therefore allows a greater portion of the visible spectrum to be absorbed than does that of Cu_2O whose width is approximately 2.5 eV.

2. CuO Films. the pure CuO films obtained by sputtering in 10% and 50% oxygen show definite signs of preferred orientation. The presence of only the (111) and (222) reflections in the diffraction patterns of these specimens is clear evidence that the films are oriented with the (111) planes parallel to the substrate surface. Frey[43] has similarly observed that r.f. sputtered NiO films on silica are oriented with the (200) planes parallel to the substrate. The (200) planes in NaCl type lattices, such as that in NiO, consist of a 1:1 ratio of nickel and oxygen ions in a close packed array.

Evidently, nearly equal concentrations of nickel and oxygen species are necessary to build up the NiO structure during sputtering.[43]

The (111) orientation of the CuO films prepared during this study suggests that film formation involves a deposition process similar to that of NiO. The (111) planes in the CuO lattice are composed of copper and oxygen ions in equal concentrations. However, due to the unusual coordination in CuO, the cations and anions do not lie in exactly the same plane, as in the (200) planes of NiO. The oxygen ions are slightly displaced above and below the single plane formed by the copper ions.

It is surprising that CuO films sputtered onto glass are oriented with the (111) planes parallel to the substrate surface. The surface of glass is largely composed of oxygen ions and it would seem logical that a layer of copper atoms might be the first layer to form followed by alternating layers of oxygen and copper. The (100) type planes of CuO alternate in this manner. However, if the deposition of CuO occurs largely by the collection of molecular species, then the (111) orientation would be more likely since it represents a stoichiometric arrangement of the component atoms.

Further discussion of the orientation effect observed in sputtered oxide films is complicated due to the dependence of orientation on substrate nature and temperature. Neugebauer[55] has indicated that orientation of the closest packed planes parallel to the substrate represents the most energetically favorable film structure, providing that the substrate does not introduce any ordering effects. The type

of ordering is also a function of substrate temperature because totally amorphous oxide films may result at cryogenic deposition temperatures where the surface mobility of the deposited species is very low.[43]

Substrate temperature during deposition also affects crystallite size. It is well known that larger crystallites are formed at higher deposition temperatures due to the increased surface mobility.[52] Submicron sized CuO crystallites are obtained at deposition temperatures of about 120°C. Subsequent annealing at 300°C results in an increase in crystallite size as indicated in the SEM micrographs. The narrowing of diffraction peaks during annealing of the CuO films is also indicative of crystallite growth.

The lattice parameters of the CuO films sputtered in 10% and 50% oxygen are greater than those of the target material or those listed in the powder diffraction file. The density and film composition data presented by Frey[44] for NiO films, and shown in Figure 3, reveals that a large amount of excess oxygen is trapped in the film lattice during sputtering. Density changes on the scale depicted in Figure 3 would require at least one nickel vacancy per unit cell or else large amounts of interstitial oxygen. Since the oxygen ion is probably too large to fit in either the NiO or CuO lattice interstitially, the major defects are probably metal ion vacancies. In either case, large numbers of such defects could conceivably result in an expanded lattice due to the repulsive forces exerted by the large oxygen ions. Therefore, the decrease in lattice parameter observed after annealing the CuO films can be attributed to the loss of oxygen.

Cupric oxide films, sputtered in the presence of oxygen, exhibit extrinsic p-type semiconduction. Cation vacancies, resulting from the large quantities of excess oxygen in the lattice, introduce new energy levels within the forbidden gap which are capable of accepting thermally excited electrons from the valence band. The p-type semiconduction results from the motion of positively charged electron vacancies or holes remaining in the valence band.

As the oxygen content of the CuO films increases, the acceptor levels within the band gap broaden into an acceptor band. The decrease in activation energy with increasing oxygen content indicates that the bottom of the acceptor band approaches the top of the valence band. The greater number of defects in the oxygen rich CuO films increases the number of holes in the valence band of these specimens and therefore brings about a decrease in resistivity.

Resistivity may be expressed as

$$\rho = 1/Nq\mu$$

where N is the carrier concentration, q is the electronic charge, and μ is the carrier mobility. Carrier mobility, regardless of conductivity type, decreases with increasing temperature due to the increased thermal scattering of the carriers.[56] Therefore, the exponential decrease in resistivity of the CuO films with temperature is due entirely to an increase in carrier concentration governed by the extrinsic activation energy. The presence of two activation energies, in each of the resistivity curves shown in Figure 28,

indicates the possibility of two sets of acceptor levels or perhaps the ionization of defects which would free extra holes in the valence band.[57]

The increased resistivity and activation energy observed in the annealed CuO films is primarily due to the loss of oxygen in the films. However, changes in film orientation, indicated by the appearence of additional diffraction peaks, also occurred during annealing. The effects of reorientation, combined with those of crystallite growth, on electrical properties cannot be fully evaluated at this time. The fact that the resistivities and activation energies of the films sputtered in 10% and 50% oxygen remained different after annealing, is important. Structural variations might be responsible for the retention of different amounts of oxygen in these films. It is evident that the 300°C annealing temperature is not high enough to fully overcome the effects induced by the sputtering environment even though the films begin to lose oxygen at temperatures below 200°C.

Optical transmittance of the CuO films sputtered in 10% oxygen decreases with increasing film thickness throughout the wavelength region between 0.3 and 2.5 μ. These films exhibit sharp drops in visible transmittance which correspond to the absorption edge of CuO. From the transmittance curves in Figures 31 and 33 the band gap of CuO can be estimated to lie between 1.77 eV and 2.00 eV. This is in fair agreement with the results of Stecker[13] who determined a band gap of 2.22 eV from conductivity data.

In contrast to the films sputtered in 10% oxygen, those sputtered in 50% oxygen display very poorly defined absorption edges. Because these films contain a larger amount of excess oxygen, and therefore a greater number of charge carriers to interact with and absorb radiation, they are expected to be less transmitting than CuO films containing a lesser amount of oxygen.

However, the CuO films sputtered in 50% oxygen are the thinnest specimens prepared during this investigation, and this fact explains their high transmittance. The transmittance of a 5000Å thick CuO film sputtered in 50% oxygen can be estimated from the Lambert Law[59],

$$I = I_o e^{-\alpha t}$$

where I_o is the intensity of the incident radiation, and I is the intensity after traversing a medium of thickness t. The term α is defined as the absorption coefficient and may be regarded as a material constant. Rearrangement of the above relation yields the transmittance (T) such that

$$T = I/I_o = e^{-\alpha t}$$

The absorption coefficient for CuO at 0.5 μ may be calculated from the transmittance data in Table VII, taking into account that the glass slide is only 90% transmitting at this wavelength. After calculating the transmittance of a 5000Å film alone, the net transmittance of such a film on glass is only about 0.005 as compared to 0.28 for an 1100Å thick film on glass.

The optical properties of CuO films are also dependent on film stoichiometry. Cupric oxide films sputtered in the presence of oxygen, and then annealed, exhibit much higher visible transmittance than similar unannealed specimens. Annealing removes oxygen from the films and thus reduces the number of charge carriers available for optical excitation.

A more dramatic, but similar, change has been observed in NiO films.[44] Highly nonstoichiometric NiO films (oxygen excess) are black and highly absorbing as sputtered, but take on a translucent green color after annealing at $400^{\circ}C$. Changes in the color of the CuO films after annealing are not as apparent. The band gap of CuO is approximately 2.0 eV, and therefore, most of the visible radiation between 1.5 and 4.1 eV is absorbed. Near-stoichiometric NiO films transmit visible radiation due to a large band gap of about 4.0 eV.[25]

3. <u>Cu_2O Films</u>. Cuprous oxide films can be successfully prepared by reducing previously sputtered CuO/Cu_2O films in a 5% CO - 95% CO_2 atmosphere at $300^{\circ}C$. Thermodynamic analysis of the reduction reveals that control of the CO/CO_2 ratio, to yield Cu_2O only, cannot be accomplished in a practical manner. However, reduction of CuO to Cu involves the formation of Cu_2O as an intermediate step and the desired oxide can thus be obtained through control of the reaction time.

X-ray diffraction patterns of the Cu_2O films show no peaks corresponding to CuO or Cu. The films appear to be polycrystalline due to the presence of both the (111) and (200) reflections in the diffraction patterns. Orientation of these films is not likely because

the ratio of the peak intensities is very similar to that observed in powder patterns.

Reduction of the mixed films to Cu_2O decreased their room temperature resistivities and thermal activation energies. As shown in Figure 29, the electrical characteristics of three Cu_2O films formed in this manner display good reproducibility. Breaks in the resistivity-temperature curves at $125^{o}C$ have been observed in previous studies and correspond to the initial ionization of neutral copper vacancies.[31] The decrease in resistivity exhibited by each of the Cu_2O films after heating in air to $200^{o}C$ must be the result of oxygen uptake from the atmosphere. Evidently, the Cu_2O films prepared by reaction of CuO with CO are in a reduced state and readily absorb oxygen on heating. Excess oxygen in the lattice increases the number of copper vacancies and therefore the hole concentration which brings about a decrease in resistivity. Had the Cu_2O films been oxidized to CuO, their resistivities would have increased markedly.

As mentioned previously, the Cu_2O films exhibit a bright yellow color and are transparent to the eye. The sharp decrease in transmittance at 0.5 μ (2.5 eV) indicates the presence of an absorption edge. Radiation of energy less than 2.5 eV cannot excite electrons across the band gap of Cu_2O and is therefore transmitted or reflected. This observation corresponds well with the data of Wieder and Czanderna[35] who determined the band gap of Cu_2O films to be about 2.3 eV.

VI. CONCLUSIONS

From the results of this investigation the following conclusions have been reached.

1. Radio frequency sputtering of CuO in pure argon yields films composed of both CuO and Cu_2O. Addition of oxygen to the sputtering gas results in pure CuO films.
2. CuO films, when sputtered in the presence of oxygen, show definite signs of preferred orientation with the (111) planes parallel to the substrate surface.
3. Both resistivity and thermal activation energy decrease with increasing oxygen availability during deposition in accordance with the band theory of oxygen excess semiconductors.
4. All copper oxide films display p-type semiconduction. This includes CuO, Cu_2O and all mixtures thereof.
5. Films sputtered in 10% and 50% oxygen begin losing oxygen at temperatures as low as $125^{\circ}C$.
6. Annealing CuO/Cu_2O films in air at $300^{\circ}C$ oxidizes the Cu_2O to CuO and results in resistivities greater than 10^3 Ω-cm.
7. The increases in resistivity and visible transmittance, as well as the decrease in lattice parameter, encountered after annealing CuO films in air, can be attributed to the loss of excess oxygen.
8. The optical band gap of CuO lies between 1.8 and 2.0 eV. That of Cu_2O lies at approximately 2.5 eV.

9. As a consequence of the large band gaps, both CuO and Cu_2O transmit greater than 50% of the infrared radiation between 1.0 and 2.5 μ. These films would not be useful as heat reflecting coatings on architectural glass.

10. CuO films prepared on glass by r.f. sputtering display excellent adherence and long time stability on standing in air at room temperature.

11. Thin films of Cu_2O on glass can be successfully prepared by reducing previously sputtered CuO films with CO/CO_2 mixtures. The resulting films are stable up to 200°C. To be useful in photovoltaic devices, however, Cu_2O films must be prepared with much better reproducibility.

VII. FUTURE WORK

Much remains to be learned about the properties of CuO. The lack of published data dealing with the preparation and properties of CuO films makes further studies especially significant. Future work should include the following:

1. Studies of the phase relationships between CuO and Cu_2O in order to better understand the structure and properties of films containing both oxides.
2. Crystallographic studies of CuO and other oxide films which possess unusual orientations. By observing the effects of the various deposition parameters on crystal structure, a more accurate description of the deposition process might be obtained.
3. Growth and characterization of CuO single crystals. Such work is necessary if the electrical properties of CuO are to be fully understood.
4. Characterization of the optical properties of CuO films, including the effects of dopants, nonstoichiometry, and thickness on absorbance, transmittance and reflectance. This information would be useful in optimizing the performance of flat plate solar collectors.
5. Studies of Cu_2O films prepared by reactive sputtering of Cu onto various substrate materials such as metals or n-type semiconductors. Promising candidates for photovoltaic applications could be selected for further investigation.

6. Development of a device sensitive enough to measure the Hall effect in oxide thin films of low electrical conductivity. The carrier concentration and mobility could thus be directly determined.
7. Studies of stable oxides in which the outermost occupied energy levels of the cation are completely filled. The high carrier mobilities associated with Cu_2O, ZnO, and CdO indicate that a definite trend might exist. Further examples of potential high mobility oxides are Ag_2O, In_2O_3, and HgO.

REFERENCES

1. T. R. Viverito, "Solar Radiation Control by Pyrolytic Oxide Thin Films," M.S. Thesis, Virginia Polytechnic Institute and State University (1974).

2. V. A. Baum and A. V. Sheklein, "Choice of Materials for Selective Transparent Insulation," Geliotekhnika, 4 (2) 50 (1968).

3. P. Kokoropoulos, E. Salam, and F. Daniels, "Selective Radiation Coatings. Preparation and High Temperature Stability," Solar Energy, 3 (4) 19 (1959).

4. L. O. Grondahl, "New Contact Rectifier," Physical Review, 27, 813 (1926).

5. L. C. Olsen and R. C. Bohara, "Experimental and Theoretical Studies of Cu_2O Shottky Barrier Solar Cells," Record of the Eleventh IEEE Photovoltaic Specialists Conference, May 6-8, p. 381 (1975).

6. G. Tunnel, E. Posnjak, and C. J. Ksanda, "Crystal Structure of Tenorite", J. Wash. Acad. Sci., 23, 195 (1933).

7. H. E. Swanson and E. Tatge, NBS Circular 539, Vol. I, 49 (1953).

8. R. D. Shannon and C. T. Prewitt, "Effective Ionic Radii in Oxides and Fluorides," Acta. Cryst. B, 25 (5) 925 (1969).

9. L. E. Orgel and J. D. Dunity, "Stereochemistry of Cupric Compounds," Nature 179 (455) 462-465 (1957).

10. F. A. Cotton, "Ligand Field Theory," J. Chem. Ed., 41 (9) 466 (1964).

11. Y. D. Tretyakov, et al., "Nonstoichiometry and Defect Structures in Copper Oxides and Ferrites," J. Solid State Chem., 5, 157 (1972).

12. K. Lark-Horowitz, "Conductivity in Semiconductors," Electrical Engineering, December, 1047 (1949).

13. K. Stecker, "The Semiconducting Properties of Cuprous Oxide XII," Ann. Physik, 3 (7) 55 (1959).

14. I. P. Shapiro, "Determination of the Forbidden-Zone Width from Diffuse Reflection Spectra" Optika i Spektroskopiya, 4, 256 (1958).

15. E. J. W. Verwey, "Semiconducting Materials," Butterworth's Scientific Publications Ltd., London, p. 151 (1951).

16. R. R. Heikes and W. D. Johnston, "Mechanism of Conduction in Li-Substituted Transition Metal Oxides," J. Chem. Phys., 26 (3) 582 (1957).

17. A. P. Young, et al., "Effect of High Pressure on Electrical Properties of NiO, CoO, CuO, and Cu_2O," Phys. Rev., 121 (1) 77 (1961).

18. Ya. M. Ksendov, et al., "Current Carrier Mobility in NiO Containing Li as an Impurity" Fiz. Tverd. Tela 5, 1537 (1963).

19. L. F. Mattheiss, "Procedure for Calculating Electronic Energy Bonds," Phys. Rev. B5, 590 (1972).

20. G. K. Wertheim and S. Huffner, "X-Ray Photoemission Band Structure of Some Transition-Metal Oxides," Phys. Rev. Lett., 28 (16) 1028 (1972).

21. D. P. Bhattacharyya and P. N. Mukherjee, "The Catalytic Activity and Electronic Property of Cupric Oxide Semiconductor," J. Appl. Chem., Biotechnol., 22, 889-898 (1972).

22. Z. M. Jarzebski, "Oxide Semiconductors," Pergamon Press, Inc., New York, Chapter 4, 57 (1973).

23. P. Kofstad, "Nonstoichiometry, Diffusion, and Electrical Conductivity in Binary Metal Oxides," John Wiley and Sons, Inc., New York, Chapter 14, 328 (1972).

24. W. D. Kingery, "Introduction to Ceramics," John Wiley and Sons, Inc., New York, Chapter 19, 673 (1960).

25. W. H. Strehlow and E. L. Cook, "Compilation of Energy Band Gaps in Elemental and Binary Semiconductors and Insulators," J. Phys. Chem. Ref. Data, 2 (1) (1973).

26. W. H. Brattain, "The Copper Oxide Rectifier," Revs. Modern Phys., 23 (3) 203 (1951).

27. A. R. Hutson, in "Semiconductors", Ed. N. B. Hannay, Reinhold Publishing Corporation, New York, 1959, p. 541.

28. F. P. Koffyberg, "Electronic Conduction and Defect Equilibria in CdO Single Crystals," J. Sol. State Chem., 2, 176 (1970).

29. S. Hüfner and G. K. Wertheim, "X-Ray photoemission Band Structure of Some Transition-Metal Compounds," Phys. Rev. B, 8 (10) 4857 (1973).

30. R. S. Toth, et al., "Electrical Conductivity of Single Crystal Cuprous Oxide at High Temperatures", Phys. Rev., 122 (2) 482-488 (1961).

31. R. Kuzel and F. L. Weichman, "Surface Layers and Their Conductivity on High Resistance Copper (I) Oxide," Can. J. Phys. 48 (13) 1585 (1970).

32. R. Derry, et al., "Variations in the Semiconductivity of Thin Films of Copper Oxide by Oxygen Adsorption," J. Chim. Phys., 51, 670 (1954).

33. A. W. Smith and H. Wieder, "Oxygen Sorption and Electrical Conductivity of Copper Oxide Films," J. Phys. Chem., 63, 2013 (1959).

34. H. Wieder and A. W. Czanderna, "Optical Properties of Copper Oxide Films," J. Appl. Phys., 37 (1) 184-187 (1966).

35. H. Wieder and A. W. Czanderna, "The Oxidation of Copper Films to $CuO_{0.67}$," J. Phys. Chem., 66, 816 (1962).

36. V. I. Yakerson, "Mechanism for the Thermal Decomposition of Salts of Carboxylic Acids," Isv. Akad. Nauk SSSR, Octd. Khim. Nauk, 1003 (1963).

37. G. Perny, et al., "Preparation and Structure of Copper Oxide Films Obtained by Reactive Sputtering," J. Physique, 25 (1) 5 (1964).

38. G. Perny, et al., "Physiochemical Aspects of the Preparation of Thin Semiconductor Layers by Cold Plasma Condensation," Rev. Phys. Appl., 1 (3) 230-6 (1966).

39. H. B. Sachse and G. L. Nichols, "Determination of Stoichiometric Variations in Sputtered Oxide Films," J. Appl. Phys., 41 (10) 4237 (1970).

40. L. I. Maissel and R. Gland, "Handbook of Thin Film Technology," McGraw-Hill Book Company, New York, Chapter 4, 4 (1970).

41. J. L. Vossen and J. J. O'Neill, "R. F. Sputtering Processes", RCA Review, 29 (2) 149 (1968).

42. G. K. Wehner, "Sputtering of Metal Single Crystals by Ion Bombardment," J. Appl. Phys., 27, 1056 (1955).

43. W. J. Frey, "Preparation and Properties of Transition-Metal Oxide Films of Nickel and Iron," Ph.D. Dissertation, Rensselaer Polytechnic Institute (1969).

44. A. F. Carroll, "Semiconducting Tin Oxide and Cobalt Oxide Films for Future Solar Energy Applications," M.S. Thesis, Virginia Polytechnic Institute and State University (1976).

45. R. D. Morrison and R. R. Lachenmayer, "Thin Film Thermocouples for Substrate Temperature Measurement," Rev. Sci. Inst., 34 (1) 106 (1963).

46. R. Marshal, et al., "The Preparation and Performance of Thin Film Thermocouples," J. Sci. Inst., 43, 144 (1966).

47. Operation Manual, Å-Scope Interferometer, Nos. 980-4000/4006, Varian Vacuum Division, Palo Alto, California (1966).

48. L. B. Valdes, "Resistivity Measurements on Germanium for Transistors," Proc. IRE, 42, 420 (1954).

49. R. B. Adler, A. C. Smith, R. L. Longini, "Introduction to Semiconductor Physics," John Wiley and Sons, Inc., New York, 197 (1964).

50. Powder Diffraction File, Joint Committee on Powder Diffraction Standards, Philadelphia, PA (1960).

51. O. Kubaschewski, E. L. L. Evans, and C. B. Alcock, "Metallurgical Thermochemistry," Pergamon Press, Inc., New York, p. 318 (1967).

52. J. L. Vossen, "Control of Film Properties by r.f. Sputtering Techniques," J. Vac. Sci. Technol., 8 (5) 512 (1971).

53. A. Lupu, "Thermogravimetry of Copper and Copper Oxides," J. Thermal. Anal., 2 (4) 445 (1970).

54. "Handbook of Chemistry and Physics, 49th Edition," R. C. Weast, Ed., Chemical Rubber Company, Cleveland, Ohio, F154 (1968).

55. C. Neugebauer, "The Structure and Properties of Thin Films," Proc. 3rd Intern. Vacuum Congr., Stuttgart, pp. 29 (1965).

56. J. P. Suchet, "Crystal Chemistry and Semiconduction in Transition Metal Binary Compounds," Academic Press, Inc., New York, p. 43 (1971).

57. P. Kofstad, Ibid, p. 19.

58. H. H. Willard, L. L. Merritt, and J. A. Dean, "Instrumental Methods of Analysis," Van Nostrand Company, Ltd., London, p. 77 (1965).

APPENDIX

Reduction of CuO to Cu_2O: Thermodynamic Considerations

The thermodynamics of the reduction of CuO to Cu_2O can be derived from a table of standard free energies of reaction compiled by Kubaschewski and Evans[51]. The reactions and free energy expressions are listed below. All the free energy terms are expressed in cal/mole, and the symbols [ ] and ( ) signify solids and gases respectively.

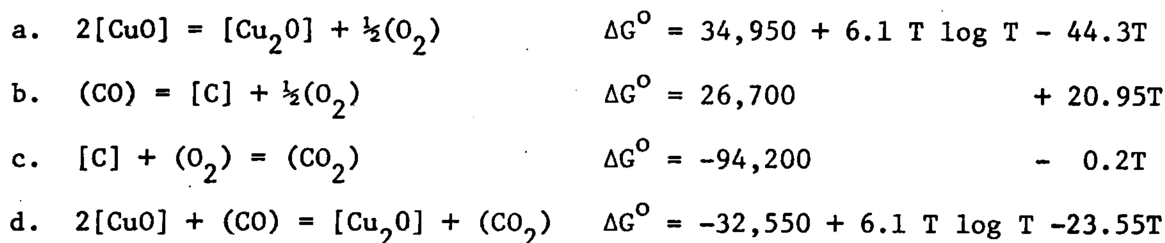

a. $2[CuO] = [Cu_2O] + \frac{1}{2}(O_2)$ $\quad \Delta G^o = 34{,}950 + 6.1\ T \log T - 44.3T$

b. $(CO) = [C] + \frac{1}{2}(O_2)$ $\quad \Delta G^o = 26{,}700 + 20.95T$

c. $[C] + (O_2) = (CO_2)$ $\quad \Delta G^o = -94{,}200 - 0.2T$

d. $2[CuO] + (CO) = [Cu_2O] + (CO_2)$ $\quad \Delta G^o = -32{,}550 + 6.1\ T \log T - 23.55T$

A second reaction, the reduction of Cu_2O to Cu metal, may also take place. Using equations (b), (c), and (e)

e. $[Cu_2O] = 2[Cu] + \frac{1}{2}(O_2)$ $\quad \Delta G^o = 40{,}500 + 3.92\ T \log T - 29.5T$

one arrives at the following relation.

f. $[Cu_2O] + (CO) = 2[Cu] + (CO_2)$ $\quad \Delta G^o = -27{,}000 + 392\ T \log T - 8.75T$

The free energy of reactions (d) and (f) may also be expressed as:

$$\Delta G^o = -RT \log_e P_{CO_2} P_{CO}$$

where R is the universal gas constant equal to 1.98 cal/mole^{o}K, T is the absolute temperature, and P refers to the partial pressure of a particular component. At 300°C (573°K) the values of ΔG^o for reactions (d) and (f) are

ΔG^o_d = -36,400 cal/mole

ΔG^o_f = -25,800 cal/mole

Solving for the P_{CO_2}/P_{CO} ratio in both cases yields

$(P_{CO_2}/P_{CO})_d = 8.6 \times 10^{13}$

$(P_{CO_2}/P_{CO})_f = 7.5 \times 10^{9}$

Obviously, such control of the gas mixtures to prevent formation of Cu metal is impractical. Between room temperature and 400°C equilibrium lies far to the right in the case of reactions (d) and (f). Similar results are obtained where hydrogen is used as the reducing agent.

The vita has been removed from
the scanned document

SEMICONDUCTION IN COPPER OXIDE THIN FILMS

by

Andrew J. Wnuk

(ABSTRACT)

Copper oxide thin films were prepared on glass substrates by radio frequency sputtering of a sintered CuO target in various argon-oxygen atmospheres. Films sputtered in pure argon consisted of both CuO and Cu_2O due to partial dissociation of CuO during deposition. Sputtering in 10% and 50% oxygen afforded films composed entirely of CuO_{1+x}.

All the sputtered films exhibited extrinsic p-type semiconduction. Both resistivity and thermal activation energy decreased with increasing oxygen content of the sputtering atmosphere. The resistivity of the CuO/Cu_2O films decreased with increasing Cu_2O content.

Annealing of the CuO_{1+x} films at 300°C in air increased their resistivity, activation energy, and visible transmittance, while decreasing the lattice parameters slightly. These changes were attributed to the loss of excess oxygen trapped within the film lattice during sputtering. Annealing of the CuO/Cu_2O films under the same conditions oxidized the Cu_2O to CuO and increased film resistivity to values greater than $10^3 \Omega$-cm.

A high degree of preferred orientation was observed in the films sputtered in the presence of oxygen. These films were oriented with the (111) planes parallel to the substrate surface and remained so

even after annealing in air at 300°C. The (111) planes in CuO are composed of equal concentrations of copper and oxygen atoms and were identified as the most densely packed planes in the lattice.

Films consisting of Cu_2O only were prepared by reducing previously sputtered films in a mixture of CO and CO_2 at 300°C. The technique proved to be a convenient means for obtaining Cu_2O films with reproducible properties which were useful in explaining the behavior of the CuO/Cu_2O films.